International School of Advanced Studies

Area of Neuroscience

Curriculum in Functional and Structural Genomics

SINEUP non-coding RNAs rescue defective frataxin expression and activity in a cellular model of Friedreich's Ataxia

Thesis submitted for the degree of "Doctor Philosophiae"

CANDIDATE

Carlotta Bon

SUPERVISOR

Prof. Stefano Gustincich

12th October 2018

DECLARATION

The work described in this thesis was carried out at SISSA (International School of Advanced Studies) in Trieste, between November 2014 and September 2018 with the exception of functional experiment on FRDA-derived lymphoblasts stably expressing miniSINEUPs, which were performed at the Department of Biomedicine and Prevention, Laboratory of Signal Transduction, University of Rome Tor Vergata, Rome, Italy, under the supervision of Ivano Condò, PhD.

This work was supported by Telethon Grant GGP15004 to Professor Stefano Gustincich, Ivano Condò and Professor Antonello Mallamaci and by the Italian Ministry of Education, University and Research (FIRB grant prot. RBAP11FRE9) to Professor Stefano Gustincich.

Part of the work described in this thesis is included in the following papers:

Structural determinants of the SINE B2 element embedded in the long non-coding RNA activator of translation AS Uchl1. Peter Podbevšek, Francesca Fasolo, Carlotta Bon, Laura Cimatti, Sabine Reißer, Piero Carninci, Giovanni Bussi, Silvia Zucchelli1, Janez Plavec*, and Stefano Gustincich*. *Scientific Reportsvolume 8, Article number: 3189 (2018). doi: https://doi.org/10.1038/s41598-017-14908-6*

SINEUP non-coding RNAs rescue defective frataxin expression and activity in a cellular model of Friedreich's Ataxia. Bon C, Luffarelli R, Russo R, Fortuni S, Santulli C, Fimiani C, Persichetti F, Cotella D, Mallamaci A, Santoro C, Carninci P, Testi R, Zucchelli S, Condò I* and Gustincich S*. *Manuscript submitted.*

TABLE OF CONTENTS

ABSTRACT

During the last decade RNA-based therapy had a burst of interest due to all undeniable advantages such as high selectivity, low off-target toxicity, and the potential scalability to a large repertory of untreatable human diseases. Most RNA therapeutic molecules are inhibitory RNAs and have been developed to down-regulate expression of pathogenic genes. Nevertheless, a large group of diseases would strongly benefit from the discovery of RNAs able to increase gene expression and restore physiological transcription and/or translation of a specific target when low expression is pathogenic.

Recently, gene-specific transcriptional activating RNAs (RNAa) (1) and non-degradative antisense oligonucleotide (ASOs) (2) have been largely employed to increase the expression of selected genes. On the other hand, despite its great potential, long non-coding translational activation as therapeutic tool is still at its infancy.

We have previously described SINEUPs, natural and synthetic antisense long non-coding RNAs, which promote translation of partially overlapping mRNAs through the activity of an embedded SINEB2 domain. In this study, we focused the attention on the SINEUP-mediated up-regulation as a possible treatment to rescue haploinsufficient gene-dosage.

In this context, we developed SINEUPs for Friedreich's ataxia (FRDA), a life-threatening disease with neuro- and cardio-degenerative progression (3) representing the most frequent type of inherited ataxia, and affecting more than 15,000 patients in Western countries (4). This monogenic disease is caused by the hyperexpansion of naturally occurring GAA repeats in the first intron of the frataxin (*FXN)* gene, encoding for frataxin, a protein implicated in the biogenesis of iron-sulphur clusters. As the genetic defect interferes with *FXN* transcription, FRDA patients express a normal frataxin protein but at insufficient levels. Thus, current therapeutic strategies are mostly aimed to restore physiological *FXN* expression.

The first goal of our study was to synthesize and validate in different cell systems, the strongest and shortest functional *FXN*-specific SINEUP to increase endogenous frataxin protein levels with a post-transcriptional mechanism.

Secondly, we aimed to validate SINEUPs as RNA tools of protein synthesis in FRDA-derived cell lines and, finally, to investigate its capability to functional rescue FRDA cells defects in cellular aconitase activity, one of the hallmarks of the disease.

In summary, we identify by *in vitro* screening *FXN*-specific SINEUPs promoting the recovery of disease-associated defects in patient-derived cells. Thus, we provide evidences that SINEUPs may be the first gene-specific therapeutic approach to activate *FXN* translation in FRDA and, more broadly, a novel scalable platform to develop new gene therapies for haploinsufficient diseases.

ACRONYMS

AAV, adeno-associated virus;

ACO, Aconitase enzyme;

ACT, Actin beta;

AGO2, argonaute 2;

AS Uchl1, lncRNA antisense to UchL1 mRNA;

AS, antisense;

ASOs, antisense oligonucleotides;

ATP, adenosine triphosphate;

BD, binding domain;

bp, base pair;

cDNA, complementary DNA;

CDS, coding sequence;

ciRNA, circular RNA

cox7B, cytochrome c oxidase subunit 7B;

CRISPR, Clustered Regularly Interspaced Short Palindromic Repeats;

CTCF, CCCTC-binding factor;

DGCR8, DiGeorge syndrome critical region gene 8;

DICER, endoribonuclease Dicer or helicase with RNase motif;

ds, double-stranded

ED, effector domain;

ENCODE, Encyclopedia of DNA Elements;

EPO, erythropoietin;

eRNA, enhancer RNA;

FANTOM, Functional Annotation of the Mammalian Genome;

FAST-1, frataxin antisense transcript 1;

FBS, fetal bovine serum;

FRDA, Friedreich Ataxia;

FXN, frataxin gene;

GAPDH, Glyceraldehyde-3-phosphate dehydrogenase

GFP, green fluorescent protein;

GUSB, glucuronidase beta

HDAC, Histon deacetylase;

HEK, human embryonic kidney;

HRP, horseradish peroxidase;

IC_{50}, inhibitor concentration that decreases the biotransformation of a substrate at a single, specified concentration by 50%;

iFXN, intermediate frataxin protein;

invSINEB2, inverted SINE of B2 subfamily;

invSINEB2, inverted SINEB2;

ISC, Iron-Sulphur Cluster;

lincRNA, long intergenic non-coding RNA;

LINE, long interspersed elements;

lncRNA, long non-coding RNA;

LOFA, late-onset FRDA;

mFXN, mature frataxin protein;

MIRb, mammalian interspersed repetitive (MIR) element b;

miRNA, micro RNA;

MOE, methoxyethyl;

MOI, multiplicity of infection;

MPP, mitochondrial processing peptidase;

MRC, mitochondrial respiratory chain;

mRNA, messenger RNA;

ncRNA, non-coding RNA;

NMHV, nuclear localization signal – MS2 coat protein interacting domain – HA epitope – (3x) VP16 transactivating domain;

nt, nucleotide;

ORF, open reading frame;

PD, Parkinson's disease;

piRNA, piwi-interacting RNA;

PRC2, polycomb repressor complex 2;

pri-miRNA, primary miRNA;

qRT-PCR, quantitative real time PCR;

RIKEN CLST, Center for life science technologies;

RIKEN PMI, Preventive Medicine & Diagnosis Innovation Program;

RISC, RNA-induced silencing complex;

RNA Pol, RNA polimerase;

RNAa, activating RNA;

RNAi, RNA interference;

RNase H, Ribonuclease H;

rRNA, ribosomal RNA;

RT, retrotranscriptase;

S, sense;

saRNA, small activating RNA;

SH-SY5Y, human neuroblastoma bone marrow;

shRNA, short harping RNA;

SINE, short interspersed element;

SINEB2, short interspersed element of B2 subfamily;

SINEUP, AS lncRNA with embedded inverted SINE B2 element that UP-regulate target mRNA translation;

siRNA, short-interfering RNA;

snoRNA, small nucleolar RNA;

SOD1, superoxide dismutase 1;

SSOs, spice-switching oligonucleotides;

TRBP, TAR RNA-binding protein;

tRNA, transfer RNA;

TSS, Transcriptional Start Site;

UchL1, Ubiquitin carboxyl-terminal hydrolase L1;

UTR, untranslated region;

VEGF, vascular endothelial growth factor;

VLOFA, very late-onset FRDA;

WB, Western Blot.

INTRODUCTION

RNA THERAPEUTICS: THE PRESENT STATE

The discovery of catalytic RNAs and RNA interference (RNAi) in the 1980s and the 1990s are milestones in the understanding of RNA function. No longer an intermediate between DNA and protein, but a dynamic and adaptable molecule able to regulate gene function (5) (6) (7). It's the breakthrough that will revolutionise molecular medicine, enlarging the range of "drug-able" targets and the ability to manipulate potentially every target transcript.

In this context, these new therapeutic drugs should be broadly classified as inhibitory RNAs or activatory RNAs. The former, promote gene expression down-regulation and include small antisense oligonucleotides (ASOs) (8,9), small interfering RNAs (siRNAs), and short hairpin RNAs (shRNAs,) (10) (11) . The latter, equally challenging, include RNAs able to activate gene-specific transcription (activatory RNA, RNAa) as well as enhance target translation (SINEUP, *described in the next chapter*) (12).

RNA molecules are unstable, potentially immunogenic and requires a vehicle to be driven to targeted cells. Nevertheless, dozens of RNA-based therapeutics are currently under clinical investigation, more than 50 RNA or RNA-derived therapeutics have reached clinical testing with promising results.

Inhibitory RNAs

AntiSense Oligonucleotides (ASOs)

Short, single-stranded antisense oligonucleotides (ASOs) are sequence-specific RNAs, tipically 8-50 nucleotides long, that bind target RNA molecules by Watson-Crick base pairing (13) and inhibit gene expression by altering mRNA splicing, arresting mRNA translation by blocking its recognition by the ribosomes, and inducing target degradation by RNase H (14) (15).

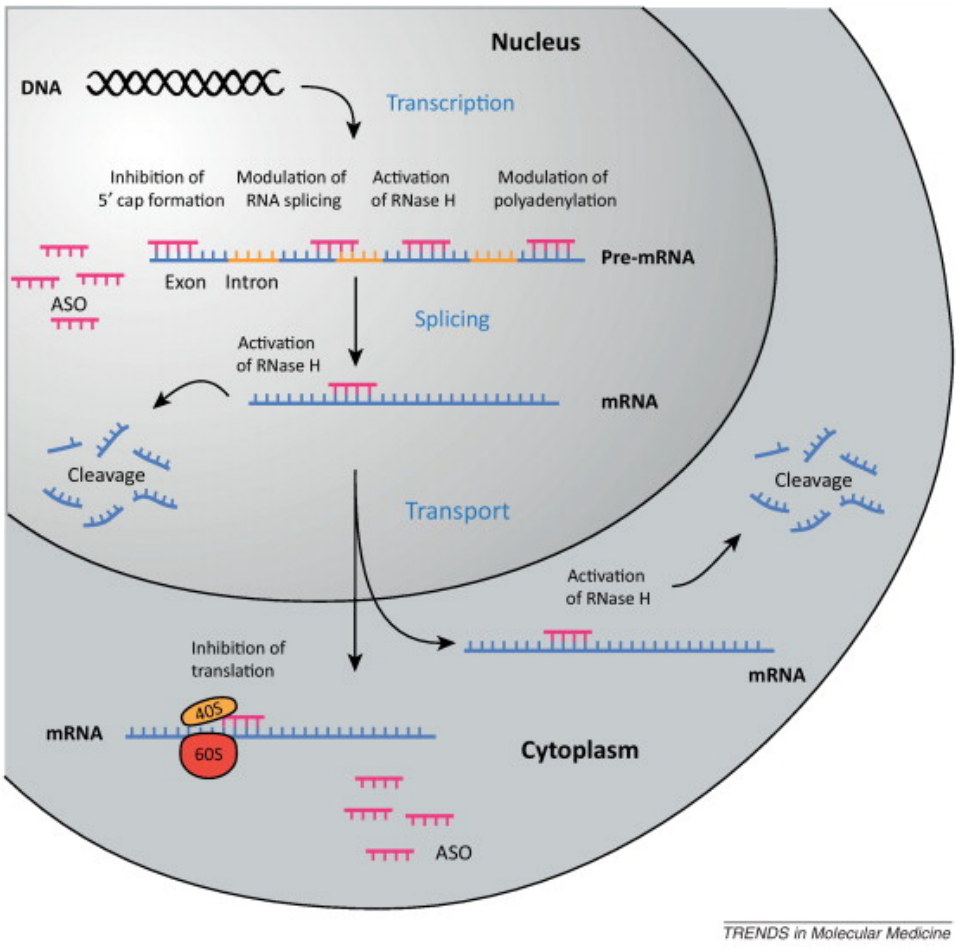

Figure 1 - **Antisense mechanisms.** ASOs can interact with RNA transcripts including both pre-mRNA and mature mRNA in the nucleus and in the cytoplasm respectively. Exonic, intronic, and untranslated region (UTR) sites may be targeted. The chemistry and design of ASOs impact on post-binding events that can be initiated including modulation of mRNA maturation, RNase H-mediated degradation, and steric translation inhibition (16).

Like others RNA-derived drugs, ASOs usually include chemical modifications to enhance its properties. Primary nucleotide sequence may be modified such as phosphorothioate (PS or PS ASOs) backbone modification; 2'-*O*-methyl (2'-O-Me),

2’-fluoro (2’-F) and 2’-*O*-methoxyethyl (2’-MOE) sugar substitution, and 2’-*O*-4’-*C*-methylene linked bicyclic ribonucleotides (locked nucleic acid, LNA) (17) (14) (18) (19).

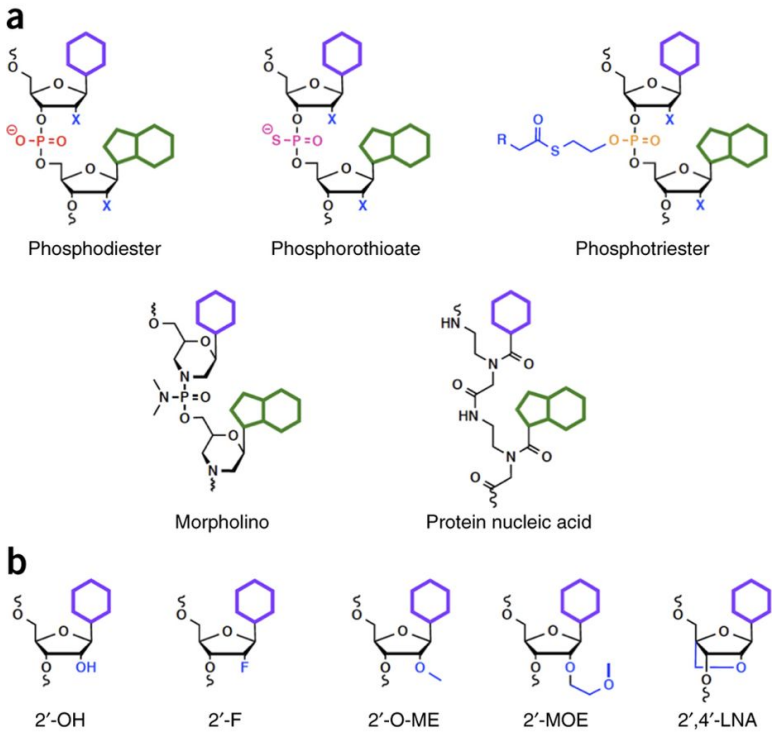

Figure 2. **Common ASO modification. a**) Phosphate backbone modifications: native, anionic charged phosphodiester; charged phosphorothioate; neutral phosphotriester; neutral morpholino backbone (PMO) and peptide nucleic acid (PNA) backbones align nucleobases with native mRNA nucleobase spacing. **b**) Common 2′ modifications of the sugar: native 2′-hydroxyl (OH), 2′-fluoro (F), 2′-hydroxymethyl (20), 2′-methoxyethyl (MOE) and 2′,4′-bicyclics that contain *O*-methylene bridge or locked nucleic acid (LNA) (21).

Modifications at the 2’-position both enhance mRNA target binding on one hand and interfere negatively with RNaseH thus preventing target RNA cleavage. “Gapmers” design have been adopted to leave the central region (gap) unmodified in between the flanking 2’-modified regions. This configuration allows RNaseH recruitment, while binding affinity and nuclease resistance are further increased (Figure 3).

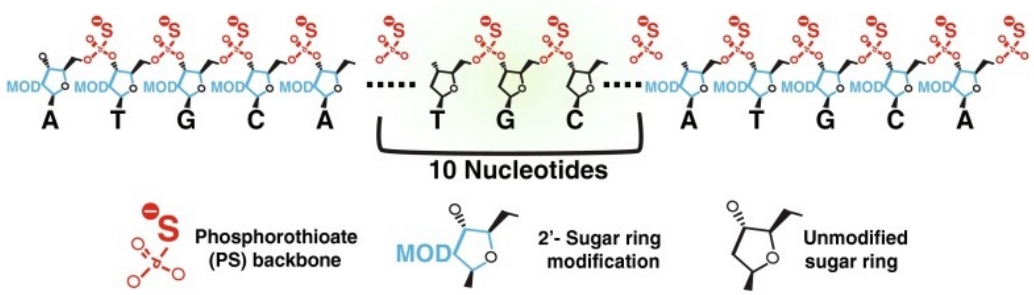

Figure 3. **Antisense oligonucleotide (ASO) 'gapmer' design.** The phosphorothioate backbone provide nuclease resistance, while the 2'-sugar modification exclusively on first and last nucleotides increases target RNA binding affinity on the outer portions of the ASO. Unmodified nucleotides allows RNaseH cleavage at the central region of the ASO (22)

To date, this class is the most widely used for therapeutical applications. In this contest, MOE ASOs gapmers targeting mutant SOD1 are the first example of ASOs tested in human clinical trials to treat ASL (Amyotrophic Lateral Sclerosis) (22).

RNA interference (RNAi)

RNA interference is the cellular process of gene expression silencing mediated by small RNA acting at both post-transcriptional and transcriptional levels, throught transcriptional gene silencing is not currently use for clinical purposes (23). microRNAs (miRNA), siRNAs and Piwi-Interacting RNAs (piRNAs) comprise small RNAs involved in RNAi. Among them, piRNAs are still poorly characterized in mammals (24) (25).

Post-transcriptional gene silencing is exploited by target mRNA degradation or cleavage. The first, is mediated by endogenous miRNA that, through imperfect complementarity, induce target degradation. On the other hand, sequence-specific cleavage is accomplished by both exogenous siRNAs or shRNAs having perfect or near-perfect base pairing with the target. After the cleavage, the target mRNA follows the natural degradation pathway, and therefore both endogenous and exogenous small RNAs-mediated processing share almost the same endogenous factor. Thus, siRNA/shRNA therapeutics may compete with natural miRNAs.

Broadly, primary miRNAs (pri-miRNAs) are processed by Drosha and DGCR8 (DiGeorge syndrome critical region gene 8) complex and then incorporated into pre-RISC (pre RNA induced silencing complex) complex formed by Dicer and TAR RNA-

binding protein (TRBP) (26). Likewise, Dicer/TRBP complex process both shRNAs and dsRNA (double-stranded RNAs) molecules into ≈21-23-nt long siRNAs. One strand of the siRNA, guide or passenger, may direct sequence-specific cleavage of target mRNA through RISC. AGO2, Argonaute 2, component of RISC has endonuclease activity by which target mRNA is cleaved and subsequently degraded by exonucleases (27). Inside RISC, the guide siRNA strand can be use to target other complementary mRNAs.

All the abovementioned properties have inspired the usage of synthetic siRNA molecules for therapeutical knockdown of endogenous and viral mRNAs (28).

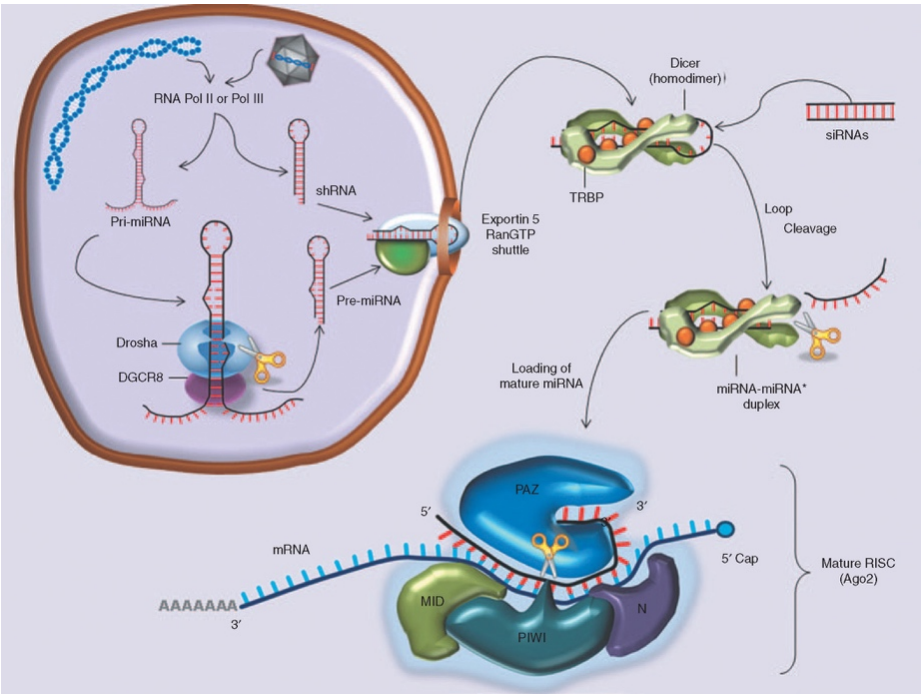

Figure 4 - **RNAi and miRNA Biogenesis**. Pri-miRNAs are transcribed from either endogenous or vector-derived genes by RNA polymerase II or polymerase III. The pri-miRNA transcript enters the microprocessor complex (Drosha & DGCR8) for its first cleavage event. The resulting pre-miRNA, as well as vector-derived shRNAs, can then be bound by the Exportin 5 RanGTP shuttle and exported though a nuclear pore into the cytoplasm. In the cytoplasm, pre-miRNAs and shRNAs associate with Dicer and TRBP. Following cleavage event results in the production of ~22-nt-long miRNA/miRNA* duplex. The guide strand of the duplex is then preferentially loaded into Ago, whereas the passenger strand is usually degraded (29).

RNAi in mammals commonly deliver synthetic siRNA molecules ≈19-23 base pairs, with overhangs at both 3', in order to mimic Dicer cleavage product. However symmetrical overhangs interfere with RISC strand choice since either guide or passenger strands can be selected. To avoid the selection bias, the dsRNA may be

designed asymmetrically with one end blunt and the second overhanging, directing preferentially the guide strand biogenesis, and thereby increasing siRNA potency and decreasing off-target effect (30).

shRNAs may constitutively be expressed from promoters and therefore induce long-lasting gene silencing for the duration of their transcription and biogenesis. However, since they are expressed through strong RNA Pol III promoters, the natural miRNA machinery could saturate resulting in severe toxicity (31) (32). To overcome saturation, multiple shRNAs may be expressed as multicistronic transcript from RNA Pol II or combined with non-RNAi therapies like rybozymes and RNA decoys (33) (34).

Recently, significant progress has been made in terms of siRNA/miRNA delivery. The most commonly used are viral vectors, both lentiviral and adeno-associated for brain delivery (35).

Anti-miRNA oligonucleotides (AntagoMIR)

Dysregulation of endogenous miRNA has been liked to numerous disorders (36) such as cancer, autoimmune disease, and neurodegeneration. Therefore, therapeutic strategies to regulate miRNA activity are emerging. To date, the expression of miRNA sponges, small RNA competitive inhibitors, and anti miRNA ASOs (antagoMIR, anti-miRNA or blockmir) (37) (38) are the main strategies could be adopted to achieve down-regulation of miRNA activity. Above all, small RNA competitive inhibitors are not currently used as therapeutical approach due to poor specificity and high IC_{50} ().

Long non-coding RNA (lncRNAs), such as lincRNAs and pseudogenes, may selectively bind miRNA and thus competing with their targets and reducing the quantity of active miRNA (39) (40). Hence synthetic sponge may be assembled as composed by long non-coding transcripts containing multiple copies of the binding site of the target miRNA. However, their usage is still restricted to *in vitro* application and some pre-clinical testing (38). Recently, a new class of nuclear-resistant lncRNAs, known as circular RNAs (circRNAs), has been discovered. Generated by covalent link of 5' and 3' termini (41) (42), may act as miRNAs sponge competing with both lncRNAs and protein-coding RNAs.

miRNA inhibition through antagoMIR, single-stranded ASOs, is currently the technique of choice. AntagoMIR targeting different miRNAs has been developed for Hepatitis C virus infection, liver cancer, heart failure, and heart metabolic disorders (2). Among them, Miravisien (SPC3649), specifically inhibiting human endogenous liver-specfic miRNA required for Hepatitis C virus infection (miR-122) had successfully completed two Phase I trials. Already indicated as well tolerated and safe, Miravisien has recently advanced to Phase II clinical study (43).

Activatory RNAs

Non-degradative ASOs

Taking advantage of its property to bind miRNAs, ASOs has also been employed for up-regulating gene expression by different mechanisms such as i.e. interfering with miRNA-mediated mRNA degradation pathway (2). Moreover, if designed against antisense (AS) lncRNAs involved in chromatin remodelling, they can block Polycomb Repressor Complex 2 (PRC2) assembly allowing transcription to restart (44). Otherwise, exon-skipping ASOs or splice-switching oligonucleotides (SSOs), can modulate mRNA processing by targeting pre-mRNA and thus interfering with splicing. (9). This last strategy has been used in the clinic for a variety of diseases, like Duchenne Muscolar Dystrophy (45) (46) (47), Ataxia Telangectasia (48,49), Frontotemporal Dementia and Parkinsonism linked to chromosome 17 (50).

RNA activation (RNAa)

Small RNAs able to enhance transcription, RNAa, were first described in 2006 by Li and colleagues (51). siRNA-like molecules have been found to elicit a specific and prolonged stimulation of Cadherin E, p21 and VEGF transcription by targeting their promoters. Later on, several reports have corroborated natural RNAa as a pervasive phenomenon (52) (53) (54) (55) (56).

Commonly referred as small activating RNAs (saRNAs), they may be sense or antisense oriented (56) and usually directed against transcription start sites (57) (58) (59) or surrounding polyA-site sequences (60), conserved *cis*-active elements of the gene of interest (56), and the transcribed region of the gene (61).

Although RNAa dynamics are still poorly understood, two classes of molecular mechanism can be identified. saRNAs may act binding AS transcript and theredore preventing down-regulation of its sense cognate (62) (63) (1) or saRNAs may convey transactivating macromolecular complexes to gene locus (62) (59) (64). Even if mismatches are quietly tolerated, they should not involve saRNA 5' end (58).

Two key features make them extremely promising, they display a later onset compared to RNAi and may exert a prolonged effect over 7 days (58). They elicit mRNA up-regulation that is usually within physiological ranges (56) (52) (65).

NMHV transcription factors

Recently, a new class of artificial transactivators has been developed. These are RNA-programmable enzymes, named NMHV (Nuclear localization signal - MS2 coat protein RNA interacting domain - HA epitope - (3x) VP16 transactivating domain) (66). This small and non-CRISPR-based device mainly consists of a fully synthetic, ribonucleoproteic transcription factor that stimulates transcription and a non-coding RNA "bait" domain that specifically drives the whole ribonucleoprotein to the target gene of interest (66). The two elements are kept together by two ancillary domains. A polypeptidic MS2 RNA-interacting domain (67), covalently joined to the ribonucleoproteic transcription factor and forming the polypeptidic "apo-factor", and its corresponding hairpin RNA interactor (68) (69), covalently joined to the non-coding RNA "bait" domain forming the RNA "co- factor".

This transactivator is 7-fold smaller than the CRISPR counterpart and, moreover, is active only where genes are normally expressed. Hence, it avoids potentially detrimental ectopic gene activation. Potentially capable of *ad libitum* gene stimulation, NMHV elicit a transcriptional gain around 2-folds. Although extremely promising to rescue insufficiency, NMHV requires further experimental validation.

SINEUPs: A NEW FUNCTIONAL CLASS OF ANTISENSE LNCRNAS

Large-scale genomic projects, such as FANTOM (70); FANTOM Consortium and the RIKEN PMI and CLST (DGT) and ENCODE (71) (72) marked the beginning of the so called "post-genomic era", by developing of full genome sequencing techniques. In this context, it was discovered that the vast majority (70-80%) of the mammalian genome is transcribed. Protein-coding gene represent just a small fraction (1-2%) of the transcriptionally active regions, therefore this prevalent transcription produces an extensive repository of non-coding (ncRNAs), including small ncRNAs, long non-coding RNAs (lncRNAs) and RNAs of Transposable Elements (TEs), increasing complexity in gene regulatory networks.

Among them, lncRNAs represent the widest and most heterogeneous class of transcripts exceeding 200 nucleotides in length. According to LNCipedia v3.1, the human genome counts more then 90000 lncRNAs transcripts differing in size, anatomical properties, subcellular localization and biological functions (73) (74). However, they share features which include: being transcribed by RNA polymerase II, to undergo splicing, to present 5′ caps and being polyadenylated (75). Moreover, their organization into discrete domains seems to represent an additional common denominator, by which lncRNAs can recruit and coordinate the activity of multiple effectors. Despite, their primary sequences are poorly conserved, whilst showing several similarities in lncRNAs modes of action, thus reinforcing the importance of RNA structures in determining function.

Based on genomic location relative to their neighbouring protein-coding genes, lncRNAs can be classified as intergenic (long intergenic non-coding RNAs or lincRNAs) if they do not overlap with any other gene or, alternatively, may overlap to genes in exonic, intronic or fully overlapping configuration.

lncRNAs contribute to gene expression regulation and, moreover, have been reported to be involved in normal organism development as well as in disease (76) (77) (78). While nuclear lncRNAs can regulate transcription in *cis* or *trans* (79), cytoplasmic ones contribute to post-transcriptional gene expression regulation by "sponging" miRNAs, sequestering specific proteins, modulating translation, and finally interacting with ribosomes (80) (81) (82) (39) (83) (84). Interestingly, examples

of lncRNAs shuttling across different cellular districts in response to specific stimuli have also been reported (82) (85). lncRNAs function are summarized in Figure 5.

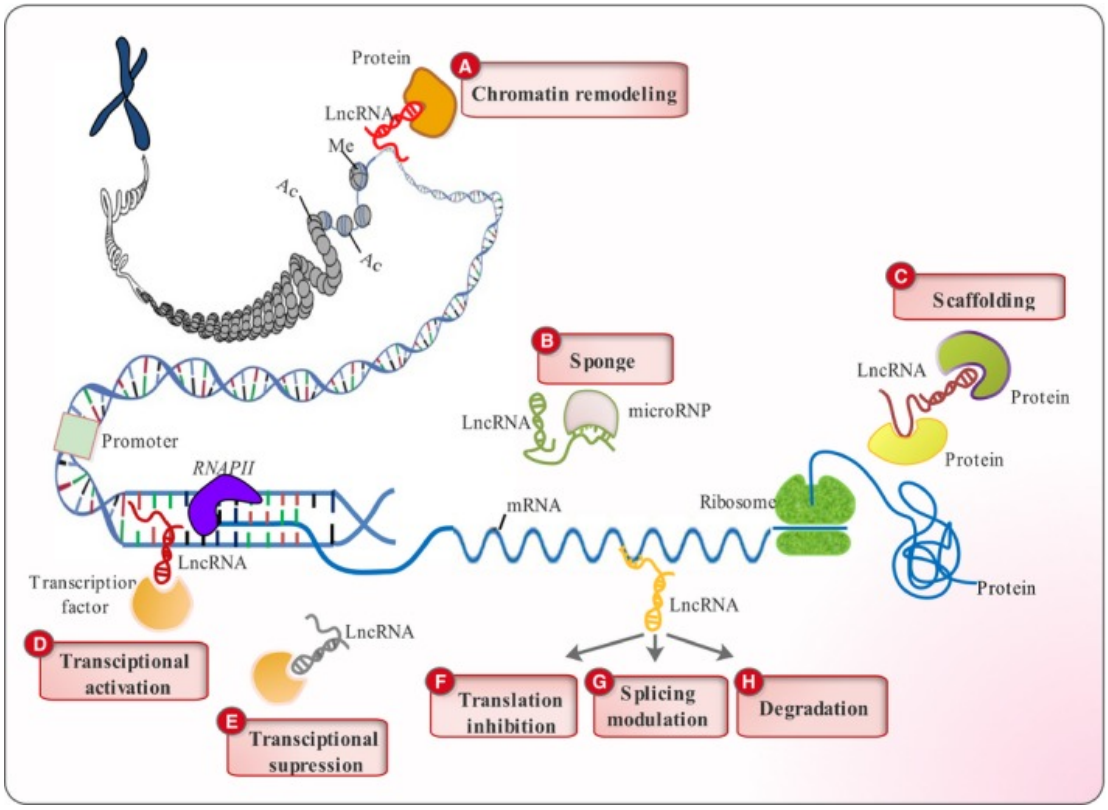

Figure 5 - **Classification of lncRNA functions.** (A) LncRNAs can recruit different protein components of the chromatin remodelling complex to change the chromatin organizational patterns. (B) They can act as 'sponges' by base pairing with their complementary miRNAs and reducing their effects. (C) LncRNAs can play scaffolding roles by providing docking sites for proteins that function together in the same biological pathway. (D) They activate transcription of certain genes by guiding transcription factors to their promoters. (E) LncRNAs are capable of suppressing transcription by sequestering transcription factors and keeping them away from their promoters. They can modulate mRNA functioning through base pairing with them and (F) inhibiting their translation (G) altering their splicing patterns and (H) subjecting them to degradative pathways (86).

One of the main features of genomes is that different genes residing in opposite DNA strands can co-exist within the same genomic region. As a result of bidirectional transcription, overlapping natural sense/antisense (S/AS) pairs are generated (72) (87) (88). Approximately 61-72% of all transcribed regions in mouse and human present lncRNAs that are in antisense orientation to adjacent protein-coding genes (87) (89).

S/AS pairs are classified according to their reciprocal genomic organization as 5' head-to-head divergent, 3' tail-to-tail convergent or fully overlapping configurations (Figure 6).

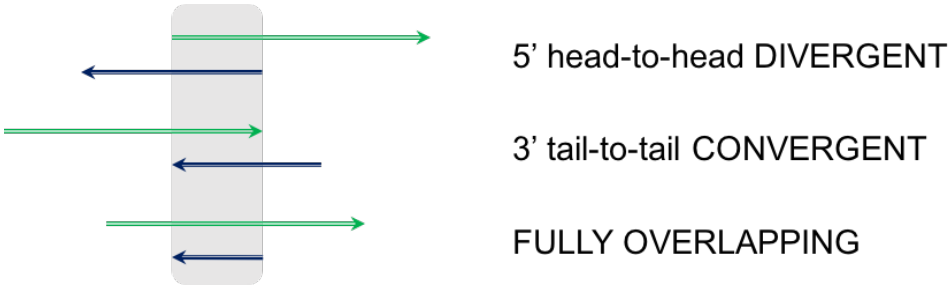

Figure 6 - **Classification of sense/antisense (S/AS) pairs.** Sense genes are in green, AS genes in blue. Arrows indicate 5′ to 3′ direction. Gray box indicates regions of overlap. Adapted from (90)

AS lncRNAs have been demonstrated to modulate cognate protein-coding gene expression in different modes (91), by affecting the epigenetic state of chromatin (92), exerting transcriptional control, regulating splicing (93) and mRNAs stability (94).

AS Uchl1

Among the mouse genomic loci of Parkinson's disease-associated genes, Carrieri and colleagues identified a spliced lncRNA transcript in the murine Ubiquitin carboxy terminal hydrolase 1 (Uchl1)/PARK5 gene, mapping in antisense orientation to its protein-coding counterpart (82).

Named Antisense Uchl1 (AS Uchl1), this 5' head-to-head divergent lncRNA, initiates within the second intron of Uchl1 and overlaps the first 73 nts of the sense (S) mRNA including the AUG codon (-40/+33 from ATG). The non-overlapping part of the transcript contains two embedded repetitive sequences, SINEB1 of the F1 subclass (Alu) and SINEB2 of the B3 subclass (82) (Figure 7).

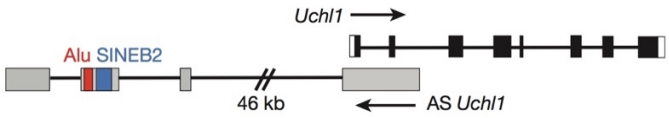

Figure 7 - Uchl1/AS Uchl1 genomic organization. Uchl1 exons are in black: 3' and 5' UTRs are in white; AS Uchl1 exons are in grey; repetitive elements are in red (Alu) and in blue (SINEB2); introns are indicated as lines. Adapted from (82).

In mouse, AS Uchl1 is co-expressed in 40% of tissues that present Uchl1 mRNA, but no AS Uchl1 is found in the absence of sense transcript (82). The two transcripts are differently localized. While mature Uchl1 mRNA is predominantly detected in the cytoplasm, AS Uchl1 is in the nucleus (82).

Overexpression of AS Uchl1 is accompanied by an increase of UCHL1 endogenous protein. Interestingly, produces no changes in Uchl1 mRNA levels, thus suggesting that AS Uchl1 expression regulation occurs at post-transcriptional level (82). Selective deletion of AS Uchl1 sequence elements to have led to the identification of two functional domains responsible for AS Uchl1-mediated translation upregulation: the 5' overlapping region and the inverted SINEB2 element.

AS Uchl1 physiologically accumulates in the nucleus of dopaminergic neurons. However, it shuttles into the cytoplasm upon cellular stress - as induced by rapamycin, an inhibitor of CAP-dependent translation – where promotes translation of sense protein-coding mRNA by enhancing its association to heavy polysomes (82).

Natural SINEUPs

A large group of lncRNAs shares similar features to S/AS Uchl1, in which FANTOM3 identified 31 natural S/AS pairs. Recently, functional validation proved their analogous function (90), as is the case of AS Uxt reported to enhance endogenous Uxt protein synthesis when overexpressed in MN9D cells with unaffected Uxt mRNA levels (82). AS Uchl1 can therefore be considered as the representative member of a new functional class of natural antisense lncRNAs capable of up-regulating translation of sense overlapping transcripts. The combination of two RNA elements provides its biological activity: the overlapping region (Binding Domain, BD) confers target specificity, while the embedded inverted SINEB2 element (Effector Domain, ED) is required for translation enhancement (Figure 8). These lncRNAs are referred to as SINEUPs, as they rely on a SINEB2 sequence to UP-regulate translation in a gene-specific manner (90,95).

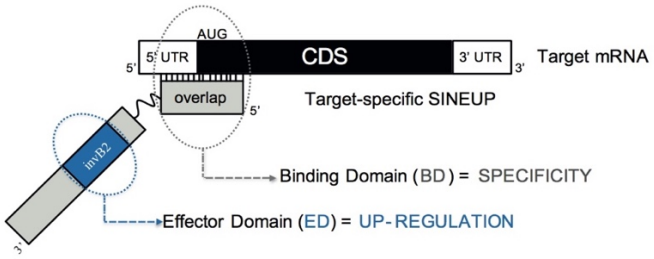

Figure 8 - **Schematic representation of SINEUPs. SINEUP modular structure.** SINEUP binding domain (grey): SINEUP sequence that overlaps, in antisense orientation, to the sense protein-coding mRNA. SINEUP effector domain (blue): non-overlapping portion of SINEUPs (grey), containing the inverted SINEB2 element (invB2) that confers activation of protein synthesis. 5′ to 3′ orientation of sense and antisense RNA molecules is indicated. Structural elements of protein-coding mRNA are shown: 5′ untranslated region (5′UTR, white), coding sequence (CDS, black) and 3′ untranslated region (3′UTR, white).

The modular organization of SINEUPs strongly reflects the role of embedded TEs in shaping lncRNAs functional features (82) (95). In particular, TEs could provide binding sites for specific molecular complexes regulating SINEUP activity. At the same time, antisense, overlapping regions may confer target specificity through RNA/RNA and RNA/DNA pairing.

However, the exact mechanism underlying the activity of the inverted SINEB2 as ED of SINEUPs remains elusive.

invSINEB2: structure and function

Recently, Podbevšek and colleagues described the secondary structure of the invSINEB2 element of AS Uchl1 (183 nts long) taking advantage of chemical footprinting and NMR studies. It folds into a structure with mostly helical secondary structure elements and it exhibits several bulges, asymmetric internal loops and hairpins (Figure 9).

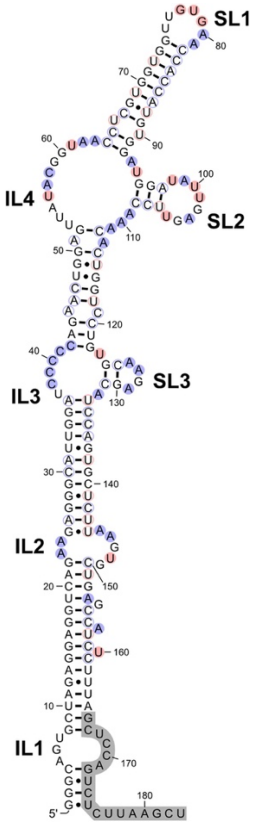

Figure 9 - Secondary structure of the inverted SINEB2/183 effector domain of AS Uchl1. tDMS and CMCT reactive nucleotides are shaded in blue and red, respectively. Internal loops and stem-loops are labelle as ILx and SLx, respectively. Non-reactive nucleotides are only circled. The segment shaded in gray corresponds to the DNA primer hybridization site (96).

Moreover, within invSINEB2, the terminal SL1 represent a crucial structural determinant required for AS Uchl1 activity. The deletion of nucleotides 68–77 of invSINEB2 (ΔSL1) from the full length AS Uchl1 (ΔSL1 mutant) completely abolish the ability of AS Uchl1 RNA to up-regulate UchL1 protein levels (Figure 10)

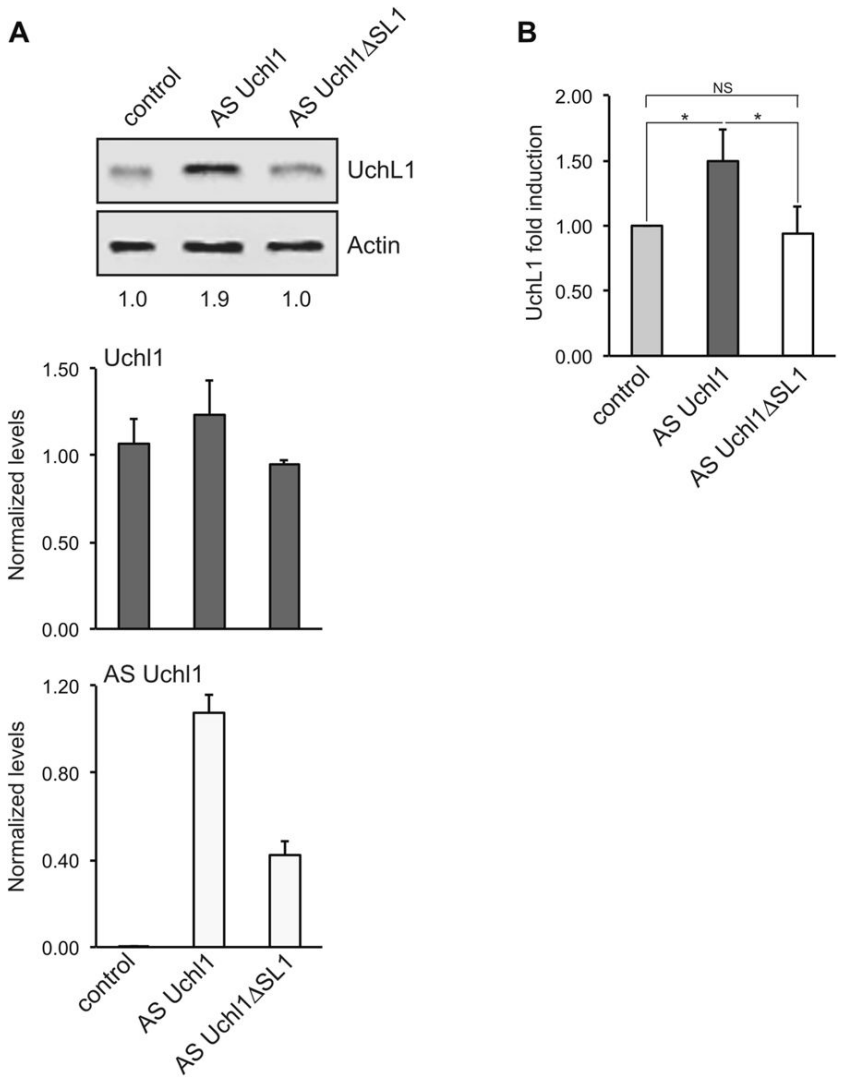

Figure 10 - The SL1 hairpin contributes to AS Uchl1 activity. (A) Murine neuroblastoma N2a cells were transfected with AS Uchl1 and ΔSL1 mutant constructs. Control cells were transfected with an empty control plasmid. Protein (97) and RNA (bottom) levels showed killed activity of ΔSL1 mutant RNA. (B) Graphical representation of AS Uchl1 and ΔSL1 translation enhancement activity on endogenous Uchl1 mRNA in N2a cells (N=5). *, p=0.01; NS, not significant (p>0.5) (96).

Further studies are needed to elucidate the precise mechanism to increase protein translation by the embedded invSINEB2 and to determine whether the SL1 motif is the sole ED portion responsible for AS Uchl1 activity.

Synthetic SINEUPs

Carrieri and colleagues engineered a chimeric construct, named AS GFP, by swapping AS Uchl1 BD to Uchl1 with a complementary sequence to EGFP mRNA in antisense orientation, maintaining the whole 3' tail (about 1200 nucleotides), the inverted SINEUB2 and the partial Alu repeat (Figure 11). This first synthetic SINEUP succeeded in up-regulating GFP protein translation when co-transfected with corresponding sense GFP-encoding DNA in HEK 293T cells, with no effects on GFP mRNA levels (Figure 11) (82) (95).

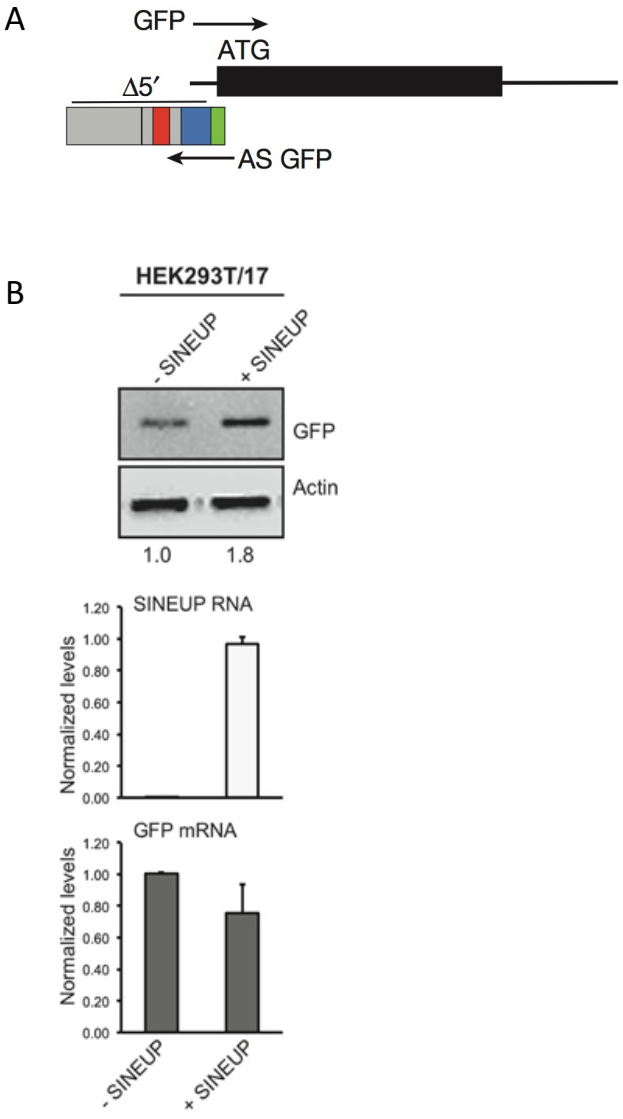

Figure 11 - Synthetic AS lncRNA increases target protein levels. (A)Scheme of antisense GFP construct. Δ 5' AS Uchl1 with repetitive elements (SINEB2, red; Alu, blue) and the overlap (green) regions are indicated. (B) SINEUP-GFP Activity. Adapted from (82) (95)

Moreover, Yao and co-workers showed that GFP mRNA is recruited to heavy polysomes in AS GFP (there referred to as RNAe)-transfected cells (98) as previously shown for Uchl1 mRNA recruitment triggered by natural AS Uchl1 (82).

Collectively, taking advantage of SINEUPs domain architecture, artificial SINEUPs may be designed by manipulating the BD to enhance target mRNA translation of any target of interest. Therefore, the translational regulatory properties of natural SINEUPs are retained by synthetic ones, likely shearing common molecular mechanisms, suggesting their applications as tools to selectively modulate gene expression *in vitro* and *in vivo*.

miniSINEUPs

Evidence of SINEUPs scalability paves the way towards a potential application as therapeutic approach, particularly in haploinsufficient diseases. However, its applicability is limited by RNA length. About 1200 nts long transcripts are suitable for delivery systems such as viral vectors, but incompatible with the use as naked RNA therapeutic molecules.

The laboratory of Prof. Gustincich demonstrated that deletions in redundant portions of the non-overlapping regions of AS Uchl1 don't affect its functionality. The exclusive combination of the invSINEB2 sequence with AS GFP BD, called miniSINEUP-GFP, promotes GFP protein up-regulation at post-transcriptional level (Figure 12). Then, they showed that ≈250 nt long transcripts are able to retain both activity and mechanisms of their full-length counterparts for a wide spectrum of targets and in different cell types (95) (99) (100).

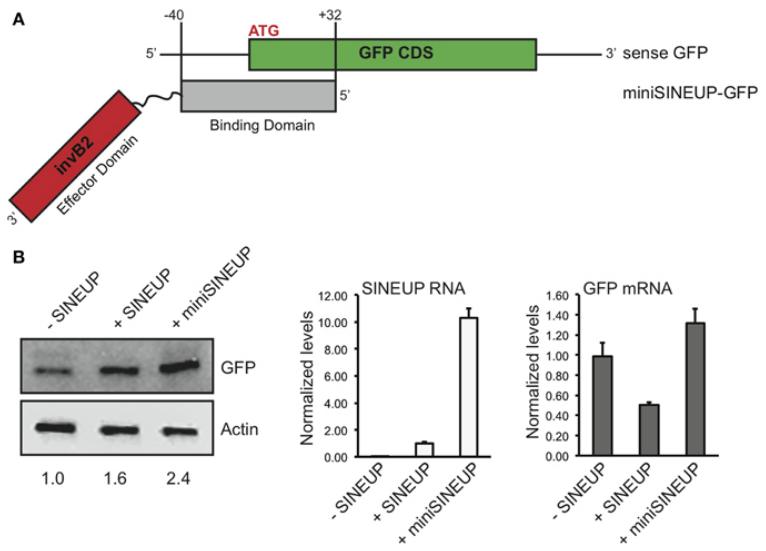

Figure 12 – miniSINEUP-GFP Activity. (A) Domain organization of miniSINEUP-GFP. Binding (gray) and effector (invB2, red) domains are indicated. **(B)** HEK 293T/17 cells were co-transfected with sense GFP vector together with empty vector (-SINEUP), SINEUP-GFP as positive control (+SINEUP) and miniSINEUP-GFP (+miniSINEUP). From (95).

SINEUPs as a new platform for increasing gene expression

The discovery of a new functional class of natural and synthetic antisense lncRNAs that stimulate translation of sense mRNAs paves the way to interesting biotechnological and therapeutical applications. The modular architecture of SINEUPs enables engineering synthetic molecules against potentially any target of interest, by swapping the BD.

Three major applications can be envisioned.

1. *Molecular biology*. SINEUPs can be used as a toolkit for increasing expression of the gene of interest in molecular biology experiments. Scientists may consider them as a counterpart of siRNA technologies.
2. *Biotechnology*. They can be used to increase efficiency of protein manufacturing procedures. Data are shown by different laboratories that SINEUPs can increase i.e. production of recombinant antibodies.
3. *Therapy*. SINEUP technology presents two critical properties for their use in therapy: high specificity and low side effects. The former is ensured by fine-tuned BD design. The latter derives from the capability to gently elicit translational gains within physiological range. Moreover, target gene stimulation occurs only where the gene is normally expressed, avoiding detrimental ectopic translational activation. In this context, there are several examples when genes causing haploinsufficient diseases may lead to other diseases when duplicated or their protein products are over-expressed in large quantities. A miniaturized version, known as miniSINEUP, implements the power of the tool, overhauling length as the main obstacle of SINEUP application in RNA therapeutics: However, delivery systems and chemical modifications to ensure SINEUP activity preservation are still under investigation. These features determine the applicability of SINEUPs as a new platform for increasing gene expression *in vivo* for therapy. Currently, several therapeutic needs for haploinsufficiency treatments are still unmet. Since the reduction to 50% or less of gene expression results in an abnormal, pathological phenotype, an efficient and specific SINEUP activity would be in principle curative by restoring physiological target levels of gene

expression. Many complex and metabolic diseases, where the increase of pro-survival factors and dysregulated enzymes may impact the well being of patients, could as well benefit from its usage. Even if its application is still in its infancy, two recent studies reported SINEUPs efficiency of modulating protein production *in vivo,* encouraging their future deployment as RNA drugs (101) (102). SINEUP technology has been tested in a medakafish model of microphthalmia with linear skin defects (MLS) syndrome, caused by mutations in players of the mitochondrial respiratory chain (MRC) including the subunit 7B of cytochrome c oxidase (COX) (101). SINEUP targeting the endogenous *cox7B* mRNA has been injected in MLS morphants resulting in restored MRC function and phenotype. Interestingly, SINEUP injection fully rescued microphthalmia and microcephaly in about 50% of embryos, whereas the injection of a control SINEUP did not result in amelioration of the phenotype by reinforcing validation of SINEUP specificity (101). SINEUP-based therapy, referred to as RNAe, has also been proposed by Longo and colleagues. Evidence of SINEUP activity has been reported in transgenic mice targeting RNAe antisense to the growth hormone gene, causing heavier body weight and longer body length compared to control mice (102).

FRIEDREICH'S ATAXIA

Friedreich's ataxia (FRDA) was firstly described by Dr. Nicholaus Friedreich in 1863 as inherited ataxia involving spinal cord, peripheral nerves and cerebellum (103). The pathogenic mutation in FRDA is a guanidine-adenine-adenine (32) trinucleotide repeats expansion on chromosome 9q13 (104) that leads to transcriptional silencing of the frataxin gene (*FXN*) (4). Broadly, the decrease of *FXN* transcription perturbs iron homeostasis promoting cardio- and neurodegeneration (105) (4).

Clinical features

Patients (75% affected individuals) typically show degeneration of large sensory neurons of the dorsal root ganglia, Betz pyramidal neurons of the cerebral cortex and lateral cortico-spinal and spinocerebellar tracts, as well as lesions in the dentate nucleus of the cerebellum (4). The main age of onset of symptoms is ten to fifteen (106). Within five years after, individuals exhibit lower-extremity weakness, diminished or absent joint-position, vibration sense distally, and dysartria. The latter, is generally of three type: mild dysarthria, hypernasality, and increased strained-strangled vocal quality (107). Dysphagia, relates to oropharyngeal coordination, weakness and spasticity, is also common (92% of affected individuals) (108).

In addition, non-neurological degeneration causes hypertrophic cardiomyopathy and increased incidence of diabetes mellitus. This occurs in up to 30% of patients (109) whereas impaired glucose tolerance is seen in up to an additional 49% (110) (111). Two thirds of affected individuals show increased interventricular septum thickness (112). Systolic dysfunction and left ventricular wall thickness appear as the disease progresses (113). Based on the ejection fraction, two main groups should be identified. The first, approximately represent 80% of affected individuals, "low risk" group with a normal ejection fraction that even though declined, it remains into the normal range. The latter, "high risk" group, had a decrease ejection fraction into the abnormal range combined with high mortality rate.

Neurodegenerative motor symptoms typically appear before adolescence with progressive gait instability and loss of coordination, while the cardiac impairment usually occurs in the later stages of the disease (114). Atrial fibrillation and congestive

heart failure are the most common cause of mortality (115) at a mean age of 40 years (116).

FRDA individuals with Late-Onset (LOFA - 26-39 years) and Very Late-Onset (VLOFA - after age 40 years), represent approximately 15% of patients (117) (118).

Genetic basis of the disease

FXN gene

Frataxin is a small highly conserved acidic protein (≈ 17 kDa) (NP_000135.2), encoded via a major transcript (NM_000144.4) in the nucleus, expressed in the cytoplasm and imported in the mitochondrion through an import signal in the N-terminus. This transcript is composed of five exons (1-5a) and encodes for 210-amino acid protein (isoform A). Alternative splicing produces minor transcripts with exon 5b instead of 5a, in the presence of an additional non-coding exon 6 that may or may not be present (isoform B and isoform B1 respectively) (Figure 13) (119).

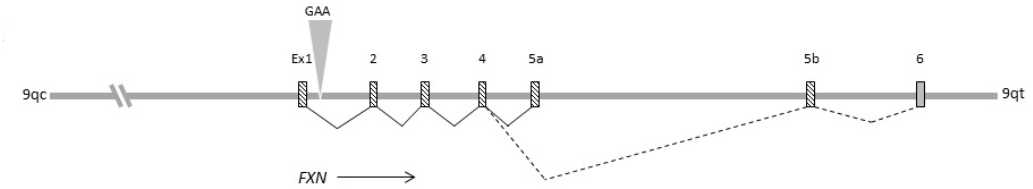

Figure 13 - **Schematic representation of the genomic structure of FXN** on the long arm of chromosome 9 (position 9q13) with centromeric (9qc) to telomeric (9qt) orientation indicated. Two alternate transcripts are shown. Adapted from (120).

Two major transcription start sites (57) were identified in the *FXN* gene: TSS1 (119) and TSS2 (121) respectively 221bp and 62bp upstream of the ATG translation start site. The region in-between is thought to be TATA-less downstream promoter, transcription factors binding sites (122), as well as insulator protein CCCTC-binding factor (CTCF) (Figure 14) (123).

GAA triplet repeat expansion

The human *FXN* locus is located on chromosome 9q21 and contains normally from 10 to 66 GAA-triplet repeats within the first intron, whereas FRDA patients carry an intronic homozygous expansion of natural tandem repeats up to 1700 triplets (119). In a small percentage of cases, however, patients are compound heterozygotes for GAA expansion on one *FXN* allele and a small insertion, deletion or point mutation in *FXN* open reading frame on the other (124). In contrast, in rare instances, GAA repeats are interrupted by other nucleotides usually closed to the 3' end of the repeat tract. Such "rare interrupted *FNX* alleles" may be associated with a later onset of the disease (125). All pathogenic variants result in a loss of frataxin function. Apart from (32) n repeats, a number of repetitive DNA element have been identified at *FXN* locus, including L2 (LINE) (126), Alu (SINE), and MIRb (119) (127). Their precise function in *FXN* regulation is still not known.

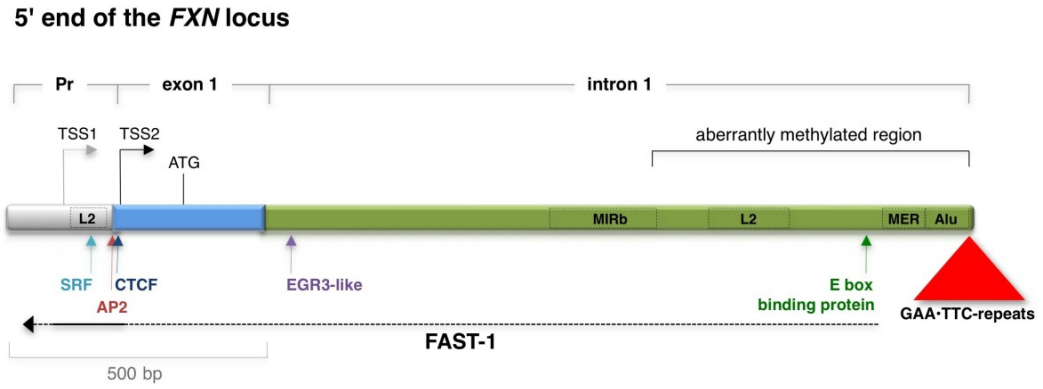

Figure 14 – **Graphical rappresentation of 5' end of the frataxin gene.** Minimal promoter, exon 1 and the promoter proximal end of intron 1 are shown. TSS1 and TSS2 refer to transcription start sites described in two different studies. The positions of various interspersed repeated sequences are indicated by the rectangles outlined with black dashed lines. The dotted black arrow indicates the estimated extent of the FXN antisense transcript-1 (FAST-1) transcript based on nested PCR. Arrows indicate the location of the binding sites for serum response factor (SRF), activator protein 2 (AP2), CCCTC-binding factor (CTCF), an early growth response protein 3 (EGR3)-like factor and an E-box binding protein which have been shown to be positive regulators of FXN expression. From (121).

Deficiency of *FXN* transcript levels and ultimately of frataxin protein results in a secondary deficiency of iron-sulfur cluster-containing enzymes, mislocalization of cellular iron, and increased sensitivity to oxidative stress, and therefore an impaired mitochondrial respiratory function.

Despite the clinical outcome is not precisely predictable based on genotype, it has been demonstrated that longer hyperexpansions result in a more severe phenotype with an earlier onset and faster progression (128) (129) (130) (131). This inverse correlation it is clear even from both LOFA (<500 repeats) and VLOFA (<300 repeats) individuals (132) (133). Moreover, cardiomyopathy is more present in patient with large expansions (130) (128) (129,134) (135).

FXN transcription inhibition

Although the mechanism by which GAA triplet repeat expansion leads to *FXN* silencing is still not precisely understood, two main hypotheses has been proposed.

Firstly, GAA repeat expansions may impair *FXN* transcription by inducing the formation of triple helical DNA structures (sticky DNA) (136) or persistent DNA/RNA hybrids (R-loops) (137) that infers with elongation. On the other hand, epigenetic silencing, via repressive chromatin formation in the sequence flanking the expanded GAA region or near the *FXN* promoter, may interfere with both transcriptional initiation and elongation (138) (123) (139) (121) (140) (141,142) (143) (Figure 15).

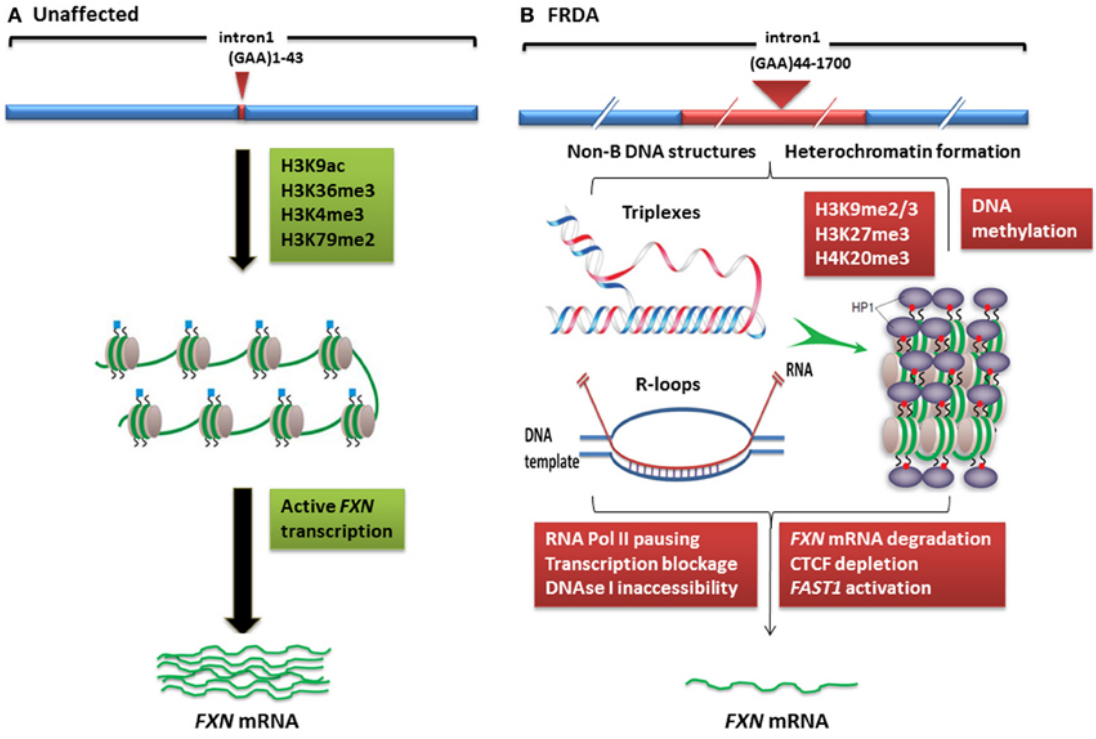

Figure 15 - **Models of FXN gene silencing in FRDA.** (A) Unaffected individuals, contain active histone marks of gene transcription initiation and elongation at the FXN promoter and intron 1 regions. (B) Potential silencing mechanisms in FRDA patients: (i) the GAA•TTC repeat may adopt abnormal non-B DNA structures (triplexes) or DNA•RNA hybrid structures (R loops), which impede the process of RNA polymerase and thus reduce FXN gene transcription, (57) increased levels of DNA methylation and HP1 and significant enrichment of repressive histone marks at the FXN gene trigger heterochromatin formation that may lead to more pronounced FXN gene silencing (144)

Antisense RNA transcripts are known to play a crucial role in gene regulation, and have previously associated with TNR expansion disease e.g. Huntington disease (145) (123). Moreover, the CCCTC-binding factor (CTCF) protein has a fundamental role of preventing DNA methylation spreading. Bidichandani and colleagues found increased levels of frataxin antisense transcript (FAST-1) in patient-derived cell lines associated to depleted CTCF binding site, suggesting involvement of these factor in heterochromatin formation and perhaps in FXN silencing (Figure 16) (144) (123) (138). However, since DNA methylation at the CTCF-binding site within the 5' UTR region of FXN gene has not been detected (123) (138), further evidences are needed, since they likely should be highly relevant for an epigenetic-based therapy for FRDA.

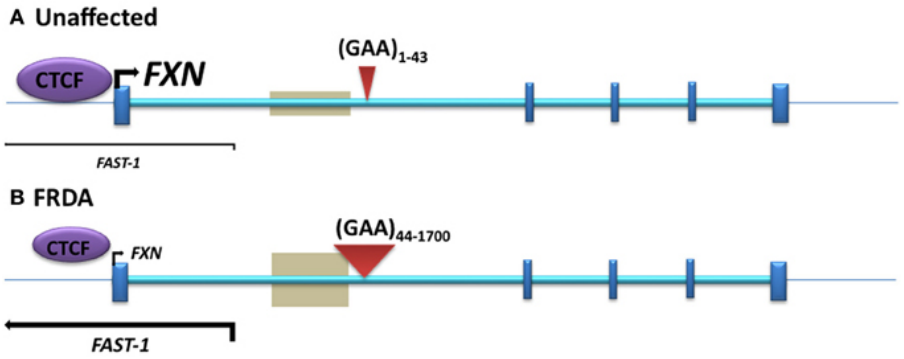

Figure 16 - (A) Unaffected: normal-sized GAA repeat (B) FRDA: GAA repeat expansion. Gray boxes represent regions of disease-associated DNA methylation and hydroxymethylation. Arrow marks represent the directions and levels of transcription for FXN and FAST-1. Blue bars represent exons of the FXN gene. Red triangles indicate GAA repeats within intron 1 of the FXN gene. From (144) (123) (138).

Lastly, based on the ability of repeats to bind splicing factors, it has been suggested that *FXN* mRNA deficit results from an altered splicing (146). Reduced splicing is related to intron length in yeast, where the largest one is <1 Kb (147). However, many efficiently spliced human introns are much longer, including normal *FXN* intron 1 (11 Kb). Since a very unstable splice isoform has been shown in FRDA cells (117) (148), this issue is still unsolved.

Epigenetic changes associated with FRDA

DNA methylation and hydroxymethylation, post-traslational histone modification, chromatin remodelling, and non-coding RNA effects are laid down in epigenetic mechanisms that produce effects on gene expression without involving changes in the primary DNA sequence. A potential involvement in FRDA disease was firstly suggested by heterochromatin-sensitive cell surface reporter gene silencing in transgenic mice by position effect variegation (PEV) mediated by a nearby long GAA expansion (149). Further studies have subsequently identified epigenetic changes, which may be involved in *FXN* gene silencing in FRDA (138) (140) (148) (121) (123) (139) (150) (151) (152) (153) (154).

Initial investigation of DNA methylation within *FXN* gene revealed hypermethylation of three out of fifteen specific CpG sites up-stream the expansion in patient-derived lymphoblasts compared to healthy controls (151). Sandi and colleagues corroborated previous finding in FRDA patient autopsy brain, heart, and cerebellum tissues (138). Moreover, direct correlation between expansion length and the extend of DNA methylation in FRDA patient blood samples has also be found.

Post-translational histone modification is associated with heterochromatin formation and gene silencing, particularly histone hypoacetilation (e.g. H3K9) and increased histone methylation (e.g. H3K9me2, H3K9me3, HeK27me3, and H4K20me3). Modification at the *FXN* locus were first identified by Gottesfeld and colleagues by identifying increased H3K9me2 and H3K9me3 in FRDA lymphoblastoid cells (139). Further studies reported changed histone modification at the *FXN* 5'UTR region, *FXN* promoter, up- and down-stream GAA repeat expansion in FRDA patient and mouse models (138) (123) (150) (151). Recent studies have shown decreased level of H3K9me3, HeK27me3, and H4K20me3 at the up- and down-stream GAA repeats expanded region indicating transcription elongation impairment. Moreover, unchanged modification at the promoter region has recently been reported. This indicates that an elongation defect occurs rather than an early transcription initiation deficit (121) (148) (153).

In summary, frataxin expression deficiency in FRDA is mainly caused by GAA expansion-induced transcriptional silencing mediated by epigenetic modification.

Frataxin

Structure

Frataxins are small proteins highly conserved from bacteria to mammals, mainly, but not exclusively, confined inside the mitochondrial matrix (155) (156) (157). Musco and colleagues determined the structure of human frataxin isoform A (158), as well as the *E. coli* homologue CyaY and the mature form yeast homologue Yfh1. All these structures shared similar fold reflecting high degree of sequence conservation, thus suggesting a common function. As confirmed by De-Phaganon end colleagues, frataxin structure consists in six-stranded β-antiparallel sheet, flanked by N- and C-terminal α-helices, with no main surface cavity (Figure 17) (159). Residues on the α-helices are negatively charged, which can be responsible of iron-binding. Unlikely, β-antiparallel sheet surface is mostly uncharged, probably involved in protein-protein interactions.

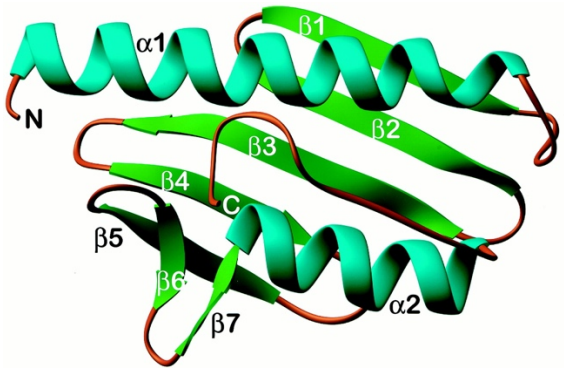

Figure 17 - **Structure of frataxin.** Compact αβ sandwich, with α helices in turquoise and β strands in green. Strands β1–β5 form a flat antiparallel β sheet that interacts with the two helices, α1 and α2. The two helices are nearly parallel to each other and to the plane of the large β sheet. A second, smaller β sheet is formed by the C terminus of β5 and strands β6 and β7. Adapted from (159).

Processing

Encoded in the nucleus, human frataxin protein is synthesized in the cytoplasm as 210 amino acid precursor (23 kDa). The N-terminal portion contains mitochondrial import sequence (41 amino acid long) that directs its transport into the mitochondrial matrix (155) (156). Here, it is converted into the functional mature form through the two-step proteolytic maturation mediated by mitochondrial processing peptidase (MPP) enzymes. An initial cleavage, within Gly41 and Leu42, generates the intermediate form (iFXN; 19 kDa) by removing the transit peptide (160). However, longer intermediate form may be produced in some normal cells when the normal processing is impaired (161).

The second site of cleavage has longly been controversial (162) (160) (163) (164). Based on the putative second site, three mature forms have been proposed by different *in vitro* studies: m_{56}-FXN (Ala55 and Ser56; 17 kDa) (162), m_{81}-FXN (Lys80 and Ser81; 14.2 kDa) (160), and m_{78}-FXN (Asn77 and Leu78; 14.5 kDa) (163). Moreover, both m_{81}-FXN and m_{78}-FXN has been reported as degradation products (d-FXN) in human heart extracts (165) (163) (158) (162). In addition, further confusion turned out from the abnormal mobility observed on SDS-PAGE for yeast, murine, and human frataxin, attributed to its acidic nature (164) (166) (162) (167). Lastly, Schmucker and colleagues provided greater clarity that the endogenous mature frataxin corresponds to m_{81}-FXN, supporting previous results (160). Most importantly, they demonstrated m_{81}-FXN capability to rescue the survival of deficient murine fibroblasts. (Figure 18) (168).

The two-step processing by MPP (mitochondrial processing peptidase) should also have regulatory function, since it has been demonstrated in rat liver mitochondria that the second cleavage is finely tuned. While the precursor is rapidly cleaved, the intermediate cleavage is slower, limiting m_{81}-FXN rate in certain conditions (162) (161).

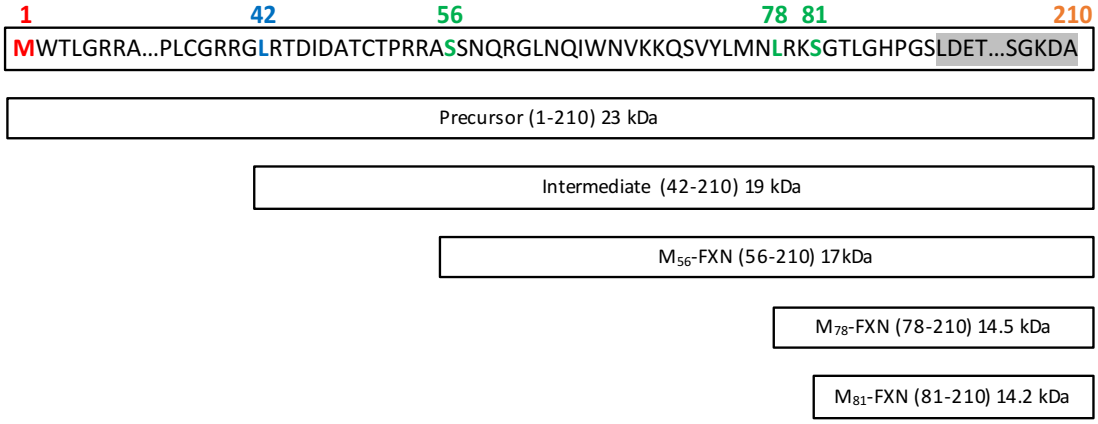

Figure 18 – **Schematic representation of the different forms of frataxin.** The precursor is targeted to the mitochondrion and undergoes a two-step maturation process. The intermediate and the three described mature forms are represented. The conserved globular domain which starts at amino acid 90 is indicated by the gray area. Scheme is not drown in scale.

The mystery of frataxin cellular function

Frataxin down-regulation causes deregulation of the mitochondrial iron metabolism pathway and subsequent mitochondrial iron loading. Three major pathways are involved: iron-sulfur cluster (ISC) biosynthesis, haem biogenesis and mitochondrial iron storage (105). The various proposed molecular functions derive from the capability of the protein to bind iron (Figure 19).

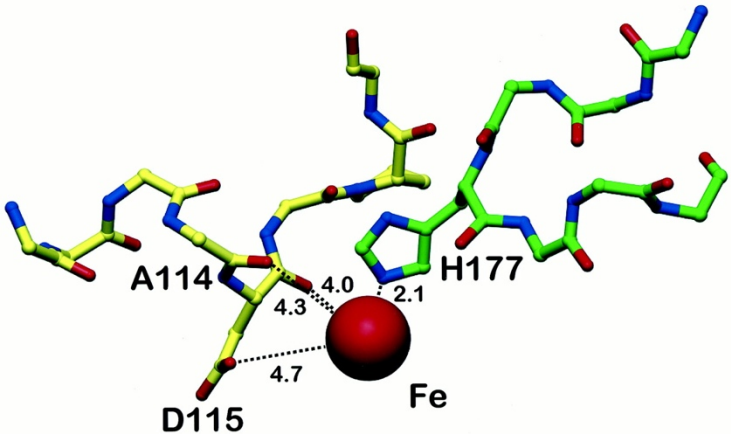

Figure 19 - **Iron binding.** Adjacent frataxin molecules are colored green and yellow. Iron, depicted as a red sphere, is coordinated to His-177. Distances in Å (dotted lines) are between the nucleus of iron and its closest neighbours. Adapted from (159).

Initially, due to the observation of Yfh1 oligomers and multimers with ferroxidase activity in presence of an excess of iron, frataxin has been proposed as iron storage protein. That same activity prompted the protective function from iron-

mediated oxidative stress resulting from toxic reactive oxygen species (ROS) and abnormal mitochondrial deposits (103). Some evidence suggests iron chaperone or "donor" function in iron-dependent reactios, such as ISC and heam biosynthesis. Related alternative hypothesis indicates frataxin as metabolic switch, shifting iron from one metabolic pathway (e.g. ISC biosynthesis) to another (e.g. heam biosynthesis) (169). Interestingly, CyaY may function as iron sensor inhibiting the rate of ISC biosynthesis in case of both high iron availability and low disposal of downstream ISC apo-receptor. The latter remains to be demonstrated in eukaryotes (170).

In summary, although its primary function is still debated (171), mature frataxin is a key component of the iron-sulphur cluster (172) biosynthetic apparatus (173) (168) (174), which provides the essential cofactor to all ISC-dependent enzymes of the cell (175) (176). As consequence of insufficient *FXN* expression, defective ISC biosynthesis triggers a series of vicious cycles leading to deregulated intracellular iron homeostasis, impaired mitochondrial electron transport chain and higher sensitivity to trigger oxidant- and stress-induced cell death (177) (178) (179). Despite many studies, the rationale behind the impact of frataxin deficiency is still poorly understood.

Therapeutical approaches in FRDA: goals and objectives

Numerous therapeutical approaches in FRDA are currently in various phases of development and testing, and may broadly be classified into two major categories: drugs aiming to treat typical FRDA manifestation and those intended to increase frataxin content (180) (181). As far as our interest on protein up-regulation, here only treatments aiming to up-regulate frataxin protein content and mRNA transcription will be presented.

Erythropoietin (EPO) is a glycoprotein produced in the kidney as hypoxia response and it is currently accepted for chronic anemia treatment. Moreover, it has cyto-protective and tissue regeneration properties. Previous study reported that human erythropoietin raises the amount of frataxin protein without increasing FXN mRNA levels (182). The observed increase was hypothesized to be attributable to a post-translational mechanism, as by influencing frataxin protein half-life (183). However, the exact pathway by which erythropoietin upregulates frataxin remains unknown and a role in protein translation process cannot be ruled out.

Histon deacetylase (HDAC) inhibitors are chromatin-modifying enzymes, reported to revert *FXN* silencing by interfering with hypoacetylation and hypermethylation of histones, usually seen in association to GAA repeat expansion in FRDA (184) (185). Nicotinamide, also known as vitamin B_3, treatment was associated with *FXN* mRNA and protein levels upregulation to levels seen in asymptomatic heterozygous carriers. However, adverse events were often encountered upon dose escalation, thus suggesting that dosage should be individually adjusted (181) (150). Similarly, RG2833, another HDAC inhibitor, up-regulates *FXN* mRNA, but it is poorly adsorbed in central nervous system. In addition, a possible conversion into a toxic metabolite led to the premature termination of its phase II trial (185). To date, a new generation of molecules is under development to enhance potency as well as to prevent formation of dangerous metabolites.

Resveratrol is a natural polyphenol with antioxidant, anticancer, and neuroprotective properties and it was found to up-regulate frataxin in both FRDA patient-derived cells and mouse model (186). However, it presents several important side effects as well as delivery issues.

Interferon-γ is an endogenous cytokine involved in both immune response and iron redistribution upon viral infection (187) (188). It is a currently FDA-approved treatment for chronic granulomatous disease and severe malignant osteopetrosis (180). Interferon-γ has been reported to enhance FXN expression in FRDA fibroblasts as well as in dorsal root ganglia of mouse model, probably by enhancing transcription and or stabilizing *FXN* mRNA (189). However, several pilot studies in phase III trials showed no statistical significant differences between individuals taking interferon-γ and placebo.

New promising approaches are represented by **gene therapy**, **gene and protein modulation**, and **protein replacement**.

A novel delivery system, known as trans-activator transcription (57), represents an innovative delivery approach. TAT is short peptidic fragment able to reach multiple tissue and cellular organelles, including mitochondrion. A knock-out mice injection of engineered small fusion-protein (TAT-FXN) resulted in a prolonged life span (up to 53% longer than untreated mice) and an improvement of cardiac function with increased heart rate, growth velocity, and cardiac output. Treated mice showed enhanced cardiac aconitase levels suggesting improvement in iron-sulfur dependent protein regulation (190). Therefore, exogenous protein replacement of missing frataxin represent a promising approach for therapeutic intervention in FRDA. Clinical trials are expected to begin within a few years.

An analogous approach, recombinant *FXN* mRNA nanoparticles, avoiding naked mRNA degradation, was successfully delivered in mice, resulting in effective frataxin translation. However, further optimization is still required (191).

The mechanism of frataxin degradation is not fully elucidated. Benini and colleagues recently identified RNF126 as selective E3 ligase responsible of frataxin ubiquitination and therefore degradation (192). Therefore, hopefully down-regulation of FXN breakdown should also represent a novel potential therapeutical approach.

Recently, oligonucleotide-based approach has got off an auspicious start in RNA therapeutics with the latest FDA approval of nusinersen in Spinal Muscular Atrophy (SMA) (193) (194) (195). Even though the mechanism trigging *FXN* transcriptional silencing is still incompletely elucidated, chromatin modification it is well known to

elicit FXN expression repression. In FRDA the pathological expanded GGA triplet repeats could bind the complementary genomic DNA, resulting in the formation of R-loops that infer with transcription. Oligonucleotides (synthetic duplex RNAs) targeting the expanded mRNA repetitive region, by obstructing interaction with genomic DNA result in frataxin up-regulation to normal levels (4-6fold increase) by normalizing *FXN* gene expression (3-4folds) in patient-derived cells. Employment of single-stranded locked nucleic acid (LNA) oligonucleotide has been also revealed effective.

Lastly, oligonucleotides may be applied on antisense lncRNAs degradation (FAST-1), also responsible of FXN repression, if coupled with RNAse-H enzyme that catalyzes RNA cleavage and degradation (51) (196).

Oligonucleotide-based strategy could theoretically be targeted also on downstream events, such as gene methylation as well as miRNAs suppression (120). To date, no clinical candidates have been defined, even though PGC1α and NRF2 down-regulation have been recently proposed (180).

Up to date, the most promising potential therapy to ameliorate or restore frataxin levels in patients is the gene therapy. The rescue of frataxin loss may be achieved either by gene editing or by the delivery of wild type FXN by intravenous administration of viral vectors. In the former case, CRISPR-Cas9 and related technology were successfully applied in mice (197) (198). In the latter, AAV9-frataxin injection reverses the functional features of cardiomyopathy when injected in pre-symtomatic - cardiac frataxin - knock-out mice. More importantly, same results have been reported with those experiencing heart failure (199). Moreover, increased frataxin expression reduces cardiac hypertrophy, and prolong life span when compared with untreated mice. However, the potential risk of over-replacement is still the major concern (200).

In addition, infection with TALE (transcription activator-like effector) proteins coupled with a TAD (transcription activation domain) specifically directed at the human frataxin promoter leads to a 2fold increase in the expression of frataxin, both mature mRNA and protein content (201). However, immunological tolerance to specific proteins is still an open issue of this method.

The serious risk of aberrant overexpression is shared by all above mentioned new promising strategies. Controversial results have been published on the effectiveness of

overexpression itself. While frataxin up-regulation shows evident phenotype amelioration in different disease models (200) (202) (203), it may even be toxic due to its disturbing effect on Fe-S biogenesis and increasing oxidative stress (204) (205). Taking advantage of the HEK-c*FXN* inducible model (206) effects of overexpression have been monitored over time. Surprisingly, it led to a prominent decreased ATP production and an even more pronounced oxidative stress (205). It is worth noting that negative outcomes refers to a healthy environment, since HEK cells normally produce frataxin. Indeed, Navarro and colleagues, observed deleterious effects at the biochemical, histological and behavioural levels in transgenic overexpressing flies, yet at the same time also indicated complete rescue of aconitase activity in knockdown flies' mutants (204). Thus, the understanding of the exact amount of frataxin required to revert patient phenotypes without any side effects still remain a crucial unmet issue. These results may further strengthen the use of SINEUPs as potentially ideal therapeutic strategy to restore physiological levels.

MATERIAL AND METHODS

OLIGONUCLEOTIDES

The complete list of oligonucleotides used for cloning, quantitative real-time PCR experiments and lentivirus titration is included in Supplementary Information (Figure S1).

CONSTRUCTS

SINEUP-FXN were generated using pcDNA 3.1(-)- Δ5'-AS Uchl1 as backbone (82) lacking the region of overlap (BD) to Uchl1 and retaining AS Uchl1 ED.

BDs were designed in antisense orientation to the most widely expressed human *FXN* mRNA, targeting the first or the second AUG, with longer or shorter overlapping region, following pairing roles of S/AS Uchl1 (82). Oligonucleotides were annealed and cloned into recipient plasmid.

For the plasmid-driven expression of miniSINEUP-FXN, we constructed a DNA cassette containing the H1 RNA polymerase III promoter followed by the BDs of SINEUP-FXN of interest, the invSINEB2 of AS Uchl1 (95), and a minimal polyadenylation signal (207). The cassette was cloned into the AseI restriction site of pEGFP-C2 vector (Clontech), with the H1 promoter oriented in the opposite direction with respect to the CMV promoter. The resulting family of plasmids is designed to constitutively express a miniSINEUP of interest and the enhanced Green Fluorescent Protein (EGFP) as a reporter, and is renamed miniSINEUP_DUAL.

All SINEUP and miniSINEUP-containing vectors were verified by sequencing.

CELL LINES

HEK 293T/17 were obtained from ATCC® (Cat. No. CRL-11268™) and maintained in culture with Dulbecco's Modified Eagle Medium (DMEM) GlutaMAX™ Supplement (Gibco by Life Technologies, Cat. No. 41090-028) supplemented with 10% fetal bovine serum (Euroclone, Cat. No. ECS0180L) and 1% antibiotics (penicillin/streptomycin), as suggested by the vendor.

SH-SY5Y cells were obtained from ATCC® (Cat. No. CRL-2266™) and maintained in culture with RPMI supplemented with GlutaMAX, 10% fetal bovine serum not inactivated (Euroclone, Cat. No. ECS0180L) and 1% antibiotics (penicillin/streptomycin).

Human GM04078 fibroblasts, from a clinically affected FRDA patient homozygous for the GAA expansion in the *FXN* gene with alleles of approximately 541 and 420 repeats, were obtained from NIGMS Human Genetic Repository, Coriell Institute for Medical Research (Camden, NJ, USA). Cells were maintained in culture with Minimum Essential Medium (41) HEPES, GlutaMAX™ Supplement (Gibco by Life Technologies, Cat. No. 42360024) supplemented with 15% fetal bovine serum heat inactivated (Euroclone, Cat. No. ECS0180L), 1% non-essential amino acids and 1% antibiotics (penicillin/streptomycin).

Human GM16214 lymphoblasts from a clinically affected FRDA patient homozygous for the GAA expansion in the *FXN* gene with alleles containing approximately 700 and 600 repeats and human GM16215 lymphoblasts from a clinically unaffected parent with only one allele containing 830 repeats (mother of affected GM16214), were obtained from NIGMS Human Genetic Repository, Coriell Institute for Medical Research (Camden, NJ, USA). Both cell lines were maintained in culture with RPMI 1640 Medium (Euroclone ECB9006) supplemented with 15% fetal bovine serum heat inactivated (Hyclone CHA1115L),100 U/mg penicillin/streptomycin (Euroclone ECB3001D) and 2 mM L-glutamine (Euroclone ECB3000D).

TRANSFECTIONS

HEK 293T/17 and SH-SY5Y cells were plated in 6 well-plates the day before transfection at 60% confluency ($4x10^5$ cells/well) and transfected with 4 μg of SINEUPs or miniSINEUPs encoding plasmids using Lipofectamine® 2000 (Invitrogen™ by Life Technologies, Cat. No. 11668019) and following manufacturer's instructions. Cells were collected 48 hours after transfection. RNA and protein were obtained from the same transfection in each replica.

RECOMBINANT LENTIVIRUS PRODUCTION AND TITRATION.

Selected miniSINEUP-FXN were cloned into a TetON-controlled lentiviral vector, based on the pCCLsin.PPT.hPGK.EGFP.Wpre backbone (208). Recombinant third generation self-inactivating (SIN) lentiviruses were produced and titrated as previously described (208). Briefly, HEK 293T/17 cells were transfected using LipoD293™ DNA In Vitro Transfection Reagent (SignaGen Laboratories, Cat. No. SL100668-5) with the transfer vector plasmid plus three auxiliary plasmids (pMD2 VSV.G; pMDLg/pRRE; pRSV-REV). The conditioned medium was collected after 24 and 48hs, filtered and ultra-centrifuged at 50000 RCF on a fixed angle rotor (JA 25.50 Beckmann Coulter) for 165 min at 4°C. Viral pellets were resuspended in DPBS without BSA (Gibco, Cat. No. 14190250). miniSINEUP-expressing lentiviral particles were titrated by Real Time quantitative PCR after infection of HEK293T/17 cells. One end-point fluorescence-titrated lentivirus was included in each PCR titration session and PCR-titers were converted into fluorescence-equivalent titers throughout the study.

INFECTION OF HUMAN FRDA FIBROBLASTS

At least 8.5 *10^5 FRDA fibroblasts were plated onto a 100 mm plate with medium supplemented with Hexadimethrine bromide at a final concentration of 0.009 μg/ml and infected with the appropriate miniSINEUP-expressing lentiviral vector (multiplicity of infection, MOI 10) together with trans-activating lentiviral vector (MOI 10). Cells were treated with doxycycline (1 ¥ g/ml) every 48 hours after transduction and collected after 4 days of treatment. RNA and proteins were obtained from the same infection in each replica.

STABLE TRANSFECTIONS OF FRDA LYMPHOBLASTS

FRDA GM16214 lymphoblasts were transfected by electroporation as already described (156). Briefly, 15x10^6 cells were incubated in 0.4 ml of RPMI 1640 for 10 min on ice with 30 μg of pMiniSINEUP-FXN constructs or relative empty vector. After electroporation at 260 V/950 microfarads (Bio-Rad GenePulser II), cells were left 30 min on ice and resuspended in 5 ml of complete RPMI 1640 medium. After 4 h, live cells were recovered by Lympholyte-Human (Cedarlane Laboratories) density

gradient centrifugation and re-plated. Stable transfectants were obtained from cultures in selection medium containing 600 μg /ml G418 (Sigma) for at least 15 days.

ACONITASE ASSAYS

Whole-cell extracts from GM16215 lymphoblasts, GM16214 lymphoblasts and GM16214 lymphoblasts stably expressing miniSINEUPs were prepared in ice-cold CelLytic M buffer (Sigma–Aldrich) supplemented with 2 mM sodium citrate and Complete EDTA-free protease inhibitor cocktail (Roche Diagnostic). Spectrophotometric aconitase assays were performed at 25°C with 100 μg of cell extracts using the BIOXYTECH Aconitase-340 Assay (OxisResearch 21041). Spectrophotometric citrate synthase activities were assessed at 25°C with 10 μg of cell extracts using the Citrate Synthase Assay Kit (Sigma–Aldrich CS0720). For the calculation of the activities, one unit of enzyme was expressed as the amount of protein that converted 1 μmol of substrate per minute at 25°C.

WESTERN BLOT

Transfected HEK 293T/17 and SH-SY5Y cells were washed twice and collected in PBS 1X. Cell pellets were directly lysed in 300 μL of Laemmli sample buffer, briefly sonicated, boiled and loaded 10-20 μl/each sample on 10-15% SDS-PAGE gel.

Infected human FRDA fibroblasts were collected in PBS 1X. Cell pellets were dissolved in 100 μL of Laemmli sample buffer, briefly sonicated, boiled and loaded 20 μl/each sample on 10-15% SDS-PAGE gel.

Proteins were transferred to nitrocellulose membrane (Amersham™, Cat. No. GEH10600001) for 1 hour at 100V. Membranes were blocked with 3% Bovine Serum Albumin (SIGMA, Cat. No. A2058) in TBST 1X solution for 1 hour at room temperature and then incubated with primary antibodies. The following antibodies were used: anti-FXN 4μg/ml (Abcam, Cat. No. 18A5DB1) overnight at 4°C followed by 1-hour incubation at room temperature with horseradish peroxidase-conjugated goat anti-mouse antibody (DakoCytomation, Glostrup, Denmark), anti-β-Actin-Peroxidase 1:20000 (SIGMA, Cat. No. A3854). Proteins of interest were visualized with the Amersham™ ECL™ Detection Reagents (GE Healthcare by SIGMA, Cat. No. RPN2105) or LiteAblot TURBO Extra-Sensitive Chemioluminescent Substrate

(EuroClone, Cat. No. EMP012001). Western blotting images were acquired using with Alliance LD2-77WL system (Uvitec, Cambridge) and band intensity was calculated using *ImageJ* software.

FRDA lymphoblasts extracts were prepared in ice-cold lysis buffer (50 mM Tris-HCl pH 7.5, 150 mM NaCl, 1% Igepal CA-630, 5 mM EDTA, 5 mM EGTA) supplemented with Complete Protease Inhibitor Cocktail (Roche Diagnostics). Lysates were clarified by centrifugation, supernatants were mixed with 10× Laemmli sample buffer and boiled for 5 min at 95°C. 50 μg of protein extracts were resolved by 12% SDS-PAGE gels and transferred to 0.2 μM nitrocellulose membrane (Trans-Blot Turbo Transfer pack, Bio-Rad). Membranes were blocked with 5% non-fat dry milk in PBS/0.1% Tween 20 and incubated with the indicated primary and secondary antibodies: mAb anti-FXN (MAB-10876 Immunological Sciences), mAb anti-α-tubulin (clone DM1A, Sigma-Aldrich) and secondary antibody horseradish peroxidase (HRP)-conjugated goat anti-mouse (Thermo Fisher Scientific). The immunoreactive bands were detected by enhanced chemiluminescence (ECL, GE Healthcare) and imaged with a ChemiDoc XRS system (Bio-Rad). Densitometric analysis was performed using ImageLab 5.2 software (Bio-Rad).

RNA ISOLATION, REVERSE TRANSCRIPTION AND QUANTITATIVE RT-PCR

Total RNA was extracted from cell pellets using TRIzol® Reagent (Thermo Fisher, Cat. No. 15596026) and following manufacturer's instructions.

For HEK 293T/17, SH-SY5Y and GM04078 fibroblasts, RNA samples were subjected to TURBO™ DNase (Invitrogen, Cat. No. AM1907) treatment, to avoid plasmid DNA contamination. A total of 1 μg of RNA was subjected to retrotranscription using iScript™cDNA Synthesis Kit (Bio-Rad, Cat. No. 1708890), according to manufacturer's instructions. qRT-PCR was carried out using SYBR green fluorescent dye (iQ SYBR Green Super Mix, Bio-Rad, Cat. No. 1708884) and an iCycler IQ Real time PCR System (Bio-Rad). The reactions were performed on diluted cDNA (1:8). Human GAPDH was used as normalizing control in all qRT-PCR experiments.

For GM16214 and GM16215 lymphoblasts, cDNA was prepared using the SuperScript VILO cDNA synthesis kit (Thermo Fisher). Levels of human *FXN* mRNA

and miniSINEUPs RNA expression were assessed by real-time qPCR using the StepOne Plus Instrument (Applied Biosystems), normalized with the control genes expression. The assays were performed using the TaqMan primers listed in Sup.Fig.1 (Applied Biosystems). GUSB, GAPDH and ACT were used as control housekeeping genes.

The amplified transcripts were quantified using the comparative Ct method and the differences in gene expression were presented as normalized fold expression with ΔΔCt method (209).

STATISTICAL ANALYSIS

In all experiments the significance of differences between groups was evaluated by unpaired t-test with Welch's correction, $p<0.05$ were considered significant. Quantitative data are presented as mean ± SEM of at least three independent experiments.

RESULTS

1. SYNTHETIC SINEUP-FXN: DESIGN AND SCREENING

Since SINEUPs target the mRNA sequence around the starting AUG, the precise knowledge of the real sites of transcription initiation is crucial, especially in cells and tissues relevant for the gene of interest and its associated disease. In our experience, we have found that the annotation of the reference sequence is often not representative of the cell-type-specific usage of transcription start sites (TSSs) and of 5'UTRs in endogenous mRNAs. To build *FXN*-specific SINEUPs, we interrogated FANTOM5 collection of Cap Analysis of Gene Expression (CAGE) datasets, which represents the widest catalogue of annotated promoters and TSSs in mammalian samples (57). Using the Zenbu Genome Browser Tool for data visualization (210), we monitored TSS usage at the human *FXN* locus with a specific focus on human cells lines and tissues relevant for FRDA (Figure 20).

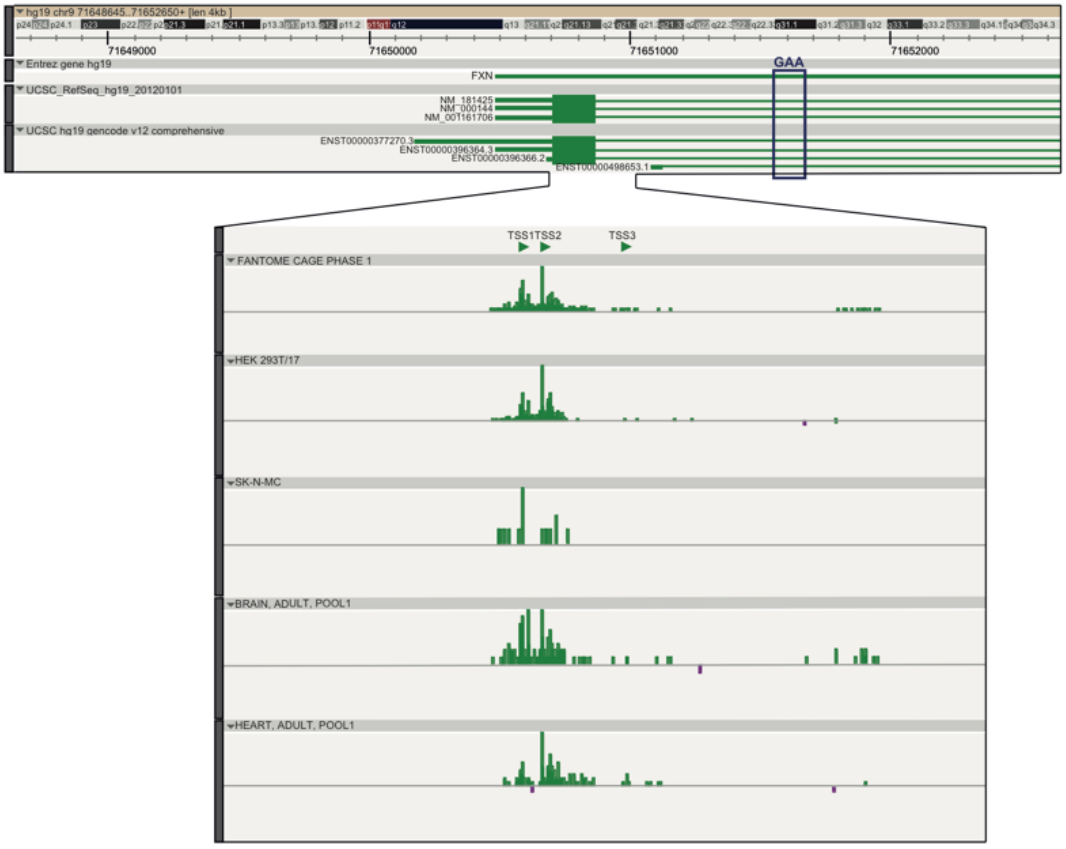

Figure 201 – **FXN locus view.** ZENBU genome browser view of FXN locus showing FXN alternative TSS usage (TSS1, TSS2 and TSS3) in FANTOM5 samples and selected libraries. FXN reference sequences and Gencode annotated transcripts are indicated. The genomic position of the GAA triplet.

Unexpectedly, we found that the annotated reference sequences are poorly representative in human samples. Rather, at least two additional variants (TSS1 and TSS2) of human *FXN* mRNA exist that are positioned more closely to the initiating AUG and are supported by "robust" statistical definition of promoters in FANTOM5. The use of these alternative TSSs finds further confirmation in the Gencode catalogue of transcripts (ENST00000396366, ENST00000498653) (Figure 20).

Based on TSS analysis, we designed FXN-specific SINEUPs (SINEUP-FXN) in antisense orientation to the most widely expressed variant of human *FXN* mRNA and following the pairing rules of S/AS Uchl1 (82). BDs were initially designed according to the canonical -40/+32 anatomy (95) and its shortest -40/+4 BD variant (211) (100). Although *FXN* mRNA has a very short 5' UTRs, we included the -40 versions of SINEUPs to investigate whether extra sequences at the 5' of the overlapping region could influence SINEUP activity. We then generated additional SINEUP-FXN by trimming BD sequences at both extremes, following a strategy previously used to optimize SINEUPs for overexpressed mRNAs but not yet tested for endogenous genes. Finally, since another methionine (M76) is positioned in frame in the second exon after the GAA-triplets repeat, we designed three additional BDs overlapping this sequence, immediately after or across the exon I/exon II boundary (Figure 21).

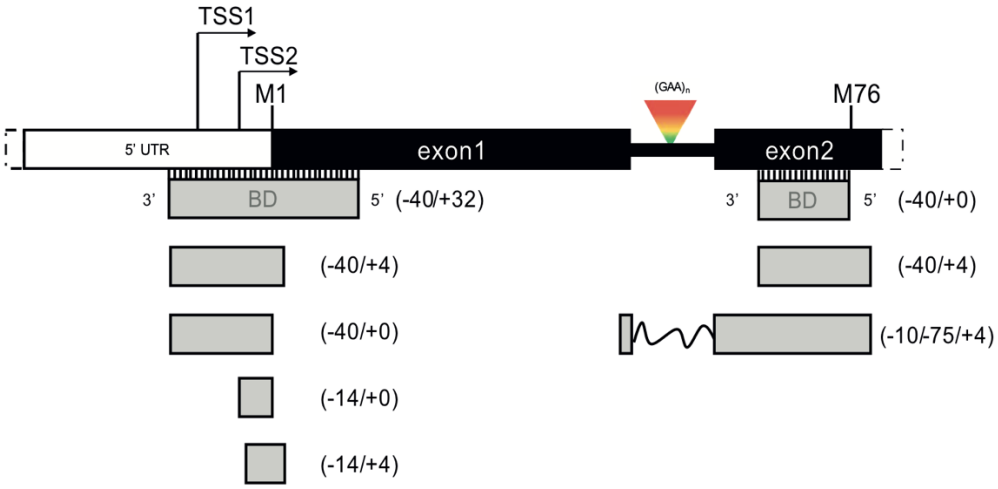

Figure 21. **Scheme of human *FXN* gene (5' end) and BDs design of synthetic SINEUP-FXN.**

Each BD variant was combined with the ED of the natural AS Uchl1 that so far represents the most potent translational activation domain for SINEUPs (Figure 22). To screen the activity of SINEUP-FXN, we took advantage of HEK 293T/17 cells which own the same TSSs of cells relevant for the pathology and have been proven to support SINEUP activity of a variety of SINEUPs targeting endogenous genes (95) (unpublished results).

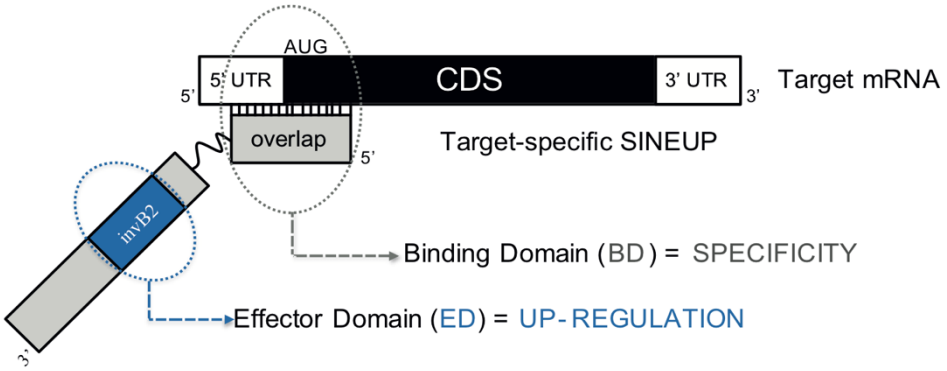

Figure 22 - **Schematic representation of SINEUPs functional domains.** The binding domain (overlap) provides SINEUP specificity and is in antisense orientation to the sense protein-coding mRNA (Target). The inverted SINEB2 element (invB2) is the effector domain (blue) and confers enhancement of protein synthesis.

HEK 293T/17 cells were transfected with SINEUP-FXN (+SINEUP) or an empty control vector (-SINEUP). SINEUP activity was estimated as fold changes in protein levels in +SINEUP compared to –SINEUP conditions by western blotting (Figure 23/a). qRT-PCR quantification of *FXN* mRNA was carried out to confirm SINEUPs act at post-transcriptional levels (Figure 23b).

We found that SINEUP activity varies significantly according to the overlapping region. When SINEUP-FXN were designed around the initiating AUG as transcribed from both TSS1 and TSS2 and maintaining extra sequences at the 5' end, we found that the activity is regulated by the length of overlap to the coding sequence (CDS). In particular, the canonical configuration of -40/+32 showed no effects on frataxin levels (data not shown). Instead, BDs with minimal (-40/+4) or no (-40/+0) overlap to the CDS induced up-regulation of mature frataxin in the range of 1.4-fold. Minimal up-regulation was also obtained with SINEUPs targeting 5'UTRs from TSS1, albeit with some variability. When the overlapping region corresponds exactly to the 5'UTR from TSS2, as it is the case for -14/+0 and -14/+4 configurations, SINEUPs reached the highest potency (1.7- to 2-fold increase).

When BD was designed at -40/+4 (exon 2) and -10/-75/+4 (exon1-exon2) relative to internal in frame M76-AUG, we could not measure any increment in frataxin protein relative to controls. Instead, when the BD did not overlap the M76-AUG sequence but retained a complementarity to its preceding regions, as in the -40/+0 (M76) configuration, it generated a SINEUP that could substantially up-regulate frataxin up to 1.5-fold (Figure 23a)

In summary, we successfully designed synthetic SINEUPs able to increase the quantity of frataxin protein with no effects on its mRNA levels (Figure 23b). SINEUP-mediated up-regulation was in the range of 1.4- to 2.4-fold increase (Figure 23a).

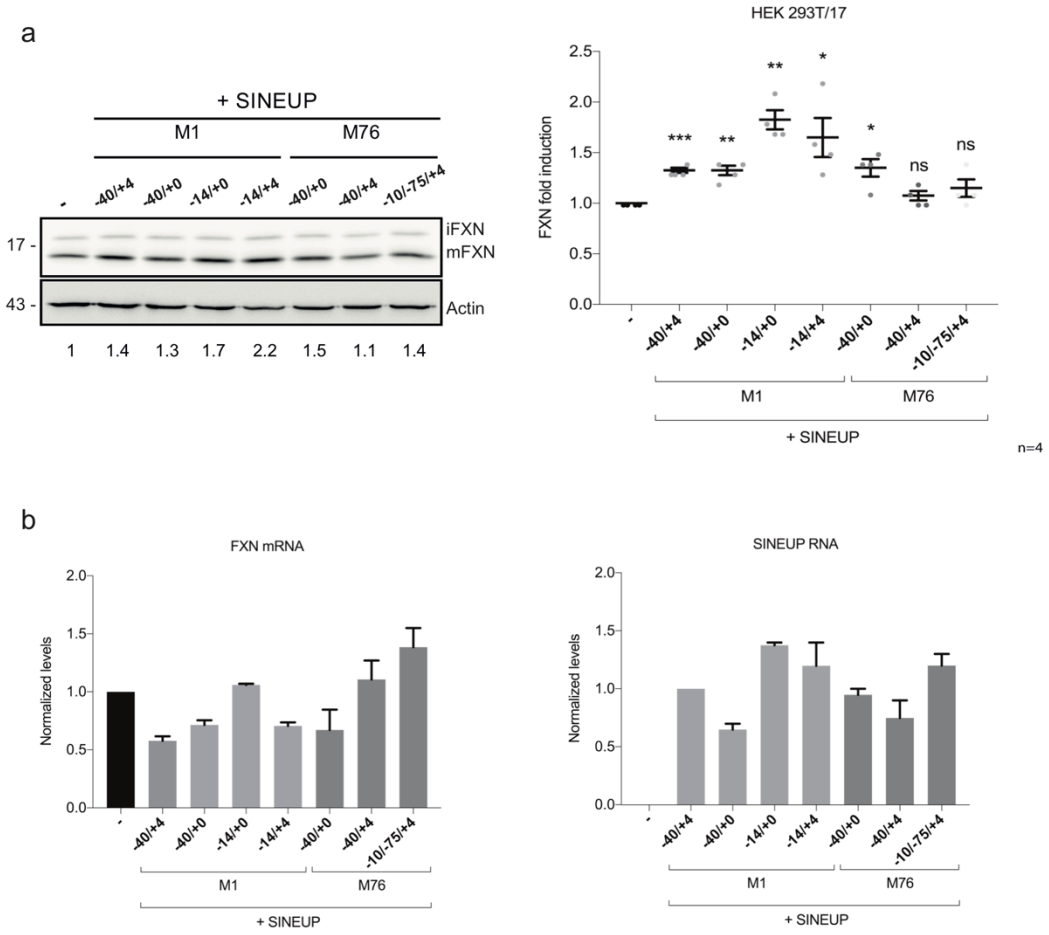

Figure 23 – SINEUP-fxn screening a) SINEUP-FXN variants were screened in HEK 293T/17 cell line. Control cells were transfected with empty vector. Protein levels were analyzed by western blot with anti-FXN antibody and SINEUP activity was calculated as increase in protein quantities relative to empty control samples (fold changes are shown). Summary of data on SINEUP activity (bottom), as frataxin protein quantities in HEK293T/17 cells. Data indicate mean ± SEM and are representative of four independent experiments. *p* values are calculated by unpaired t-test with Welch's correction. *, p<0,05; **, p<0,01, ***, p<0,001; ns, non-significant; b) RNA levels were analyzed by qRT- PCR with target-specific and SINEUP primers, respectively. In all conditions, *FXN* mRNA quantities were stable (ns, p > 0.05).

2. SYNTHETIC MINISINEUP-FXN ARE ACTIVE *IN VITRO*

Synthetic SINEUPs derived from natural AS Uchl1 RNA are about 1200 nucleotides long. For their potential usage as RNA therapeutics, shorter functional molecules retaining SINEUP translation enhancement activity are needed. Therefore, each BD variant of the most effective SINEUP-FXN was combined exclusively with the invSINEB2 (ED) sequence, producing ≈250 nucleotides long transcripts (miniSINEUP-FXN) (Figure 24). Four different BDs were selected (-40/+0, -14/+4, 14/+0 on M1 and -40/+0 on M76), covering various anatomies of overlap to *FXN* mRNA.

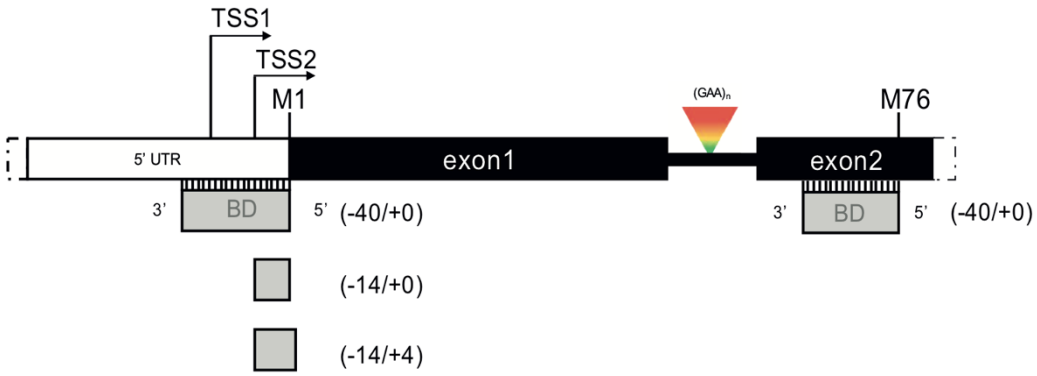

Figure 24 - **Schematic representation of miniSINEUPs functional domains and design.**

miniSINEUPs were then tested in HEK293T/17 cells as before. We found that SINEUP miniaturization did not alter the activity of the selected molecules towards endogenous frataxin (Figure 25), strongly supporting the modularity of SINEUPs. As one of the prominent FRDA phenotypes involves the central nervous system, we monitored miniSINEUP-FXN in human neuroblastoma SH-SY5Y cell line confirming their activities (data not shown). Moreover, to asses the specificity we performed BD blast analysis that showed three different miniSINEUPs off-targets, with different degrees of confidence. By westerblot analysis, extracts derived from replicas taken into account for the validation were tested for those off-targets, resulting in any protein perturbation as a result of putative unspecific binding (Figure S2).

Altogether, miniSINEUPs promoted protein induction consistently in the range of 1.4- to 2.0-fold, proving that miniSINEUP-FXN retain the same mechanism and efficiency of their full-length counterpart with the advantage of being shorter (Figure 25a).

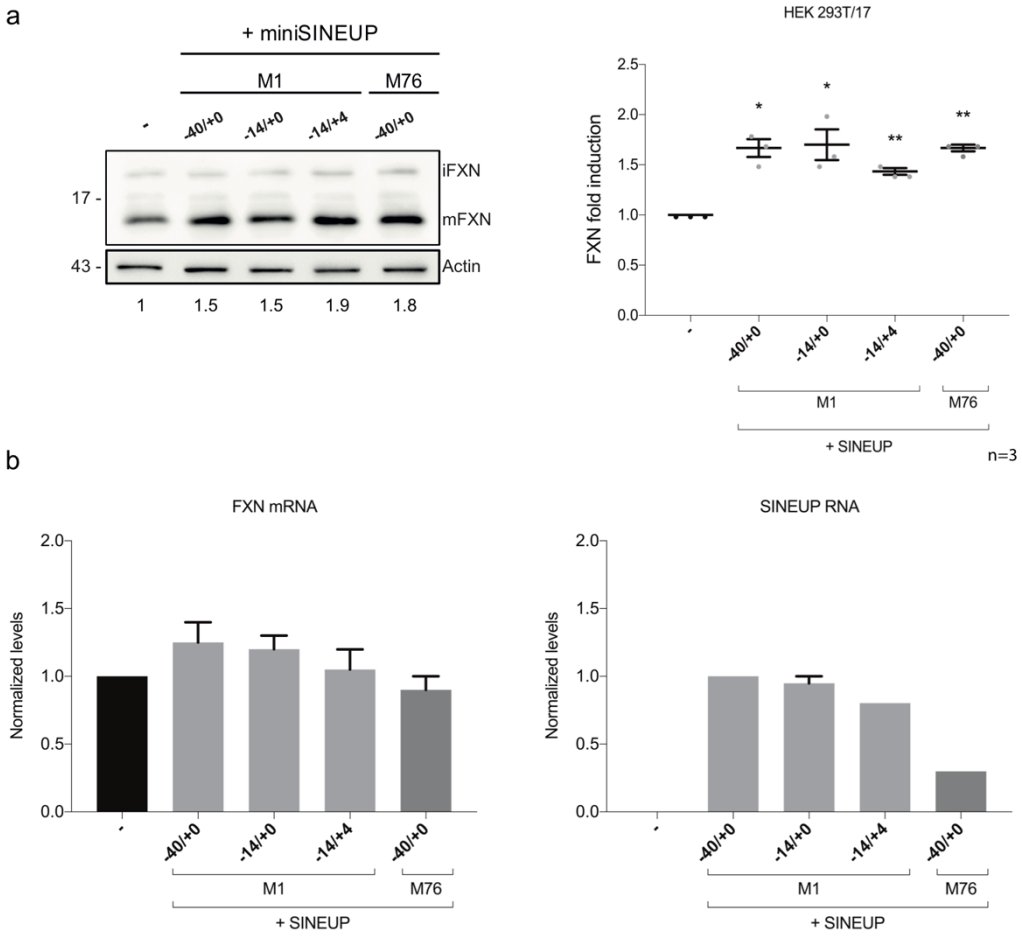

Figure 25 - **miniSINEUP-FXN activity in HEK293T/17 cell line. a)**Protein levels were analyzed by western blot with anti-FXN antibody and SINEUP activity was calculated as increase in protein levels relative to empty control samples (fold changes are shown). Summary of data on SINEUP activity (bottom), as frataxin protein quantities in HEK293T/17 cells. Data indicate mean ± SEM and are representative of four independent experiments. *p* values are calculated by unpaired t-test with Welch's correction. *, p<0,05; **, p<0,01, ***, p<0,001; **b)** RNA levels (bottom) were analyzed by qRT-PCR with target-specific and SINEUP primers, respectively. In all conditions, FXN mRNA quantities were stable (ns, p>0.05).

3. PROTEIN RESCUE IN FRDA-DERIVED FIBROBLASTS

FRDA-derived cells represent the most relevant cellular model to test therapeutic strategies for patients, as they carry the complete *FXN* locus together with pathogenic GAA-triplet repeat expansions (212). The most promising miniSINEUP-FXN were cloned into a lentiviral expression vector, in-between the doxycycline-controlled TREt promoter and BGHpA to build inducible recombinant lentiviral particles (LVs miniSINEUP-FXN). We took advantage of LVs, paired with a constitutive rtTA2S-M2 trans-activator, to drive delayed and TetON-controlled expression of miniSINEUP-FXN. An additional virus, lacking miniSINEUPs, was used as a negative control. To optimize induction conditions, lentiviral particles were transduced in SH-SY5Y cells, and miniSINEUP expression and frataxin levels were measured at different time points, following a single or a double doxycycline (Doxo) induction (Figure S3a) We found that a single Doxo stimulation, combined with tests at 48 hours, was not sufficient to trigger SINEUP-mediated increase in frataxin quantities. Instead, a double treatment protocol was crucial to promote protein induction (Figure S3b). We then applied the double-Doxo protocol to infected FRDA cells as a proof of principle that SINEUPs could be exploited in a pathological context. Among available patients-derived cells, we selected primary FRDA fibroblasts (GM04078) carrying a hyper-expansion of about 541 repeats on one allele and 420 repeats on the other, and showing an intermediate phenotype. All LV-miniSINEUPs led to an increase in frataxin quantities in the range of 1.6 to 2.1 fold (Figure 26a), as observed in cells with physiological numbers of GAA repeats. Importantly, the position of SINEUP BD relative to the GAA expansion and the presence of the pathological expansion itself did not interfere with the observed protein increase in patients' cells. Considering that GM04078 cells show reduced levels of frataxin, averaging around 40% when compared to age- or sex-matched healthy-derived cells (213), SINEUP activity rescued physiological protein quantities in this FRDA cellular model.

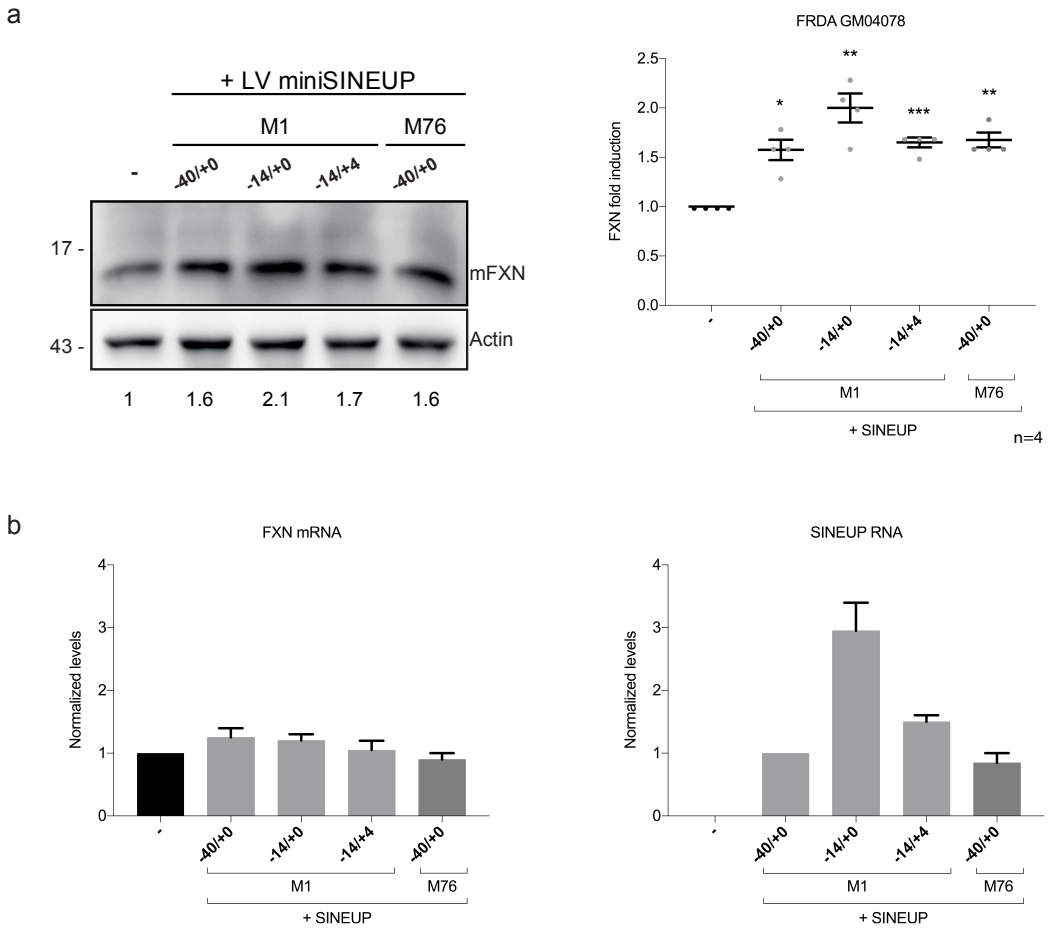

Figure 26 - **Protein rescue in frda-derived fibroblasts.** a) Primary fibroblasts derived from a FRDA patient (GM04078) were infected with inducible lentiviral vectors driving miniSINEUP-FXN expression. Control cells were infected with empty virus. Protein levels were analyzed by western blot with anti-FXN antibody and SINEUP activity was calculated as increase in protein levels relative to empty control samples (fold changes are shown). Summary of the effects of miniSINEUPs on frataxin protein quantities in FRDA cells. Data indicate mean ± SEM and are representative of four independent experiments. *p* values are calculated by unpaired t-test with Welch's correction. *, p<0,05; **, p<0,01, ***, p<0,001; b) RNA levels (bottom) were analyzed by qRT-PCR with target-specific and SINEUP primers, respectively. In all conditions, *FXN* mRNA quantities were stable (ns, p > 0.05).

4. THERAPEUTICAL PROTEIN RESCUE IN FRDA-DERIVED LYMPHOBLASTS

The ability of miniSINEUP-FXN to up-regulate endogenous frataxin levels in patient's fibroblasts prompted us to evaluate their therapeutic potential in a different FRDA cellular model. To this purpose, we employed FRDA-derived lymphoblasts, which carry the pathogenic expansion of GAA repeats and show reduced levels of the protein when compared to controls.

Frataxin-deficient lymphoblasts derived from a FRDA patient (GM16214) were stably transfected either with the miniSINEUP-FXN targeting the initiating AUG (BD -40/+0 on M1) or an empty vector as negative control. Following antibiotic selection, independent clonal subpopulations were monitored by western blot (Figure 27a) and real-time PCR analysis (Figure 27b) Frataxin protein levels were evaluated in whole cell extracts from different clones and compared to untransfected lymphoblasts. As expected, extracts from FRDA cells showed a significant deficit of *FXN* expression with respect to control lymphoblasts derived from the healthy heterozygous patient's mother. Analysis of independent miniSINEUP clones revealed a strong rescue of frataxin levels while negative control transfectants showed no significative change. In particular, we observed an upregulation ranging from 1.5- to 3.8-fold when compared to negative controls (Figure 27a). *FXN* mRNA expression was quite similar in FRDA patient cells, negative control clones and miniSINEUP-FXN clones, confirming their post-transcriptional mode of action (Figure 27b). Next, we investigated whether a miniSINEUP-FXN targeting the AUG downstream GAA expansions (BD -40/+0 on M76) could exert the same activity in these cells. To this purpose, we generated new stably transfected FRDA cells. As shown in Fig. 5a, this miniSINEUP-FXN was able to increase frataxin protein levels from 1.6- to 2.3-fold (Figure 27a). According to the translational mechanism, levels of *FXN* mRNA never showed significant changes. Collectively, data indicate that each miniSINEUP-FXN variant restored physiological levels of frataxin protein in FRDA-derived cells.

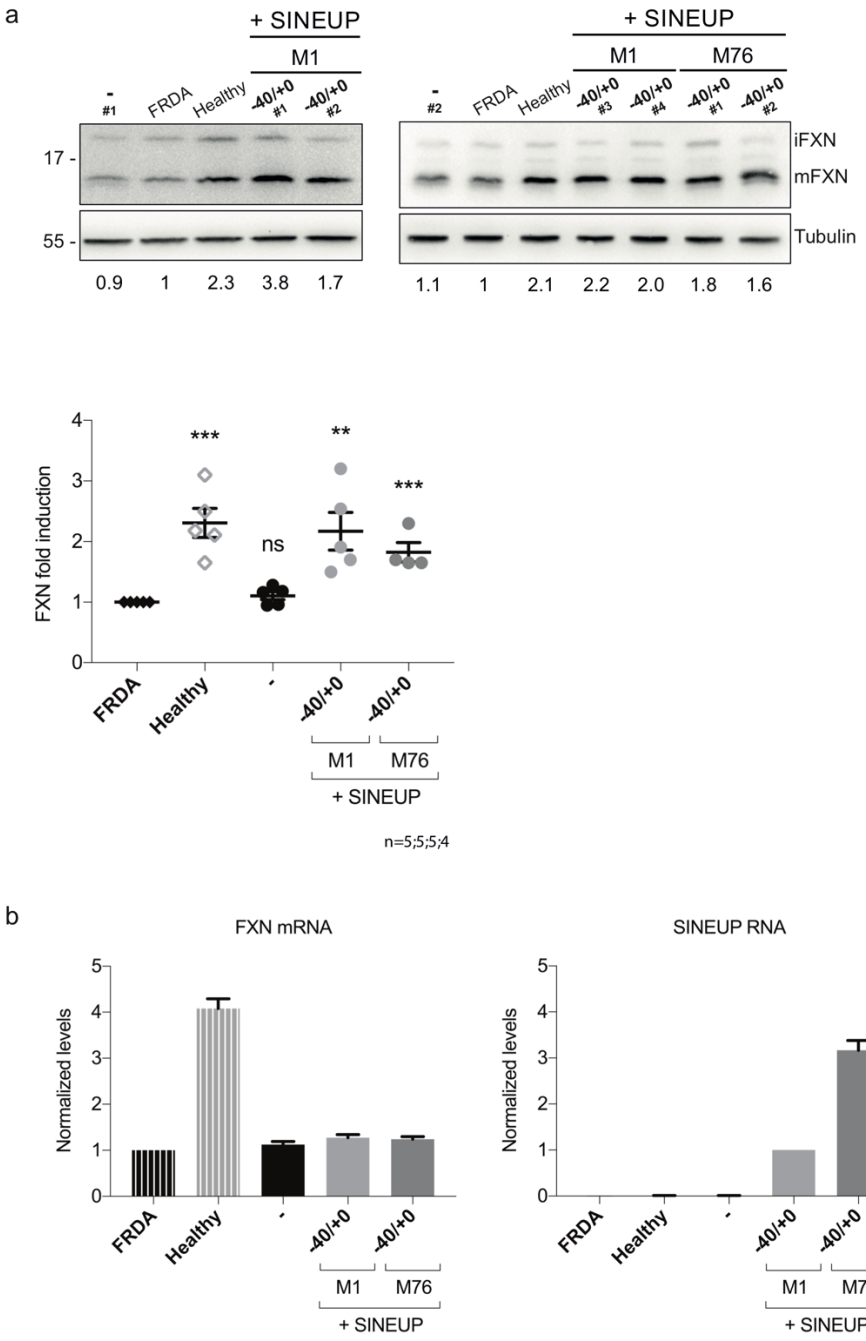

Figure 27 - **Therapeutical protein rescue in frda-derived lymphoblasts.** Lymphoblasts derived from a FRDA patient (GM16214) were stably transfected with miniSINEUP-FXN constructs targeting the M1 AUG (-40/+0) or the M76 AUG (-40/+0). Control cells were stably transfected with empty vector. a) Upper panel: representative western blot analysis with anti-FXN antibody shows protein levels in GM16214 cells (FRDA), GM16215 cells (Healthy) and different FRDA clones transfected with empty vector (-), miniSINEUP-FXN M1 (-40/+0) or M76 (-40/+0). Frataxin fold changes are relative to untransfected FRDA cells. Lower panel: summary of frataxin protein levels in untransfected and transfected cells. Data indicate mean ± SEM from at least four independent experiments. *p* values are calculated by unpaired t-test with Welch's correction (**, p<0,01, ***, p<0,001). b) RNA levels were analyzed by qRT-PCR in untransfected and transfected cells described in (a). Left panel: *FXN* mRNA quantitation. Right panel: SINEUP RNA quantitation. In all conditions referring to FRDA cells, *FXN* mRNA quantities were stable (ns, p > 0.05).

5. FUNCTIONAL RESCUE OF DISEASE-ASSOCIATED PHENOTYPE

As previously reported by several studies, frataxin-deficient cells are primarily affected by defective ISC biosynthesis. Accordingly, insufficient frataxin levels trigger a typical loss in the activity of aconitases, two different ISC-dependent enzymes located in mitochondrial and cytosolic compartments. To assess the functional impact of SINEUPs, aconitase activity was chosen as a functional readout of restoring frataxin physiological levels on the above-described FRDA stable transfectants. To evaluate the status of aconitases, enzyme activity was monitored in total lysates from miniSINEUP-FXN clones and untrasfected lymphoblasts by spectrophotometric assays. Extracts from these FRDA-derived cells exhibited a loss of aconitase activity close to 50% when compared to healthy-derived cells from the patient's parent. Total aconitase activity was strongly rescued in FRDA lymphoblasts stably expressing miniSINEUP-FXN targeting the initiating AUG (BD -40/+0 on M1) while it was not restored in negative control cells. Furthermore, the deficit was also rescued in cells expressing the miniSINEUP-FXN variant, which targets internal AUG (BD -40/+0 on M76) and is capable as well to increase mature frataxin quantities (Figure 28a) Measured as a control, activity of citrate synthase, the Krebs cycle enzyme catalyzing the preceding step respect to aconitase, but lacking ISC, did not show significant fluctuations in assayed extracts (Figure 28b). These results demonstrate the rescue of the major disease-associated phenotype in cells derived from an FRDA patient. Altogether, our data prove that a treatment with miniSINEUPs targeting frataxin achieved protein physiological levels and a consistent rescue of pathophysiological defects in FRDA-derived cells.

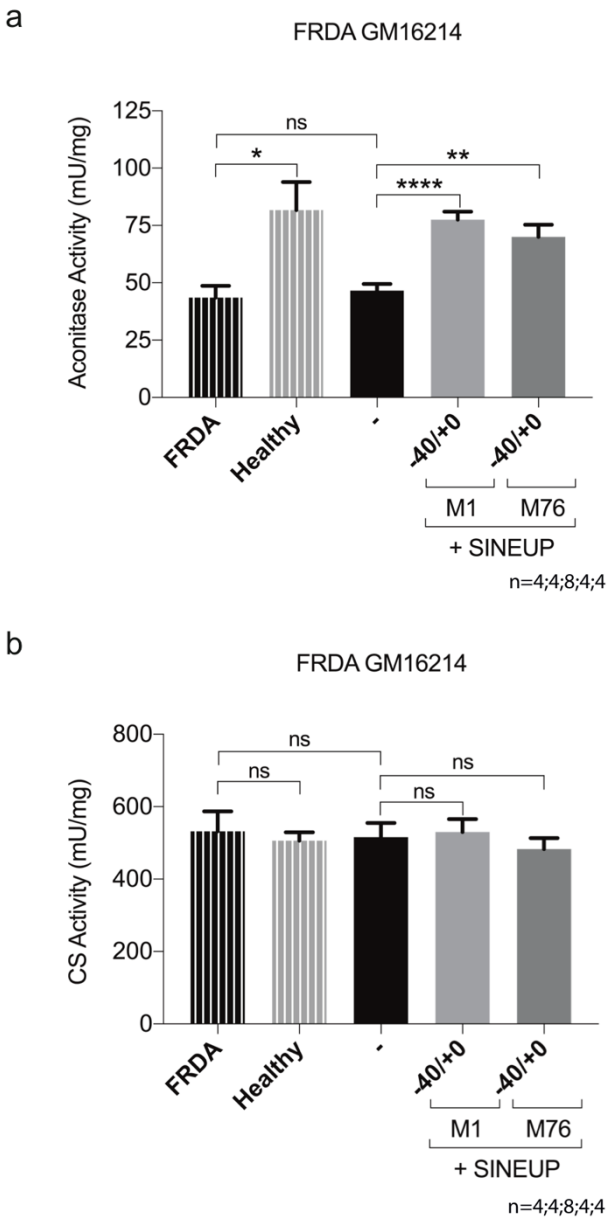

Figure 28 – **Aconitase Activity Assay.** Enzyme assays on lymphoblasts derived from a FRDA patient (GM16214) stably transfected with miniSINEUP-FXN constructs targeting the M1 AUG (-40/+0) or the M76 AUG (-40/+0). Control cells were stably transfected with empty vector. a) Aconitase assay shows enzyme activity in GM16214 cells (FRDA), GM16215 cells (Healthy) and FRDA clones transfected with empty vector (-), miniSINEUP-FXN M1 (-40/+0) or M76 (-40/+0). b) Citrate Synthase assay shows enzyme activity in untransfected and transfected cells described in (a). All data indicate mean ± SEM from at least four independent experiments. *p* values are calculated by unpaired t-test with Welch's correction (*, p<0,05; **, p<0,01; ***, p<0,001; ns, p > 0.05).

DISCUSSION

FRDA is a rare genetic disorder caused by an insufficient quantity of frataxin protein. Since its discovery in 1996, the understanding of frataxin functions has grown rapidly (171). However, no effective therapy is currently available to the patients (214). The main root of the pathology is the impaired transcription of *FXN* gene as result of GAA repeat expansion. Disease onset, severity and rate of progression are strictly dependent on the length of repeat expansion and ultimately frataxin levels. Homozygous GAA expansion leads to a pronounced drop in protein levels, up to only 20-30% compared to non-carrier's healthy individuals. Interestingly, heterozygous carriers are clinically healthy with protein levels ranging from 50% to 70% of controls (215,216).

During the last decade RNA-based therapy had a burst of interest because of both the high selectivity and the potential scalability to a large repertory of untreatable human diseases. Most RNA therapeutic molecules are inhibitory RNAs and have been developed to down-regulate expression of pathogenic genes. Among them, Small Inhibitory RNAs (siRNAs) and Anti-Sense Oligonucleotides (ASOs) are currently being tested in clinical trials for different disorders. Despite a huge improvement in terms of RNA stabilization, off-target effects reduction and on-target activity maximization, delivery still requires to be optimized. To this purpose, advanced carrier nanoparticles and new-generation adenoviral-associated vectors may eventually lead to new efficient target-specific drugs delivery. Furthermore, nucleic acid-based drugs can be directly delivered into the brain by intratechal injection. Thus, among others, a modified ASO targeting ISS-N1 (Intronic Splicing Silencer N1) has been successfully administrated in human CNS by intratechal injection (217) and it has been recently approved by FDA for spinal muscular atrophy treatment.

On the other hand, a large group of diseases would strongly benefit from transcriptional- or translation-stimulating drugs able to rescue physiological levels of a specific target protein (12).

Currently, there are no therapies to treat the disease or prevent its progression. The most promising approaches point to restore sufficient frataxin levels (180), mostly by enhancing *FXN* transcription. Among them, IFN-γ (189) and dyclonine (97) have

been identified as encouraging candidates by drug repositioning programs. Synthetic histone deacetylase (HDAC) inhibitors have been described to increase *FXN* mRNA in FRDA-derived cells and in FRDA animal models (139) (218). More recently, synthetic nucleic acids were successfully employed targeting GAA repeats, acting as R-loops inhibitors (51). Moreover, polyamide-based transcription factors capable of binding GAA microsatellite were developed (219). Interestingly, protein replacement therapy, based on TAT-frataxin delivery (190), and frataxin degradation prevention, by a class of ubiquitin-competing small molecules (220), have been recently proposed as potential treatments targeting the frataxin polipeptide. Finally, an effective gene replacement strategy in the FRDA mouse model opened new opportunities for gene therapy in the future (199).

Recently, gene-specific transcriptional activating RNAs (RNAa) (1) and non-degradative ASOs (2) have been employed to increase the expression of selected genes. As insufficient amounts of *FXN* mRNA are responsible for frataxin deficiency, this latter class of activating RNAs should be beneficial. It has been demonstrated that GAA expansion leads to DNA-RNA hybrid (R-loop) formation *in vitro* (221) (222) and inhibition of transcription due to RNA polymerase arrest. Interestingly, ASOs targeting *FXN* GAA repeat and R-loop structure are able to increase *FXN* mRNA in different FRDA patient-derived cell lines (223).

Almost all investigated molecules capable of elevating frataxin are currently aimed at increasing *FXN* transcription. In this context, SINEUPs represent a new and alternative approach to increase *FXN* expression, acting at post-transcriptional level. SINEUP-FXN are in antisense orientation 5' head-to-head to the most widely expressed *FXN* mRNA. Starting from canonical -40/+32 on M1, we screened different BDs to identify the shortest ones, while maintaining specificity. Each variant was combined with the ED of AS Uchl1 that so far represents the most potent translational activation domain for SINEUPs. Here we show that synthetic SINEUPs against the endogenous mRNA of *FXN* are able to increase its protein synthesis. Furthermore, we demonstrate BD's flexibility designing them around the initiating AUG of target mRNA as well as covering an internal in-frame methionine. While AUG overlap is crucial to retain SINEUP activity when targeting over-expressed mRNAs (100), we

prove it is not for endogenous transcripts. In addition, shrinking the BD down to 14 nts still maintains strong target protein up-regulation.

The vast majority of RNA-based therapeutics has been demonstrated to be too charged and/or too large to enter cells (21). Therefore, SINEUPs miniaturization is required to favour its delivery (95). Here we provide further evidence that miniSINEUP-FXNs are equally active than their longer counterparts. Chemical footprinting of invSINEB2 has recently identified several structural regions that are required for the ability of AS Uchl1 to increase translation, including a short terminal stem loop hairpin structure (SL1) as key structural determinant (96). Therefore, it is tempting to speculate that an even shorter and more active ED could be obtained based on structural data, thus providing further optimization of SINEUPs towards their therapeutic application (Gustincich S., unpublished; Carninci P., unpublished).

Finally, we demonstrate for the first time that *FXN* expression can be targeted specifically at translational level, providing evidence that synthetic SINEUPs and miniSINEUPs positively regulate frataxin in human healthy cell lines (from 20% to 50%). More importantly, FRDA-derived fibroblasts and lymphoblasts showed an accumulation of mature frataxin in the range of two folds of the amounts in untreated cells, without increasing *FXN* mRNA levels. In this context, miniSINEUP-FXN targeting the first AUG in FRDA lymphoblasts re-establishes *FXN* physiological levels, indistinguishable from those of healthy controls. The role of frataxin as activator of the ISC biosynthetic machinery (168,173,174) and as iron-chaperone, that provides ferrous iron in a bioavailable form (224-226), are the most well-defined molecular functions for this protein. In this context, frataxin is dually linked to cellular aconitases activity. The role of frataxin in the biosynthesis of ISC impacts on cellular availability of the prosthetic group required for both enzymes' function (227). Furthermore, frataxin can physically interact with mitochondrial and cytosolic aconitase, with the ability to protect or reactivate the enzyme's cofactor (226,228). Accordingly, rescue of aconitase defects has been associated to therapeutic increase of frataxin levels in cellular and animal models of FRDA (183,197,218,229). Therefore, we proved that the additional frataxin protein, as induced by miniSINEUPs, was functional and able to rescue the activity of ISC-dependent enzymes to physiological

levels in patient's lymphoblasts. It is striking that we observed the recovery of more than 90% of aconitase activity in presence of the most effective miniSINEUP-FXN.

In conclusion, we provide strong evidence that synthetic SINEUPs enhance endogenous protein expression to the physiological range in a cellular model of a monogenic disease.

Their ability to revert pathophysiological phenotypes in human patients' cells warrants the pre-clinical evaluation of a SINEUP-based therapy to treat FRDA. More broadly, these evidences support that synthetic SINEUPs represent a scalable platform to treat haploinsufficiency disorders.

CONFERENCE PROCEEDINGS

1. **Bon C**†, Lu arelli R, Fortuni S, Zucchelli1 S, Condó I and Gustincich S. *Synthetic SINEUPs rescue defective phenotype in a cellular model of Friedreich's Ataxia.* UMass Medical School, RNA therapeutics Conference 2018 - From Base Paires to Bedsides - Worcester MA, June 28-29, 2018

2. Matey T. A, Zucchelli S, Fasolo F, **Bon C**, Santulli C, Takahashi H, Cotella D, Jones M. H, Santoro C, Carninci P and Gustincich S. *SINEUPs: a new class of natural and synthetic antisense long non-coding RNAs (lncRNAs) that activate translation.* Cold Spring Harbor Laboratory - Regulatory Non-Coding RNAs. - New York, May 15-19, 2018.

3. **Bon C**, Carninci P, Cotella D, Damiani D, Espinoza S, Persichetti F, Santoro C, Takahashi H, Zucchelli S and Gustincich S. *SINEUPs: A Versatile Tool to Increase Protein Synthesis.* Keystone Symposia - Noncoding RNAs: Form, Function, Physiology - Keystone, Colorado USA, February 25 - March 1, 2018

4. Zucchelli S, **Bon C**†, Fimiani C, Tigani W, Fortuni S, Lu arelli R, Condó I, Mallamaci A and Gustincich S. *RNA therapeutics for Friedreich's Ataxia.* 2nd International Ataxia Research Conference - Pisa, Italy, September 27-30, 2017

5. Zucchelli S, **Bon C**, Fasolo F, Tettey Matey A, Santulli C, Takahashi H, Cotella D, Jones MH, Santoro C, Carninci P, and Gustincich S. *SINEUPs: a new class of natural and synthetic antisense long non-coding RNAs that activate translation.* Keystone Symposia - Noncoding RNAs: From disease to Targeted Therapeutics - Ban , Alberta, Canada, February 5-9, 2017.

6. Zucchelli S, **Bon C**, Fasolo F, Tettey Matey A, Santulli C, Takahashi H, Cotella D, Jones MH, Santoro C, Carninci P, and Gustincich S. *SINEUPs: a new class of natural and synthetic antisense long non-coding RNAs that activate translation.* Global Technology Comunity (GTC) - 7th Non-Coding RNA and RNAi Therapeutics Conference - Boston MA, September 14-15, 2016.

Labelled with † the conferences where I presented a talk or a poster.

LIST OF PUBBLICATIONS

1. Bon C, Lu arelli R, Russo R, Fortuni S, Santulli C, Fimiani C, Persichetti F, Cotella D, Mallamaci A, Santoro C, Carninci P, Testi R, Zucchelli S, Condó I and Gustincich S. **SINEUP non-coding RNAs rescue defective frataxin expression and activity in a cellular model of Friedreich's Ataxia.** (submitted)

2. Fasolo F, Patrucco L, Volpe M, Peano C, Mignone F, Bon C, Carninci P, Persichetti F, Santoro C, Zucchelli S, Sblattero D, Sanges R, Cotella D and Stefano Gustincich. The RNA-binding protein ILF3 binds to the embedded inverted **SINEB2 element of SINEUP AS Uchl1 long non-coding RNA influencing its nuclear localization.** (submitted)

3. Podbevöek P, Fasolo F, Bon C, Cimatti L, Reißer S, Carninci P, Bussi G, Zucchelli S, Plavec J, Gustincich S. **Structural determinants of the SINE B2 element embedded in the long non-coding RNA activator of translation AS Uchl1.** Sci Rep. 2018 Feb 16;8(1):3189.

SUPPLEMENTARY FIRGURES & TABLES

SUPPLEMENTARY FIGURE S1

Cloning Oligo Name:	Sequence (5' → 3'):	Features:
FXN.9 FWD	TCGAGGCTGCTCCGGGTCTGCCGCCCGCTCCGCCCTCCAGCGCTG	BD
FXN.9 REV	CAGCGCTGGAGGGCGGAGCGGGCGGCAGACCCGGAGCAGCC	BD
FXN.10 FWD	TCGAGGCTGCTCCGGGTCT	BD
FXN.10 REV	AGACCCGGAGCAGCC	BD
FXN.11 FWD	TCGAGACATGCTGCTCCGGGTCT	BD
FXN.11 REV	AGACCCGGAGCAGCATGTC	BD
FXN.12 FWD	TCGAGTCATCAAATAGACACTCTGCTTTTTGACATTCCAAATCTGGTTG	BD
FXN12. REV	CAACCAGATTTGGAATGTCAAAAAGCAGAGTGTCTATTTGATGAC	BD
FXN.13 FWD	TCGAGCAAATAGACACTCTGCTTTTTGACATTCCAAATCTGGTTG	BD
FXN13. REV	CAACCAGATTTGGAATGTCAAAAAGCAGAGTGTCTATTTGC	BD
FXN.14 FWD	TCGAGCAAATAGACACTCTGCTTTTTGACATTCCAAATCTGGTTGAGGCCACGTTGGTTCGAACTTGCGCGGCGG	BD
FXN14. REV	CCGCCGCGCAAGTTCGAACCAACGTGGCCTCAACCAGATTTGGAATGTCAAAAAGCAGAGTGTCTATTTGC	BD
SyberGreen Assay qRT-PCR Oligo Name:	**Sequence (5' → 3'):**	**Features:**
hGAPDH FWD	TCTCTGCTCCTCCTGTTC	Housekeeping gene
hGAPDH REV	GCCCAATACGACCAAATCC	Housekeeping gene
mAS3' Uchl1 FWD	CTGGTGTGTATTATCTCTTATGC	ED (SINEUP)
mAS3' Uchl1 REV	CTCCCGAGTCTCTGTAGC	ED (SINEUP)
pTSinvB2 FWD	CAGTGCTAGAGGAGGTCAGAAGA	ED (miniSINEUP)
pTSinvB2 REV	GGAGCTAAAGAGATGGCTCAGCACTT	ED (miniSINEUP)
hFXN FWD1	GTGATCAACAAGCAGACGCCAAACAAGCA	FRDA Fibroblast
hFXN REV1	GTACACCCAGTTTTTCCCAGTCCAGTCA	FRDA Fibroblast
hFXN FWD2	CCTTGCAGACAAGCCATACACGTTTGAG	FRDA Fibroblast
hFXN REV2	CTGCTTGTTGATCACATAGGTTCCTAGATC	FRDA Fibroblast
hFXN FWD	GGAAACGCTGGACTCTTTAGC	Human Cell lines
hFXN REV	CCAGTTTGACAGTTAAGACACCA	Human Cell lines
TaqMan Assay qRT-PCR Oligo Name:	**Sequence (5' → 3'):**	**Features:**
FXN	Hs00175940_m1	Target
hGAPDH	Hs99999905_m1	Housekeeping gene
GUSB	Hs00939627_m1	Housekeeping gene
ACTB	Hs99999903_m1	Housekeeping gene
miniSINEUP ED FWD	GGTCAGAAGAGGGCATTGGA,	ED (miniSINEUP)
miniSINEUP ED REV	CCACCACGAGGTTACCGTATAAC	ED (miniSINEUP)
Probe	CCCCCAGAACTGG	ED Probe

Figure S1 – **List of primers.** Complete list of oligonucleotides used in this study for cloning and quantitative PCR experiments.

SUPPLEMENTARY FIGURE S2

a

Subject name	Gene hit	Subject start	Subject end	Subject ori	Genomic Location	Orientation	Query name	Query position	Query start	Query end	Query ori	Length	Score	E-val	%ID
ENST00000642330.1	FXN	1	36	Forward	9:69035747-69035782	Forward	-40/+0	M1	5	40	Forward	36	71.9	2,00E-12	100.00
ENST00000642889.1	AL358113.1	1	33	Forward	9:69035750-69035782	Forward	-40/+0	M1	8	40	Forward	33	65.9	1,00E-10	100.00
ENST00000644653.1	FXN	1	32	Forward	9:69035751-69035782	Forward	-40/+0	M1	9	40	Forward	32	63.9	4,00E-10	100.00
ENST00000396366.6	FXN	1	21	Forward	9:69035762-69035782	Forward	-40/+0	M1	20	40	Forward	21	42.1	0.001	100.00
ENST00000382387.3	C9orf66	424	442	Forward	9:215300-215318	Reverse	-40/+0	M1	6	24	Forward	19	38.2	0.023	100.00
ENST00000522870.5	HSF4	39	56	Forward	16:67164719-67164736	Forward	-40/+0	M1	10	27	Forward	18	36.2	0.089	100.00
ENST00000406434.5	FAM49A	13	30	Forward	2:166657799-166657816	Reverse	-40/+0	M1	12	29	Forward	18	36.2	0.089	100.00
ENST00000381323.7	FAM49A	19	36	Forward	2:166657799-166657816	Reverse	-40/+0	M1	12	29	Forward	18	36.2	0.089	100.00
ENST00000523360.1	AC074143.1	399	416	Forward	16:67164719-67164736	Forward	-40/+0	M1	10	27	Forward	18	36.2	0.089	100.00
ENST00000580114.5	AC074143.1	873	890	Forward	16:67164719-67164736	Forward	-40/+0	M1	10	27	Forward	18	36.2	0.089	100.00
ENST00000376991.6	DRAP1	48	64	Forward	11:65919382-65919398	Forward	-40/+0	M1	11	27	Forward	17	34.2	0.35	100.00
ENST00000525501.5	DRAP1	109	125	Forward	11:65919382-65919398	Forward	-40/+0	M1	11	27	Forward	17	34.2	0.35	100.00
ENST00000215095.10	STX1B	201	220	Forward	16:31010442-31010461	Reverse	-40/+0	M1	21	40	Forward	20	32.2	1.4	95.00

Subject name	Gene hit	Subject start	Subject end	Subject ori	Genomic Location	Orientation	Query name	Query position	Query start	Query end	Query ori	Length	Score	E-val	%ID
ENST00000396364	FXN	207	224	Forward	9:71650685-71650702	Forward	-14/4	M1	1	18	Forward	18	36,2	0,011	100
ENST00000396366	FXN	8	25	Forward	9:71650685-71650702	Forward	-14/4	M1	1	18	Forward	18	36,2	0,011	100
ENST00000377270	FXN	511	528	Forward	9:71650685-71650702	Forward	-14/4	M1	1	18	Forward	18	36,2	0,011	100
ENST00000561836	STX1B	48	62	Forward	16:31021762-31021776	Reverse	-14/4	M1	1	15	Forward	15	30,2	0,68	100
ENST00000215095	STX1B	174	188	Forward	16:31021762-31021776	Reverse	-14/4	M1	1	15	Forward	15	30,2	0,68	100

Subject name	Gene hit	Subject start	Subject end	Subject ori	Genomic Location	Orientation	Query name	Query position	Query start	Query end	Query ori	Length	Score	E-val	%ID
ENST00000396364	FXN	207	220	Forward	9:71650685-71650698	Forward	-14/+0	M1	1	14	Forward	14	28,2	1,8	100
ENST00000396366	FXN	8	21	Forward	9:71650685-71650698	Forward	-14/+0	M1	1	14	Forward	14	28,2	1,8	100
ENST00000377270	FXN	511	524	Forward	9:71650685-71650698	Forward	-14/+0	M1	1	14	Forward	14	28,2	1,8	100
ENST00000561836	STX1B	48	61	Forward	16:31021763-31021776	Reverse	-14/+0	M1	1	14	Forward	14	28,2	1,8	100
ENST00000215095	STX1B	174	187	Forward	16:31021763-31021776	Reverse	-14/+0	M1	1	14	Forward	14	28,2	1,8	100

Subject name	Gene hit	Subject start	Subject end	Subject ori	Genomic Location	Orientation	Query name	Query position	Query start	Query end	Query ori	Length	Score	E-val	%ID
ENST00000396364	FXN	406	449	Forward	9:71661321-71661364	Forward	-40/+0	M76	1	44	Forward	44	87,7	3,00E-17	100
ENST00000498653	FXN	66	109	Forward	9:71661321-71661364	Forward	-40/+0	M76	1	44	Forward	44	87,7	3,00E-17	100
ENST00000396366	FXN	207	250	Forward	9:71661321-71661364	Forward	-40/+0	M76	1	44	Forward	44	87,7	3,00E-17	100
ENST00000377270	FXN	710	753	Forward	9:71661321-71661364	Forward	-40/+0	M76	1	44	Forward	44	87,7	3,00E-17	100
ENST00000484259	FXN	1	42	Forward	9:71661323-71661364	Forward	-40/+0	M76	3	44	Forward	42	83,8	5,00E-16	100
ENST00000316488	RP11-474P12,3	204	247	Forward	9:127730977-127731020	Reverse	-40/+0	M76	1	44	Forward	44	79,8	7,00E-15	97,73
ENST00000411625	RP11-474P12,3	100	143	Forward	9:127730977-127731020	Reverse	-40/+0	M76	1	44	Forward	44	79,8	7,00E-15	97,73
ENST00000559534	TUBGCP5	214	229	Forward	15:22866925-22866940	Forward	-40/+0	M76	9	24	Forward	16	32,2	1,5	100
ENST00000561214	TUBGCP5	406	421	Forward	15:22866925-22866940	Forward	-40/+0	M76	9	24	Forward	16	32,2	1,5	100
ENST00000453949	TUBGCP5	2471	2486	Forward	15:22866925-22866940	Forward	-40/+0	M76	9	24	Forward	16	32,2	1,5	100
ENST00000283645	TUBGCP5	2572	2587	Forward	15:22866925-22866940	Forward	-40/+0	M76	9	24	Forward	16	32,2	1,5	100

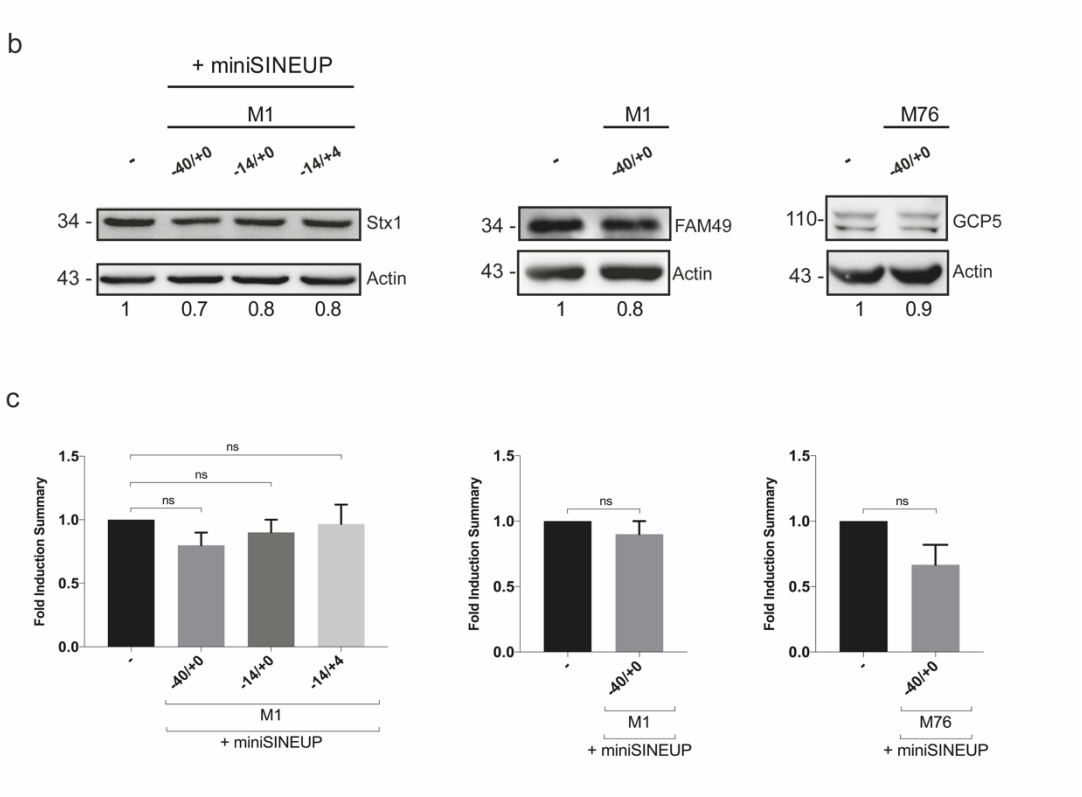

Figure S2 – **miniSINEUP specificity. a)** Blast analysis of miniSINEUPs BDs off-targets against Human Genome transcripts; highlighted in red chosen off-targets for each BD; **b)** Off-targets protein levels were analyzed by western blot with anti-stx1b, anti-fam49, anti-gcp5 antibodies staining and off-target protein levels were calculated relative to empty control samples (fold changes are shown); analysed protein lysates are relative to replicas of miniSINEUPs activity experiments (Figure 25); **c)** Summary of data of protein quantities. Data indicate mean ± SEM and are representative of four independent experiments. *p* values are calculated by unpaired t-test with Welch's correction. *, p<0,05; **, p<0,01, ***, p<0,001.

SUPPLEMENTARY FIGURE S3

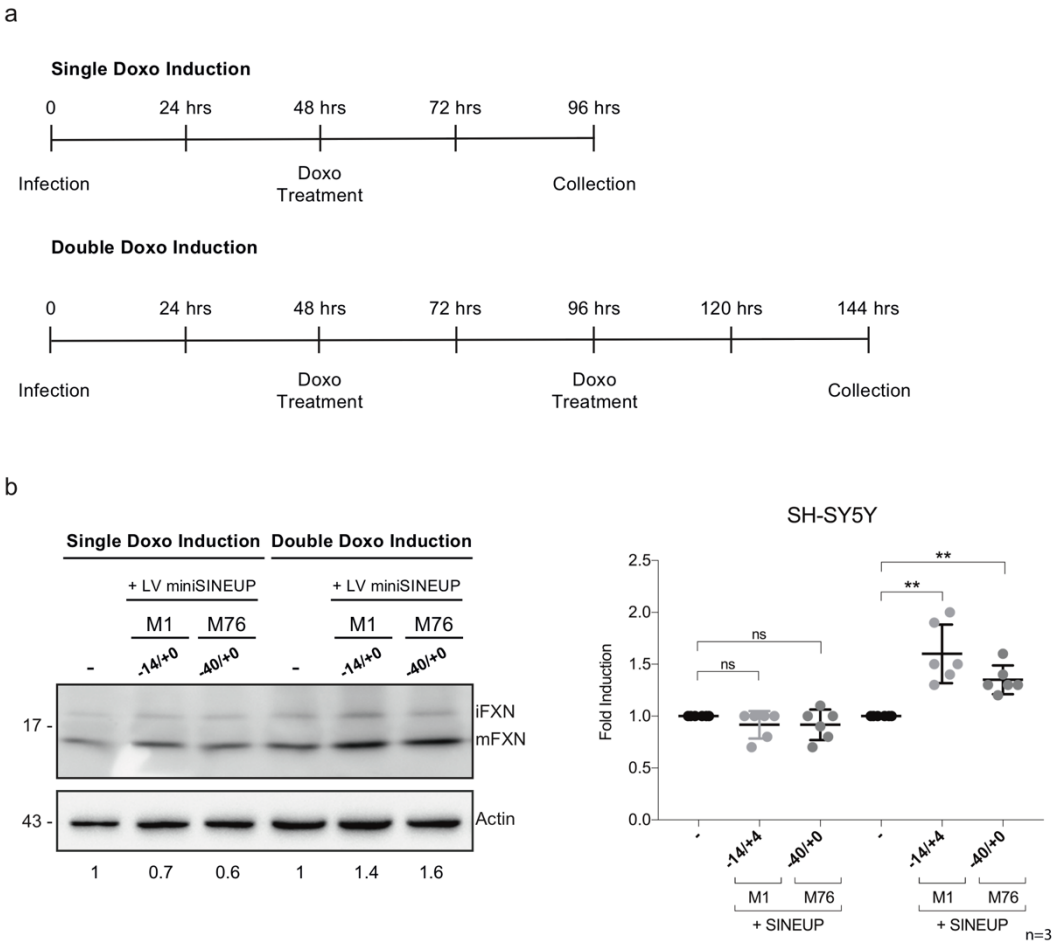

Figure S3 - **Setup of inducible lentiviral delivery of miniSINEUP *in vitro* in human cell** lines. **a)** Schematic overview of Single Induction and Double Induction protocol used with lentiviral vectors expressing miniSINEUP-FXN. The time of Infection, Induction of expression (Doxo Treatment) and Collection of RNA and protein samples are shown. **(b)** Human neuroblastoma SH-SY5Y cells were infected with lentiviral vectors expressing miniSINEUPs (LV miniSINEUP) or empty control virus (-) as indicated and following the Single Induction or Double Induction protocols. Protein levels were analyzed by western blot with anti-FXN antibody and SINEUP activity was calculated as increase in protein levels relative to empty control samples (fold changes are shown). Scatter plot graph (bottom) shows summary of results (frataxin protein fold-induction). Data indicate mean ± SEM and are representative of three independent experiments. *p* values are calculated by unpaired t-test with Welch's correction. *, p<0,05; **, p<0,01, ***, p<0,001.

ACKNOWLEDGMENTS

This thesis is the result of four-year of formative and challenging work, that would not have been possible without the experience, the idea and the critical reasoning of my Supervisor Professor Stefano Gustincich.

Special thanks to Professor Silvia Zucchelli, who led me in this project, sharing her expertise and methodology.

I am indebted to all the members of the SINEUP network - SISSA, Universita' del Piemonte Orientale, IIT, and RIKEN - for thought-provoking discussions.

I am most grateful to the collaborators, particularly to Ivano Condò and Riccardo Luffarelli, for having me in their laboratory - embracing me - and teaching me their expertise.

My sincere thanks must also go to Professor Antonello Mallamaci for the possibility to join his laboratory and to learn from their scientific experience but also for his presence and intuition.

I cannot forget the technical staff, especially Helena for her prompt support and kind care, and all the people I have dealt with here in SISSA over so many years.

Thanks will never be enough to those who were and still are my unforgettable lab-mates, that accompanied me through this tough path and fight for the PhD. Above all, Chiara without whose energy, support and laugh I wouldn't have done it.

BIBLIOGRAPHY

1. Faghihi, M.A., Kocerha, J., Modarresi, F., Engstrom, P.G., Chalk, A.M., Brothers, S.P., Koesema, E., St Laurent, G. and Wahlestedt, C. (2010) RNAi screen indicates widespread biological function for human natural antisense transcripts. *PloS one*, **5**.

2. Li, Z. and Rana, T.M. (2014) Therapeutic targeting of microRNAs: current status and future challenges. *Nature reviews. Drug discovery*, **13**, 622-638.

3. Pandolfo, M. (2009) Friedreich ataxia: the clinical picture. *Journal of neurology*, **256 Suppl 1**, 3-8.

4. Koeppen, A.H. (2011) Friedreich's ataxia: pathology, pathogenesis, and molecular genetics. *Journal of the neurological sciences*, **303**, 1-12.

5. Guerrier-Takada, C., Gardiner, K., Marsh, T., Pace, N. and Altman, S. (1983) The RNA moiety of ribonuclease P is the catalytic subunit of the enzyme. *Cell*, **35**, 849-857.

6. Kruger, K., Grabowski, P.J., Zaug, A.J., Sands, J., Gottschling, D.E. and Cech, T.R. (1982) Self-splicing RNA: autoexcision and autocyclization of the ribosomal RNA intervening sequence of Tetrahymena. *Cell*, **31**, 147-157.

7. Fire, A., Xu, S., Montgomery, M.K., Kostas, S.A., Driver, S.E. and Mello, C.C. (1998) Potent and specific genetic interference by double-stranded RNA in Caenorhabditis elegans. *Nature*, **391**, 806-811.

8. Sridharan, K. and Gogtay, N.J. (2016) Therapeutic nucleic acids: current clinical status. *British journal of clinical pharmacology*, **82**, 659-672.

9. Havens, M.A. and Hastings, M.L. (2016) Splice-switching antisense oligonucleotides as therapeutic drugs. *Nucleic acids research*, **44**, 6549-6563.

10. Bobbin, M.L. and Rossi, J.J. (2016) RNA Interference (RNAi)-Based Therapeutics: Delivering on the Promise? *Annual review of pharmacology and toxicology*, **56**, 103-122.

11. Lorenzer, C., Dirin, M., Winkler, A.M., Baumann, V. and Winkler, J. (2015) Going beyond the liver: progress and challenges of targeted delivery of siRNA therapeutics. *Journal of controlled release : official journal of the Controlled Release Society*, **203**, 1-15.

12. Gustincich, S., Zucchelli, S. and Mallamaci, A. (2017) The Yin and Yang of nucleic acid-based therapy in the brain. *Progress in neurobiology*, **155**, 194-211.

13. Lundin, K.E., Gissberg, O. and Smith, C.I. (2015) Oligonucleotide Therapies: The Past and the Present. *Human gene therapy*, **26**, 475-485.

14. Bennett, C.F. and Swayze, E.E. (2010) RNA targeting therapeutics: molecular mechanisms of antisense oligonucleotides as a therapeutic platform. *Annual review of pharmacology and toxicology*, **50**, 259-293.

15. Evers, M.M., Toonen, L.J. and van Roon-Mom, W.M. (2015) Antisense oligonucleotides in therapy for neurodegenerative disorders. *Advanced drug delivery reviews*, **87**, 90-103.

16. Southwell, A.L., Skotte, N.H., Bennett, C.F. and Hayden, M.R. (2012) Antisense oligonucleotide therapeutics for inherited neurodegenerative diseases. *Trends in molecular medicine*, **18**, 634-643.

17. Sanghvi, Y.S. (2011) A status update of modified oligonucleotides for chemotherapeutics applications. *Current protocols in nucleic acid chemistry*, **Chapter 4**, Unit 4.1.1-22.

18. Eckstein, F. (2014) Phosphorothioates, essential components of therapeutic oligonucleotides. *Nucleic acid therapeutics*, **24**, 374-387.

19. Yamamoto, T., Nakatani, M., Narukawa, K. and Obika, S. (2011) Antisense drug discovery and development. *Future medicinal chemistry*, **3**, 339-365.

20. Hacisuleyman, E., Goff, L.A., Trapnell, C., Williams, A., Henao-Mejia, J., Sun, L., McClanahan, P., Hendrickson, D.G., Sauvageau, M., Kelley, D.R. *et al.* (2014) Topological organization of multichromosomal regions by the long intergenic noncoding RNA Firre. *Nature structural & molecular biology*, **21**, 198-206.

21. Dowdy, S.F. (2017) Overcoming cellular barriers for RNA therapeutics. *Nature biotechnology*, **35**, 222-229.

22. Miller, T.M., Pestronk, A., David, W., Rothstein, J., Simpson, E., Appel, S.H., Andres, P.L., Mahoney, K., Allred, P., Alexander, K. *et al.* (2013) An antisense oligonucleotide against SOD1 delivered intrathecally for patients with SOD1 familial amyotrophic lateral sclerosis: a phase 1, randomised, first-in-man study. *The Lancet. Neurology*, **12**, 435-442.

23. Castanotto, D. and Rossi, J.J. (2009) The promises and pitfalls of RNA-interference-based therapeutics. *Nature*, **457**, 426-433.

24. Brennecke, J., Aravin, A.A., Stark, A., Dus, M., Kellis, M., Sachidanandam, R. and Hannon, G.J. (2007) Discrete small RNA-generating loci as master regulators of transposon activity in Drosophila. *Cell*, **128**, 1089-1103.

25. Vagin, V.V., Sigova, A., Li, C., Seitz, H., Gvozdev, V. and Zamore, P.D. (2006) A distinct small RNA pathway silences selfish genetic elements in the germline. *Science (New York, N.Y.)*, **313**, 320-324.

26. Han, J., Lee, Y., Yeom, K.H., Nam, J.W., Heo, I., Rhee, J.K., Sohn, S.Y., Cho, Y., Zhang, B.T. and Kim, V.N. (2006) Molecular basis for the recognition of primary microRNAs by the Drosha-DGCR8 complex. *Cell*, **125**, 887-901.

27. Rand, T.A., Petersen, S., Du, F. and Wang, X. (2005) Argonaute2 cleaves the anti-guide strand of siRNA during RISC activation. *Cell*, **123**, 621-629.

28. Davidson, B.L. and Monteys, A.M. (2012) Singles engage the RNA interference pathway. *Cell*, **150**, 873-875.

29. Borel, F., Kay, M.A. and Mueller, C. (2014) Recombinant AAV as a platform for translating the therapeutic potential of RNA interference. *Molecular therapy : the journal of the American Society of Gene Therapy*, **22**, 692-701.

30. Amarzguioui, M., Lundberg, P., Cantin, E., Hagstrom, J., Behlke, M.A. and Rossi, J.J. (2006) Rational design and in vitro and in vivo delivery of Dicer substrate siRNA. *Nature protocols*, **1**, 508-517.

31. Grimm, D., Wang, L., Lee, J.S., Schurmann, N., Gu, S., Borner, K., Storm, T.A. and Kay, M.A. (2010) Argonaute proteins are key determinants of RNAi efficacy, toxicity, and persistence in the adult mouse liver. *The Journal of clinical investigation*, **120**, 3106-3119.

32. Castanotto, D., Sakurai, K., Lingeman, R., Li, H., Shively, L., Aagaard, L., Soifer, H., Gatignol, A., Riggs, A. and Rossi, J.J. (2007) Combinatorial delivery of small interfering RNAs reduces RNAi efficacy by selective incorporation into RISC. *Nucleic acids research*, **35**, 5154-5164.

33. Gou, D., Weng, T., Wang, Y., Wang, Z., Zhang, H., Gao, L., Chen, Z., Wang, P. and Liu, L. (2007) A novel approach for the construction of multiple shRNA expression vectors. *The journal of gene medicine*, **9**, 751-763.

34. Li, M.J., Kim, J., Li, S., Zaia, J., Yee, J.K., Anderson, J., Akkina, R. and Rossi, J.J. (2005) Long-term inhibition of HIV-1 infection in primary hematopoietic cells by lentiviral vector delivery of a triple combination of anti-HIV shRNA, anti-CCR5 ribozyme, and a nucleolar-localizing TAR decoy. *Molecular therapy : the journal of the American Society of Gene Therapy*, **12**, 900-909.

35. Keiser, M.S., Kordasiewicz, H.B. and McBride, J.L. (2016) Gene suppression strategies for dominantly inherited neurodegenerative diseases: lessons from Huntington's disease and spinocerebellar ataxia. *Human molecular genetics*, **25**, R53-64.

36. Garzon, R., Marcucci, G. and Croce, C.M. (2010) Targeting microRNAs in cancer: rationale, strategies and challenges. *Nature reviews. Drug discovery*, **9**, 775-789.

37. Ebert, M.S. and Sharp, P.A. (2010) Emerging roles for natural microRNA sponges. *Current biology : CB*, **20**, R858-861.

38. Ebert, M.S. and Sharp, P.A. (2010) MicroRNA sponges: Progress and possibilities. *Rna*, **16**, 2043-2050.

39. Cesana, M., Cacchiarelli, D., Legnini, I., Santini, T., Sthandier, O., Chinappi, M., Tramontano, A. and Bozzoni, I. (2011) A long noncoding RNA controls muscle differentiation by functioning as a competing endogenous RNA. *Cell*, **147**, 358-369.

40. Tay, Y., Kats, L., Salmena, L., Weiss, D., Tan, S.M., Ala, U., Karreth, F., Poliseno, L., Provero, P., Di Cunto, F. *et al.* (2011) Coding-independent regulation of the tumor suppressor PTEN by competing endogenous mRNAs. *Cell*, **147**, 344-357.

41. Memczak, S., Jens, M., Elefsinioti, A., Torti, F., Krueger, J., Rybak, A., Maier, L., Mackowiak, S.D., Gregersen, L.H., Munschauer, M. *et al.* (2013) Circular RNAs are a large class of animal RNAs with regulatory potency. *Nature*, **495**, 333-338.

42. Salzman, J., Gawad, C., Wang, P.L., Lacayo, N. and Brown, P.O. (2012) Circular RNAs are the predominant transcript isoform from hundreds of human genes in diverse cell types. *PloS one*, **7**, e30733.

43. Lanford, R.E., Hildebrandt-Eriksen, E.S., Petri, A., Persson, R., Lindow, M., Munk, M.E., Kauppinen, S. and Orum, H. (2010) Therapeutic silencing of microRNA-122 in primates with chronic hepatitis C virus infection. *Science (New York, N.Y.)*, **327**, 198-201.

44. Zhao, J., Ohsumi, T.K., Kung, J.T., Ogawa, Y., Grau, D.J., Sarma, K., Song, J.J., Kingston, R.E., Borowsky, M. and Lee, J.T. (2010) Genome-wide identification of polycomb-associated RNAs by RIP-seq. *Molecular cell*, **40**, 939-953.

45. Hodgkinson, L., Sorbera, L. and Graul, A.I. (2016) Duchenne muscular dystrophy drugs face tough path to approval. *Drugs of today (Barcelona, Spain : 1998)*, **52**, 199-202.

46. Kole, R. and Krieg, A.M. (2015) Exon skipping therapy for Duchenne muscular dystrophy. *Advanced drug delivery reviews*, **87**, 104-107.

47. Mendell, J.R., Goemans, N., Lowes, L.P., Alfano, L.N., Berry, K., Shao, J., Kaye, E.M. and Mercuri, E. (2016) Longitudinal effect of eteplirsen versus historical control on ambulation in Duchenne muscular dystrophy. *Annals of neurology*, **79**, 257-271.

48. Du, L., Kayali, R., Bertoni, C., Fike, F., Hu, H., Iversen, P.L. and Gatti, R.A. (2011) Arginine-rich cell-penetrating peptide dramatically enhances AMO-mediated ATM aberrant splicing correction and enables delivery to brain and cerebellum. *Human molecular genetics*, **20**, 3151-3160.

49. Du, L., Pollard, J.M. and Gatti, R.A. (2007) Correction of prototypic ATM splicing mutations and aberrant ATM function with antisense morpholino oligonucleotides. *Proceedings of the National Academy of Sciences of the United States of America*, **104**, 6007-6012.

50. Peacey, E., Rodriguez, L., Liu, Y. and Wolfe, M.S. (2012) Targeting a pre-mRNA structure with bipartite antisense molecules modulates tau alternative splicing. *Nucleic acids research*, **40**, 9836-9849.

51. Li, L., Matsui, M. and Corey, D.R. (2016) Activating frataxin expression by repeat-targeted nucleic acids. *Nature communications*, **7**, 10606.

52. Janowski, B.A., Younger, S.T., Hardy, D.B., Ram, R., Huffman, K.E. and Corey, D.R. (2007) Activating gene expression in mammalian cells with promoter-targeted duplex RNAs. *Nature chemical biology*, **3**, 166-173.

53. Place, R.F., Li, L.C., Pookot, D., Noonan, E.J. and Dahiya, R. (2008) MicroRNA-373 induces expression of genes with complementary promoter sequences. *Proceedings of the National Academy of Sciences of the United States of America*, **105**, 1608-1613.

54. Portnoy, V., Huang, V., Place, R.F. and Li, L.C. (2011) Small RNA and transcriptional upregulation. *Wiley interdisciplinary reviews. RNA*, **2**, 748-760.

55. Faghihi, M.A., Zhang, M., Huang, J., Modarresi, F., Van der Brug, M.P., Nalls, M.A., Cookson, M.R., St-Laurent, G., 3rd and Wahlestedt, C. (2010)

Evidence for natural antisense transcript-mediated inhibition of microRNA function. *Genome biology*, **11**, R56.

56. Diodato, A., Pinzan, M., Granzotto, M. and Mallamaci, A. (2013) Promotion of cortico-cerebral precursors expansion by artificial pri-miRNAs targeted against the Emx2 locus. *Current gene therapy*, **13**, 152-161.

57. Forrest, A.R., Kawaji, H., Rehli, M., Baillie, J.K., de Hoon, M.J., Haberle, V., Lassmann, T., Kulakovskiy, I.V., Lizio, M., Itoh, M. *et al.* (2014) A promoter-level mammalian expression atlas. *Nature*, **507**, 462-470.

58. Li, L.C., Okino, S.T., Zhao, H., Pookot, D., Place, R.F., Urakami, S., Enokida, H. and Dahiya, R. (2006) Small dsRNAs induce transcriptional activation in human cells. *Proceedings of the National Academy of Sciences of the United States of America*, **103**, 17337-17342.

59. Schwartz, J.C., Younger, S.T., Nguyen, N.B., Hardy, D.B., Monia, B.P., Corey, D.R. and Janowski, B.A. (2008) Antisense transcripts are targets for activating small RNAs. *Nature structural & molecular biology*, **15**, 842-848.

60. Yue, X., Schwartz, J.C., Chu, Y., Younger, S.T., Gagnon, K.T., Elbashir, S., Janowski, B.A. and Corey, D.R. (2010) Transcriptional regulation by small RNAs at sequences downstream from 3' gene termini. *Nature chemical biology*, **6**, 621-629.

61. Liu, M., Roth, A., Yu, M., Morris, R., Bersani, F., Rivera, M.N., Lu, J., Shioda, T., Vasudevan, S., Ramaswamy, S. *et al.* (2013) The IGF2 intronic miR-483 selectively enhances transcription from IGF2 fetal promoters and enhances tumorigenesis. *Genes & Development*, **27**, 2543-2548.

62. Morris, K.V., Santoso, S., Turner, A.M., Pastori, C. and Hawkins, P.G. (2008) Bidirectional transcription directs both transcriptional gene activation and suppression in human cells. *PLoS genetics*, **4**, e1000258.

63. Modarresi, F., Faghihi, M.A., Lopez-Toledano, M.A., Fatemi, R.P., Magistri, M., Brothers, S.P., van der Brug, M.P. and Wahlestedt, C. (2012) Inhibition of natural antisense transcripts in vivo results in gene-specific transcriptional upregulation. *Nature biotechnology*, **30**, 453-459.

64. Matsui, M., Chu, Y., Zhang, H., Gagnon, K.T., Shaikh, S., Kuchimanchi, S., Manoharan, M., Corey, D.R. and Janowski, B.A. (2013) Promoter RNA links transcriptional regulation of inflammatory pathway genes. *Nucleic acids research*, **41**, 10086-10109.

65. Voutila, J., Saetrom, P., Mintz, P., Sun, G., Alluin, J., Rossi, J.J., Habib, N.A. and Kasahara, N. (2012) Gene Expression Profile Changes After Short-activating RNA-mediated Induction of Endogenous Pluripotency Factors in Human Mesenchymal Stem Cells. *Molecular therapy. Nucleic acids*, **1**, e35.

66. Fimiani, C., Goina, E. and Mallamaci, A. (2015) Upregulating endogenous genes by an RNA-programmable artificial transactivator. *Nucleic acids research*, **43**, 7850-7864.

67. LeCuyer, K.A., Behlen, L.S. and Uhlenbeck, O.C. (1995) Mutants of the bacteriophage MS2 coat protein that alter its cooperative binding to RNA. *Biochemistry*, **34**, 10600-10606.

68. Carey, J., Cameron, V., De Haseth, P.L. and Uhlenbeck, O.C. (1983) Sequence-specific interaction of R17 coat protein with its ribonucleic acid binding site. *Biochemistry*, **22**, 2601-2610.

69. Romaniuk, P.J., Lowary, P., Wu, H.N., Stormo, G. and Uhlenbeck, O.C. (1987) RNA binding site of R17 coat protein. *Biochemistry*, **26**, 1563-1568.

70. Carninci, P., Kasukawa, T., Katayama, S., Gough, J., Frith, M.C., Maeda, N., Oyama, R., Ravasi, T., Lenhard, B., Wells, C. *et al.* (2005) The transcriptional landscape of the mammalian genome. *Science (New York, N.Y.)*, **309**, 1559-1563.

71. Consortium, E.P. (2004) The ENCODE (ENCyclopedia Of DNA Elements) Project. *Science (New York, N.Y.)*, **306**, 636-640.

72. Derrien, T., Johnson, R., Bussotti, G., Tanzer, A., Djebali, S., Tilgner, H., Guernec, G., Martin, D., Merkel, A., Knowles, D.G. *et al.* (2012) The GENCODE v7 catalog of human long noncoding RNAs: analysis of their gene structure, evolution, and expression. *Genome research*, **22**, 1775-1789.

73. Iyer, M.K., Niknafs, Y.S., Malik, R., Singhal, U., Sahu, A., Hosono, Y., Barrette, T.R., Prensner, J.R., Evans, J.R., Zhao, S. *et al.* (2015) The landscape of long noncoding RNAs in the human transcriptome. *Nature genetics*, **47**, 199-208.

74. Volders, P.J., Verheggen, K., Menschaert, G., Vandepoele, K., Martens, L., Vandesompele, J. and Mestdagh, P. (2015) An update on LNCipedia: a database for annotated human lncRNA sequences. *Nucleic acids research*, **43**, D174-180.

75. Guttman, M., Amit, I., Garber, M., French, C., Lin, M.F., Feldser, D., Huarte, M., Zuk, O., Carey, B.W., Cassady, J.P. *et al.* (2009) Chromatin signature reveals over a thousand highly conserved large non-coding RNAs in mammals. *Nature*, **458**, 223-227.

76. Fatica, A. and Bozzoni, I. (2014) Long non-coding RNAs: new players in cell differentiation and development. *Nature reviews. Genetics*, **15**, 7-21.

77. Chen, C.K., Yu, C.P., Li, S.C., Wu, S.M., Lu, M.Y.J., Chen, Y.H., Chen, D.R., Ng, C.S., Ting, C.T. and Li, W.H. (2017) Identification and evolutionary analysis of long non-coding RNAs in zebra finch. *BMC Genomics*, **18**.

78. Sanchez, Y. and Huarte, M. (2013) Long non-coding RNAs: challenges for diagnosis and therapies. *Nucleic acid therapeutics*, **23**, 15-20.

79. Vance, K.W. and Ponting, C.P. (2014) Transcriptional regulatory functions of nuclear long noncoding RNAs. *Trends in genetics : TIG*, **30**, 348-355.

80. van Heesch, S., van Iterson, M., Jacobi, J., Boymans, S., Essers, P.B., de Bruijn, E., Hao, W., MacInnes, A.W., Cuppen, E. and Simonis, M. (2014) Extensive localization of long noncoding RNAs to the cytosol and mono- and polyribosomal complexes. *Genome biology*, **15**, R6.

81. Ingolia, N.T., Lareau, L.F. and Weissman, J.S. (2011) Ribosome profiling of mouse embryonic stem cells reveals the complexity and dynamics of mammalian proteomes. *Cell*, **147**, 789-802.

82. Carrieri, C., Cimatti, L., Biagioli, M., Beugnet, A., Zucchelli, S., Fedele, S., Pesce, E., Ferrer, I., Collavin, L., Santoro, C. *et al.* (2012) Long non-coding antisense RNA controls Uchl1 translation through an embedded SINEB2 repeat. *Nature*, **491**, 454-457.

83. Liu, H., Searle, I.R., Watson-Haigh, N.S., Baumann, U., Mather, D.E., Able, A.J. and Able, J.A. (2015) Genome-Wide Identification of MicroRNAs in Leaves and the Developing Head of Four Durum Genotypes during Water Deficit Stress. *PloS one*, **10**.

84. Tichon, A., Gil, N., Lubelsky, Y., Havkin Solomon, T., Lemze, D., Itzkovitz, S., Stern-Ginossar, N. and Ulitsky, I. (2016) A conserved abundant cytoplasmic long noncoding RNA modulates repression by Pumilio proteins in human cells. *Nature communications*, **7**.

85. Kino, T., Hurt, D.E., Ichijo, T., Nader, N. and Chrousos, G.P. (2010) Noncoding RNA gas5 is a growth arrest- and starvation-associated repressor of the glucocorticoid receptor. *Science signaling*, **3**, ra8.

86. Salehi, S., Taheri, M.N., Azarpira, N., Zare, A. and Behzad-Behbahani, A. (2017) State of the art technologies to explore long non-coding RNAs in cancer. *Journal of cellular and molecular medicine*, **21**, 3120-3140.

87. Katayama, S., Tomaru, Y., Kasukawa, T., Waki, K., Nakanishi, M., Nakamura, M., Nishida, H., Yap, C.C., Suzuki, M., Kawai, J. *et al.* (2005) Antisense transcription in the mammalian transcriptome. *Science (New York, N.Y.)*, **309**, 1564-1566.

88. Werner, A. (2013) Biological functions of natural antisense transcripts. *BMC Biology*, **11**, 31.

89. Chen, J., Sun, M. and Kent, W.J. (2004) Over 20% of human transcripts might form sense–antisense pairs. **32**, 4812-4820.

90. Zucchelli, S., Fasolo, F., Russo, R., Cimatti, L., Patrucco, L., Takahashi, H., Jones, M.H., Santoro, C., Sblattero, D., Cotella, D. *et al.* (2015) SINEUPs are modular antisense long non-coding RNAs that increase synthesis of target proteins in cells. *Frontiers in Cellular Neuroscience*, **9**.

91. Pelechano, V. and Steinmetz, L.M. (2013) Gene regulation by antisense transcription. *Nature reviews. Genetics*, **14**, 880-893.

92. Yu, W., Gius, D., Onyango, P., Muldoon-Jacobs, K., Karp, J., Feinberg, A.P. and Cui, H. (2008) Epigenetic silencing of tumour suppressor gene p15 by its antisense RNA. *Nature*, **451**, 202-206.

93. Tripathi, V., Ellis, J.D., Shen, Z., Song, D.Y., Pan, Q., Watt, A.T., Freier, S.M., Bennett, C.F., Sharma, A., Bubulya, P.A. *et al.* (2010) The Nuclear-Retained Noncoding RNA MALAT1 Regulates Alternative Splicing by Modulating SR Splicing Factor Phosphorylation. *Molecular cell*, **39**, 925-938.

94. Spigoni, G., Gedressi, C. and Mallamaci, A. (2010) Regulation of Emx2 expression by antisense transcripts in murine cortico-cerebral precursors. *PloS one*, **5**, e8658.

95. Zucchelli, S., Cotella, D., Takahashi, H., Carrieri, C., Cimatti, L., Fasolo, F., Jones, M.H., Sblattero, D., Sanges, R., Santoro, C. *et al.* (2015) SINEUPs: A new class of natural and synthetic antisense long non-coding RNAs that activate translation. *RNA biology*, **12**, 771-779.

96. Podbevsek, P., Fasolo, F., Bon, C., Cimatti, L., Reisser, S., Carninci, P., Bussi, G., Zucchelli, S., Plavec, J. and Gustincich, S. (2018) Structural determinants of the SINE B2 element embedded in the long non-coding RNA activator of translation AS Uchl1. *Scientific reports*, **8**, 3189.

97. Sahdeo, S., Scott, B.D., McMackin, M.Z., Jasoliya, M., Brown, B., Wulff, H., Perlman, S.L., Pook, M.A. and Cortopassi, G.A. (2014) Dyclonine rescues frataxin deficiency in animal models and buccal cells of patients with Friedreich's ataxia. *Human molecular genetics*, **23**, 6848-6862.

98. Yao, Y., Jin, S., Long, H., Yu, Y., Zhang, Z., Cheng, G., Xu, C., Ding, Y., Guan, Q., Li, N. *et al.* (2015) RNAe: an effective method for targeted protein translation enhancement by artificial non-coding RNA with SINEB2 repeat. *Nucleic acids research*, **43**, e58-e58.

99. Patrucco, L., Chiesa, A., Soluri, M.F., Fasolo, F., Takahashi, H., Carninci, P., Zucchelli, S., Santoro, C., Gustincich, S., Sblattero, D. *et al.* (2015) Engineering mammalian cell factories with SINEUP noncoding RNAs to improve translation of secreted proteins. *Gene*, **569**, 287-293.

100. Takahashi, H., Kozhuharova, A., Sharma, H., Hirose, M., Ohyama, T., Fasolo, F., Yamazaki, T., Cotella, D., Santoro, C., Zucchelli, S. *et al.* (2018) Identification of functional features of synthetic SINEUPs, antisense lncRNAs that specifically enhance protein translation. *PloS one*, **13**, e0183229.

101. Indrieri, A., Grimaldi, C., Zucchelli, S., Tammaro, R., Gustincich, S. and Franco, B. (2016) Synthetic long non-coding RNAs [SINEUPs] rescue defective gene expression in vivo. *Scientific reports*, **6**, 27315.

102. Long, H., Yao, Y., Jin, S., Yu, Y., Hu, X., Zhuang, F., Zhang, H. and Wu, Q. (2017) RNAe in a transgenic growth hormone mouse model shows potential for use in gene therapy. *Biotechnology letters*, **39**, 179-188.

103. Pandolfo, M. and Pastore, A. (2009) The pathogenesis of Friedreich ataxia and the structure and function of frataxin. *Journal of neurology*, **256 Suppl 1**, 9-17.

104. Chamberlain, S., Shaw, J., Rowland, A., Wallis, J., South, S., Nakamura, Y., von Gabain, A., Farrall, M. and Williamson, R. (1988) Mapping of mutation causing Friedreich's ataxia to human chromosome 9. *Nature*, **334**, 248-250.

105. Huang, M.L., Becker, E.M., Whitnall, M., Suryo Rahmanto, Y., Ponka, P. and Richardson, D.R. (2009) Elucidation of the mechanism of mitochondrial iron loading in Friedreich's ataxia by analysis of a mouse mutant. *Proceedings of the National Academy of Sciences of the United States of America*, **106**, 16381-16386.

106. Delatycki, M.B., Camakaris, J., Brooks, H., Evans-Whipp, T., Thorburn, D.R., Williamson, R. and Forrest, S.M. (1999) Direct evidence that mitochondrial iron accumulation occurs in Friedreich ataxia. *Annals of neurology*, **45**, 673-675.

107. Folker, J., Murdoch, B., Cahill, L., Delatycki, M., Corben, L. and Vogel, A. (2010) Dysarthria in Friedreich's ataxia: a perceptual analysis. *Folia phoniatrica et logopaedica : official organ of the International Association of Logopedics and Phoniatrics (IALP)*, **62**, 97-103.

108. Vogel, A.P., Brown, S.E., Folker, J.E., Corben, L.A. and Delatycki, M.B. (2014) Dysphagia and swallowing-related quality of life in Friedreich ataxia. *Journal of neurology*, **261**, 392-399.

109. Cnop, M., Mulder, H. and Igoillo-Esteve, M. (2013) Diabetes in Friedreich ataxia. *Journal of neurochemistry*, **126 Suppl 1**, 94-102.

110. Ristow, M. (2004) Neurodegenerative disorders associated with diabetes mellitus. *Journal of molecular medicine (Berlin, Germany)*, **82**, 510-529.

111. Cnop, M., Igoillo-Esteve, M., Rai, M., Begu, A., Serroukh, Y., Depondt, C., Musuaya, A.E., Marhfour, I., Ladriere, L., Moles Lopez, X. *et al.* (2012) Central role and mechanisms of beta-cell dysfunction and death in friedreich ataxia-associated diabetes. *Annals of neurology*, **72**, 971-982.

112. Delatycki, M.B., Voullaire, L., Francis, D., Petrovic, V., Robertson, A., Webber, L.M. and Slater, H.R. (1999) Directly inherited partial trisomy of chromosome 6p identified in a father and daughter by chromosome microdissection. *Journal of medical genetics*, **36**, 335-338.

113. Rajagopalan, B., Francis, J.M., Cooke, F., Korlipara, L.V., Blamire, A.M., Schapira, A.H., Madan, J., Neubauer, S. and Cooper, J.M. (2010) Analysis of the factors influencing the cardiac phenotype in Friedreich's ataxia. *Movement disorders : official journal of the Movement Disorder Society*, **25**, 846-852.

114. Dutka, D.P., Donnelly, J.E., Nihoyannopoulos, P., Oakley, C.M. and Nunez, D.J. (1999) Marked variation in the cardiomyopathy associated with Friedreich's ataxia. *Heart (British Cardiac Society)*, **81**, 141-147.

115. Tsou, A.Y., Paulsen, E.K., Lagedrost, S.J., Perlman, S.L., Mathews, K.D., Wilmot, G.R., Ravina, B., Koeppen, A.H. and Lynch, D.R. (2011) Mortality in Friedreich ataxia. *Journal of the neurological sciences*, **307**, 46-49.

116. Delatycki, M.B. and Corben, L.A. (2012) Clinical features of Friedreich ataxia. *Journal of child neurology*, **27**, 1133-1137.

117. Bidichandani SI, D.M. (1998) Friedreich Ataxia.

118. Bhidayasiri, R., Perlman, S.L., Pulst, S.M. and Geschwind, D.H. (2005) Late-onset Friedreich ataxia: phenotypic analysis, magnetic resonance imaging findings, and review of the literature. *Archives of neurology*, **62**, 1865-1869.

119. Campuzano, V., Montermini, L., Molto, M.D., Pianese, L., Cossee, M., Cavalcanti, F., Monros, E., Rodius, F., Duclos, F., Monticelli, A. *et al.* (1996) Friedreich's ataxia: autosomal recessive disease caused by an intronic GAA triplet repeat expansion. *Science (New York, N.Y.)*, **271**, 1423-1427.

120. Evans-Galea, M.V., Pebay, A., Dottori, M., Corben, L.A., Ong, S.H., Lockhart, P.J. and Delatycki, M.B. (2014) Cell and gene therapy for Friedreich ataxia: progress to date. *Human gene therapy*, **25**, 684-693.

121. Kumari, D., Biacsi, R.E. and Usdin, K. (2011) Repeat expansion affects both transcription initiation and elongation in friedreich ataxia cells. *The Journal of biological chemistry*, **286**, 4209-4215.

122. Tourtellotte, W.G. and Milbrandt, J. (1998) Sensory ataxia and muscle spindle agenesis in mice lacking the transcription factor Egr3. *Nature genetics*, **20**, 87-91.

123. De Biase, I., Chutake, Y.K., Rindler, P.M. and Bidichandani, S.I. (2009) Epigenetic silencing in Friedreich ataxia is associated with depletion of CTCF (CCCTC-binding factor) and antisense transcription. *PloS one*, **4**, e7914.

124. Galea, C.A., Huq, A., Lockhart, P.J., Tai, G., Corben, L.A., Yiu, E.M., Gurrin, L.C., Lynch, D.R., Gelbard, S., Durr, A. *et al.* (2016) Compound heterozygous FXN mutations and clinical outcome in friedreich ataxia. *Annals of neurology*, **79**, 485-495.

125. Stolle, C.A., Frackelton, E.C., McCallum, J., Farmer, J.M., Tsou, A., Wilson, R.B. and Lynch, D.R. (2008) Novel, complex interruptions of the GAA repeat in small, expanded alleles of two affected siblings with late-onset Friedreich ataxia. *Movement disorders : official journal of the Movement Disorder Society*, **23**, 1303-1306.

126. Greene, E., Entezam, A., Kumari, D. and Usdin, K. (2005) Ancient repeated DNA elements and the regulation of the human frataxin promoter. *Genomics*, **85**, 221-230.

127. Cossee, M., Schmitt, M., Campuzano, V., Reutenauer, L., Moutou, C., Mandel, J.L. and Koenig, M. (1997) Evolution of the Friedreich's ataxia trinucleotide repeat expansion: founder effect and premutations. *Proceedings of the National Academy of Sciences of the United States of America*, **94**, 7452-7457.

128. Filla, A., De Michele, G., Cavalcanti, F., Pianese, L., Monticelli, A., Campanella, G. and Cocozza, S. (1996) The relationship between trinucleotide (GAA) repeat length and clinical features in Friedreich ataxia. *American journal of human genetics*, **59**, 554-560.

129. Montermini, L., Richter, A., Morgan, K., Justice, C.M., Julien, D., Castellotti, B., Mercier, J., Poirier, J., Capozzoli, F., Bouchard, J.P. *et al.* (1997) Phenotypic variability in Friedreich ataxia: role of the associated GAA triplet repeat expansion. *Annals of neurology*, **41**, 675-682.

130. Durr, A., Cossee, M., Agid, Y., Campuzano, V., Mignard, C., Penet, C., Mandel, J.L., Brice, A. and Koenig, M. (1996) Clinical and genetic abnormalities in patients with Friedreich's ataxia. *The New England journal of medicine*, **335**, 1169-1175.

131. Monros, E., Molto, M.D., Martinez, F., Canizares, J., Blanca, J., Vilchez, J.J., Prieto, F., de Frutos, R. and Palau, F. (1997) Phenotype correlation and intergenerational dynamics of the Friedreich ataxia GAA trinucleotide repeat. *American journal of human genetics*, **61**, 101-110.

132. Lecocq, C., Charles, P., Azulay, J.P., Meissner, W., Rai, M., N'Guyen, K., Pereon, Y., Fabre, N., Robin, E., Courtois, S. *et al.* (2016) Delayed-onset Friedreich's ataxia revisited. *Movement disorders : official journal of the Movement Disorder Society*, **31**, 62-69.

133. Martinez, A.R., Moro, A., Abrahao, A., Faber, I., Borges, C.R., Rezende, T.J., Martins, C.R., Jr., Moscovich, M., Munhoz, R.P., Segal, S.L. *et al.* (2017) Nonneurological Involvement in Late-Onset Friedreich Ataxia (LOFA): Exploring the Phenotypes. *Cerebellum (London, England)*, **16**, 253-256.

134. Montermini, L., Andermann, E., Labuda, M., Richter, A., Pandolfo, M., Cavalcanti, F., Pianese, L., Iodice, L., Farina, G., Monticelli, A. *et al.* (1997) The Friedreich ataxia GAA triplet repeat: premutation and normal alleles. *Human molecular genetics*, **6**, 1261-1266.

135. Delatycki, M.B., Knight, M., Koenig, M., Cossee, M., Williamson, R. and Forrest, S.M. (1999) G130V, a common FRDA point mutation, appears to have arisen from a common founder. *Human genetics*, **105**, 343-346.

136. Sakamoto, N., Ohshima, K., Montermini, L., Pandolfo, M. and Wells, R.D. (2001) Sticky DNA, a self-associated complex formed at long GAA*TTC repeats in intron 1 of the frataxin gene, inhibits transcription. *The Journal of biological chemistry*, **276**, 27171-27177.

137. Groh, M., Lufino, M.M., Wade-Martins, R. and Gromak, N. (2014) R-loops associated with triplet repeat expansions promote gene silencing in Friedreich ataxia and fragile X syndrome. *PLoS genetics*, **10**, e1004318.

138. Al-Mahdawi, S., Pinto, R.M., Ismail, O., Varshney, D., Lymperi, S., Sandi, C., Trabzuni, D. and Pook, M. (2008) The Friedreich ataxia GAA repeat expansion mutation induces comparable epigenetic changes in human and transgenic mouse brain and heart tissues. *Human molecular genetics*, **17**, 735-746.

139. Herman, D., Jenssen, K., Burnett, R., Soragni, E., Perlman, S.L. and Gottesfeld, J.M. (2006) Histone deacetylase inhibitors reverse gene silencing in Friedreich's ataxia. *Nature chemical biology*, **2**, 551-558.

140. Evans-Galea, M.V., Carrodus, N., Rowley, S.M., Corben, L.A., Tai, G., Saffery, R., Galati, J.C., Wong, N.C., Craig, J.M., Lynch, D.R. *et al.* (2012) FXN methylation predicts expression and clinical outcome in Friedreich ataxia. *Annals of neurology*, **71**, 487-497.

141. Chutake, Y.K., Costello, W.N., Lam, C. and Bidichandani, S.I. (2014) Altered nucleosome positioning at the transcription start site and deficient transcriptional initiation in Friedreich ataxia. *The Journal of biological chemistry*, **289**, 15194-15202.

142. Chutake, Y.K., Lam, C., Costello, W.N., Anderson, M. and Bidichandani, S.I. (2014) Epigenetic promoter silencing in Friedreich ataxia is dependent on repeat length. *Annals of neurology*, **76**, 522-528.

143. Li, Y., Lu, Y., Polak, U., Lin, K., Shen, J., Farmer, J., Seyer, L., Bhalla, A.D., Rozwadowska, N., Lynch, D.R. *et al.* (2015) Expanded GAA repeats impede transcription elongation through the FXN gene and induce transcriptional silencing that is restricted to the FXN locus. *Human molecular genetics*, **24**, 6932-6943.

144. Sandi, C., Sandi, M., Anjomani Virmouni, S., Al-Mahdawi, S. and Pook, M.A. (2014) Epigenetic-based therapies for Friedreich ataxia. **5**.

145. Chung, D.W., Rudnicki, D.D., Yu, L. and Margolis, R.L. (2011) A natural antisense transcript at the Huntington's disease repeat locus regulates HTT expression. *Human molecular genetics*, **20**, 3467-3477.

146. Baralle, M., Pastor, T., Bussani, E. and Pagani, F. (2008) Influence of Friedreich ataxia GAA noncoding repeat expansions on pre-mRNA processing. *American journal of human genetics*, **83**, 77-88.

147. Klinz, F.-J. and Gallwitz, D. (1985) Size and position of intervening sequences are critical for the splicing efficiency of pre-mRNA in the yeast Saccharomyces cerevisiae. *Nucleic acids research*, **13**, 3791-3804.

148. Punga, T. and Buhler, M. (2010) Long intronic GAA repeats causing Friedreich ataxia impede transcription elongation. *EMBO molecular medicine*, **2**, 120-129.

149. Saveliev, A., Everett, C., Sharpe, T., Webster, Z. and Festenstein, R. (2003) DNA triplet repeats mediate heterochromatin-protein-1-sensitive variegated gene silencing. *Nature*, **422**, 909-913.

150. Chan, P.K., Torres, R., Yandim, C., Law, P.P., Khadayate, S., Mauri, M., Grosan, C., Chapman-Rothe, N., Giunti, P., Pook, M. *et al.* (2013) Heterochromatinization induced by GAA-repeat hyperexpansion in Friedreich's ataxia can be reduced upon HDAC inhibition by vitamin B3. *Human molecular genetics*, **22**, 2662-2675.

151. Greene, E., Mahishi, L., Entezam, A., Kumari, D. and Usdin, K. (2007) Repeat-induced epigenetic changes in intron 1 of the frataxin gene and its consequences in Friedreich ataxia. *Nucleic acids research*, **35**, 3383-3390.

152. Al-Mahdawi, S., Sandi, C., Mouro Pinto, R. and Pook, M.A. (2013) Friedreich ataxia patient tissues exhibit increased 5-hydroxymethylcytosine modification and decreased CTCF binding at the FXN locus. *PloS one*, **8**, e74956.

153. Kim, E., Napierala, M. and Dent, S.Y. (2011) Hyperexpansion of GAA repeats affects post-initiation steps of FXN transcription in Friedreich's ataxia. *Nucleic acids research*, **39**, 8366-8377.

154. Rai, M., Soragni, E., Jenssen, K., Burnett, R., Herman, D., Coppola, G., Geschwind, D.H., Gottesfeld, J.M. and Pandolfo, M. (2008) HDAC inhibitors correct frataxin deficiency in a Friedreich ataxia mouse model. *PloS one*, **3**, e1958.

155. Campuzano, V., Montermini, L., Lutz, Y., Cova, L., Hindelang, C., Jiralerspong, S., Trottier, Y., Kish, S.J., Faucheux, B., Trouillas, P. *et al.* (1997) Frataxin is reduced in Friedreich ataxia patients and is associated with mitochondrial membranes. *Human molecular genetics*, **6**, 1771-1780.

156. Condo, I., Ventura, N., Malisan, F., Tomassini, B. and Testi, R. (2006) A pool of extramitochondrial frataxin that promotes cell survival. *The Journal of biological chemistry*, **281**, 16750-16756.

157. Perez-Luz, S., Gimenez-Cassina, A., Fernandez-Frias, I., Wade-Martins, R. and Diaz-Nido, J. (2015) Delivery of the 135 kb human frataxin genomic DNA locus gives rise to different frataxin isoforms. *Genomics*, **106**, 76-82.

158. Musco, G., Stier, G., Kolmerer, B., Adinolfi, S., Martin, S., Frenkiel, T., Gibson, T. and Pastore, A. (2000) Towards a structural understanding of Friedreich's ataxia: the solution structure of frataxin. *Structure (London, England : 1993)*, **8**, 695-707.

159. Dhe-Paganon, S., Shigeta, R., Chi, Y.I., Ristow, M. and Shoelson, S.E. (2000) Crystal structure of human frataxin. *The Journal of biological chemistry*, **275**, 30753-30756.

160. Condo, I., Ventura, N., Malisan, F., Rufini, A., Tomassini, B. and Testi, R. (2007) In vivo maturation of human frataxin. *Human molecular genetics*, **16**, 1534-1540.

161. Marmolino, D. (2011) Friedreich's ataxia: past, present and future. *Brain research reviews*, **67**, 311-330.

162. Cavadini, P., Gellera, C., Patel, P.I. and Isaya, G. (2000) Human frataxin maintains mitochondrial iron homeostasis in Saccharomyces cerevisiae. *Human molecular genetics*, **9**, 2523-2530.

163. Yoon, T., Dizin, E. and Cowan, J.A. (2007) N-terminal iron-mediated self-cleavage of human frataxin: regulation of iron binding and complex formation with target proteins. *Journal of biological inorganic chemistry : JBIC : a publication of the Society of Biological Inorganic Chemistry*, **12**, 535-542.

164. Schmucker, S., Argentini, M., Carelle-Calmels, N., Martelli, A. and Puccio, H. (2008) The in vivo mitochondrial two-step maturation of human frataxin. *Human molecular genetics*, **17**, 3521-3531.

165. Adinolfi, S., Trifuoggi, M., Politou, A.S., Martin, S. and Pastore, A. (2002) A structural approach to understanding the iron-binding properties of phylogenetically different frataxins. *Human molecular genetics*, **11**, 1865-1877.

166. Gakh, O., Park, S., Liu, G., Macomber, L., Imlay, J.A., Ferreira, G.C. and Isaya, G. (2006) Mitochondrial iron detoxification is a primary function of frataxin that limits oxidative damage and preserves cell longevity. *Human molecular genetics*, **15**, 467-479.

167. Foury, F., Pastore, A. and Trincal, M. (2007) Acidic residues of yeast frataxin have an essential role in Fe–S cluster assembly. *EMBO Reports*, **8**, 194-199.

168. Schmucker, S., Martelli, A., Colin, F., Page, A., Wattenhofer-Donze, M., Reutenauer, L. and Puccio, H. (2011) Mammalian frataxin: an essential function for cellular viability through an interaction with a preformed ISCU/NFS1/ISD11 iron-sulfur assembly complex. *PloS one*, **6**, e16199.

169. Becker, E.M., Greer, J.M., Ponka, P. and Richardson, D.R. (2002) Erythroid differentiation and protoporphyrin IX down-regulate frataxin expression in Friend cells: characterization of frataxin expression compared to molecules involved in iron metabolism and hemoglobinization. *Blood*, **99**, 3813-3822.

170. Adinolfi, S., Iannuzzi, C., Prischi, F., Pastore, C., Iametti, S., Martin, S.R., Bonomi, F. and Pastore, A. (2009) Bacterial frataxin CyaY is the gatekeeper of iron-sulfur cluster formation catalyzed by IscS. *Nature structural & molecular biology*, **16**, 390-396.

171. Pastore, A. and Puccio, H. (2013) Frataxin: a protein in search for a function. *Journal of neurochemistry*, **126 Suppl 1**, 43-52.

172. Pianese, L., Turano, M., Lo Casale, M.S., De Biase, I., Giacchetti, M., Monticelli, A., Criscuolo, C., Filla, A. and Cocozza, S. (2004) Real time PCR quantification of frataxin mRNA in the peripheral blood leucocytes of Friedreich ataxia patients and carriers. *Journal of neurology, neurosurgery, and psychiatry*, **75**, 1061-1063.

173. Tsai, C.L. and Barondeau, D.P. (2010) Human frataxin is an allosteric switch that activates the Fe-S cluster biosynthetic complex. *Biochemistry*, **49**, 9132-9139.

174. Bridwell-Rabb, J., Fox, N.G., Tsai, C.L., Winn, A.M. and Barondeau, D.P. (2014) Human frataxin activates Fe-S cluster biosynthesis by facilitating sulfur transfer chemistry. *Biochemistry*, **53**, 4904-4913.

175. Braymer, J.J. and Lill, R. (2017) Iron-sulfur cluster biogenesis and trafficking in mitochondria. *The Journal of biological chemistry*, **292**, 12754-12763.

176. Rouault, T.A. and Maio, N. (2017) Biogenesis and functions of mammalian iron-sulfur proteins in the regulation of iron homeostasis and pivotal metabolic pathways. *The Journal of biological chemistry*, **292**, 12744-12753.

177. Anzovino, A., Lane, D.J., Huang, M.L. and Richardson, D.R. (2014) Fixing frataxin: 'ironing out' the metabolic defect in Friedreich's ataxia. *British journal of pharmacology*, **171**, 2174-2190.

178. Bayot, A., Santos, R., Camadro, J.M. and Rustin, P. (2011) Friedreich's ataxia: the vicious circle hypothesis revisited. *BMC Medicine*, **9**, 112.

179. Gonzalez-Cabo, P. and Palau, F. (2013) Mitochondrial pathophysiology in Friedreich's ataxia. *Journal of neurochemistry*, **126 Suppl 1**, 53-64.

180. Strawser, C., Schadt, K., Hauser, L., McCormick, A., Wells, M., Larkindale, J., Lin, H. and Lynch, D.R. (2017) Pharmacological therapeutics in Friedreich ataxia: the present state. *Expert review of neurotherapeutics*, **17**, 895-907.

181. Indelicato, E. and Bösch, S. (2018) Emerging therapeutics for the treatment of Friedreich's ataxia. *Expert Opinion on Orphan Drugs*, **6**, 57-67.

182. Acquaviva, F., Castaldo, I., Filla, A., Giacchetti, M., Marmolino, D., Monticelli, A., Pinelli, M., Sacca, F. and Cocozza, S. (2008) Recombinant human erythropoietin increases frataxin protein expression without increasing mRNA expression. *Cerebellum (London, England)*, **7**, 360-365.

183. Rufini, A., Fortuni, S., Arcuri, G., Condo, I., Serio, D., Incani, O., Malisan, F., Ventura, N. and Testi, R. (2011) Preventing the ubiquitin-proteasome-dependent degradation of frataxin, the protein defective in Friedreich's ataxia. *Human molecular genetics*, **20**, 1253-1261.

184. Soragni, E., Xu, C., Plasterer, H.L., Jacques, V., Rusche, J.R. and Gottesfeld, J.M. (2012) Rationale for the development of 2-aminobenzamide histone deacetylase inhibitors as therapeutics for Friedreich ataxia. *Journal of child neurology*, **27**, 1164-1173.

185. Soragni, E., Miao, W., Iudicello, M., Jacoby, D., De Mercanti, S., Clerico, M., Longo, F., Piga, A., Ku, S., Campau, E. *et al.* (2014) Epigenetic therapy for Friedreich ataxia. *Annals of neurology*, **76**, 489-508.

186. Li, L. (2013) Pharmacological Screening Using an FXN-EGFP Cellular Genomic Reporter Assay for the Therapy of Friedreich Ataxia. **8**.

187. Young, H.A. and Bream, J.H. (2007) IFN-gamma: recent advances in understanding regulation of expression, biological functions, and clinical applications. *Current topics in microbiology and immunology*, **316**, 97-117.

188. Ganz, T. (2009) Iron in innate immunity: starve the invaders. *Current opinion in immunology*, **21**, 63-67.

189. Tomassini, B., Arcuri, G., Fortuni, S., Sandi, C., Ezzatizadeh, V., Casali, C., Condò, I., Malisan, F., Al-Mahdawi, S., Pook, M. *et al.* (2012) Interferon gamma upregulates frataxin and corrects the functional deficits in a Friedreich ataxia model. *Human molecular genetics*, **21**, 2855-2861.

190. Vyas, P.M., Tomamichel, W.J., Pride, P.M., Babbey, C.M., Wang, Q., Mercier, J., Martin, E.M. and Payne, R.M. (2012) A TAT-frataxin fusion protein increases lifespan and cardiac function in a conditional Friedreich's ataxia mouse model. *Human molecular genetics*, **21**, 1230-1247.

191. Nabhan, J.F., Wood, K.M., Rao, V.P., Morin, J., Bhamidipaty, S., LaBranche, T.P., Gooch, R.L., Bozal, F., Bulawa, C.E. and Guild, B.C. (2016) Intrathecal delivery of frataxin mRNA encapsulated in lipid nanoparticles to dorsal root ganglia as a potential therapeutic for Friedreich's ataxia. *Scientific reports*, **6**, 20019.

192. Benini, M., Fortuni, S., Condò, I., Alfedi, G., Malisan, F., Toschi, N., Serio, D., Massaro, D.S., Arcuri, G., Testi, R. *et al.* (2017) E3 Ligase RNF126 Directly Ubiquitinates Frataxin, Promoting Its Degradation: Identification of a Potential Therapeutic Target for Friedreich Ataxia. *Cell Reports*, **18**, 2007-2017.

193. Sardone, V., Zhou, H., Muntoni, F., Ferlini, A. and Falzarano, M.S. (2017) Antisense Oligonucleotide-Based Therapy for Neuromuscular Disease. *Molecules (Basel, Switzerland)*, **22**.

194. Chiriboga, C.A., Swoboda, K.J., Darras, B.T., Iannaccone, S.T., Montes, J., De Vivo, D.C., Norris, D.A., Bennett, C.F. and Bishop, K.M. (2016) Results from a phase 1 study of nusinersen (ISIS-SMN(Rx)) in children with spinal muscular atrophy. *Neurology*, **86**, 890-897.

195. Ottesen, E.W., Seo, J., Singh, N.N. and Singh, R.N. (2017) A Multilayered Control of the Human Survival Motor Neuron Gene Expression by Alu Elements. *Frontiers in Microbiology*, **8**.

196. Ozsolak F, S.K., Wood S. et al. . (2015) Targeting the GAA-repeat region with oligonucleotides for the treatment of Friedreich's ataxia. Presented at the International Ataxia Research Conference (ARC); Windsor, UK;.

197. Li, Y., Polak, U., Bhalla, A.D., Rozwadowska, N., Butler, J.S., Lynch, D.R., Dent, S.Y.R. and Napierala, M. (2015) Excision of Expanded GAA Repeats Alleviates the Molecular Phenotype of Friedreich's Ataxia. *Molecular therapy : the journal of the American Society of Gene Therapy*, **23**, 1055-1065.

198. Ouellet, D.L., Cherif, K., Rousseau, J. and Tremblay, J.P. (2017) Deletion of the GAA repeats from the human frataxin gene using the CRISPR-Cas9 system in YG8R-derived cells and mouse models of Friedreich ataxia. *Gene therapy*, **24**, 265-274.

199. Perdomini, M., Belbellaa, B., Monassier, L., Reutenauer, L., Messaddeq, N., Cartier, N., Crystal, R.G., Aubourg, P. and Puccio, H. (2014) Prevention and reversal of severe mitochondrial cardiomyopathy by gene therapy in a mouse model of Friedreich's ataxia. *Nature medicine*, **20**, 542-547.

200. Miranda, C.J., Santos, M.M., Ohshima, K., Tessaro, M., Sequeiros, J. and Pandolfo, M. (2004) Frataxin overexpressing mice. *FEBS letters*, **572**, 281-288.

201. Chapdelaine, P., Coulombe, Z., Chikh, A., Gérard, C. and Tremblay, J.P. (2013) A Potential New Therapeutic Approach for Friedreich Ataxia: Induction of Frataxin Expression With TALE Proteins. *Molecular therapy. Nucleic acids*, **2**, e119-.

202. Runko, A.P., Griswold, A.J. and Min, K.T. (2008) Overexpression of frataxin in the mitochondria increases resistance to oxidative stress and extends lifespan in Drosophila. *FEBS letters*, **582**, 715-719.

203. Shoichet, S.A., Baumer, A.T., Stamenkovic, D., Sauer, H., Pfeiffer, A.F., Kahn, C.R., Muller-Wieland, D., Richter, C. and Ristow, M. (2002) Frataxin promotes antioxidant defense in a thiol-dependent manner resulting in diminished malignant transformation in vitro. *Human molecular genetics*, **11**, 815-821.

204. Navarro, J.A. (2011) Overexpression of Human and Fly Frataxins in Drosophila Provokes Deleterious Effects at Biochemical, Physiological and Developmental Levels. **6**.

205. Vannocci, T., Notario Manzano, R., Beccalli, O., Bettegazzi, B., Grohovaz, F., Cinque, G., de Riso, A., Quaroni, L., Codazzi, F. and Pastore, A. (2018) Adding a temporal dimension to the study of Friedreich's ataxia: the effect of frataxin overexpression in a human cell model. *Disease models & mechanisms*, **11**.

206. Vannocci, T., Faggianelli, N., Zaccagnino, S., della Rosa, I., Adinolfi, S. and Pastore, A. (2015) A new cellular model to follow Friedreich's ataxia development in a time-resolved way. *Disease models & mechanisms*, **8**, 711-719.

207. Borodulina, O.R. and Kramerov, D.A. (2008) Transcripts synthesized by RNA polymerase III can be polyadenylated in an AAUAAA-dependent manner. *Rna*, **14**, 1865-1873.

208. Follenzi, A. and Naldini, L. (2002) Generation of HIV-1 derived lentiviral vectors. *Methods in enzymology*, **346**, 454-465.

209. Schmittgen, T.D. and Livak, K.J. (2008) Analyzing real-time PCR data by the comparative C(T) method. *Nature protocols*, **3**, 1101-1108.

210. Severin, J., Lizio, M., Harshbarger, J., Kawaji, H., Daub, C.O., Hayashizaki, Y., Bertin, N. and Forrest, A.R. (2014) Interactive visualization and analysis of large-scale sequencing datasets using ZENBU. *Nature biotechnology*, **32**, 217-219.

211. Zucchelli, S., Fasolo, F., Russo, R., Cimatti, L., Patrucco, L., Takahashi, H., Jones, M.H., Santoro, C., Sblattero, D., Cotella, D. *et al.* (2015) SINEUPs are modular antisense long non-coding RNAs that increase synthesis of target proteins in cells. *Frontiers in cellular neuroscience*, **9**, 174.

212. Perdomini, M., Hick, A., Puccio, H. and Pook, M.A. (2013) Animal and cellular models of Friedreich ataxia. *Journal of neurochemistry*, **126 Suppl 1**, 65-79.

213. Gomez-Sebastian, S., Gimenez-Cassina, A., Diaz-Nido, J., Lim, F. and Wade-Martins, R. (2007) Infectious Delivery and Expression of a 135 kb Human FRDA Genomic DNA Locus Complements Friedreich's Ataxia Deficiency in Human Cells. *Molecular therapy : the journal of the American Society of Gene Therapy*, **15**, 248-254.

214. Tai, G., Corben, L.A., Yiu, E.M., Milne, S.C. and Delatycki, M.B. (2018) Progress in the treatment of Friedreich ataxia. *Neurol Neurochir Pol*.

215. Deutsch, E.C., Santani, A.B., Perlman, S.L., Farmer, J.M., Stolle, C.A., Marusich, M.F. and Lynch, D.R. (2010) A rapid, noninvasive immunoassay for frataxin: utility in assessment of Friedreich ataxia. *Molecular genetics and metabolism*, **101**, 238-245.

216. Sacca, F., Puorro, G., Antenora, A., Marsili, A., Denaro, A., Piro, R., Sorrentino, P., Pane, C., Tessa, A., Brescia Morra, V. *et al.* (2011) A combined nucleic acid and protein analysis in Friedreich ataxia: implications for diagnosis, pathogenesis and clinical trial design. *PloS one*, **6**, e17627.

217. Corey, D.R. (2017) Nusinersen, an antisense oligonucleotide drug for spinal muscular atrophy. *Nature neuroscience*, **20**, 497-499.

218. Sandi, C., Pinto, R.M., Al-Mahdawi, S., Ezzatizadeh, V., Barnes, G., Jones, S., Rusche, J.R., Gottesfeld, J.M. and Pook, M.A. (2011) Prolonged treatment with pimelic o-aminobenzamide HDAC inhibitors ameliorates the disease phenotype of a Friedreich ataxia mouse model. *Neurobiology of disease*, **42**, 496-505.

219. Erwin, G.S., Grieshop, M.P., Ali, A., Qi, J., Lawlor, M., Kumar, D., Ahmad, I., McNally, A., Teider, N., Worringer, K. *et al.* (2017) Synthetic transcription elongation factors license transcription across repressive chromatin. *Science (New York, N.Y.)*, **358**, 1617-1622.

220. Rufini, A., Cavallo, F., Condo, I., Fortuni, S., De Martino, G., Incani, O., Di Venere, A., Benini, M., Massaro, D.S., Arcuri, G. *et al.* (2015) Highly specific ubiquitin-competing molecules effectively promote frataxin accumulation and partially rescue the aconitase defect in Friedreich ataxia cells. *Neurobiology of disease*, **75**, 91-99.

221. Grabczyk, E., Mancuso, M. and Sammarco, M.C. (2007) A persistent RNA.DNA hybrid formed by transcription of the Friedreich ataxia triplet repeat in live bacteria, and by T7 RNAP in vitro. *Nucleic acids research*, **35**, 5351-5359.

222. Lin, Y., Dent, S.Y., Wilson, J.H., Wells, R.D. and Napierala, M. (2010) R loops stimulate genetic instability of CTG.CAG repeats. *Proceedings of the National Academy of Sciences of the United States of America*, **107**, 692-697.

223. Li, L., Shen, X., Liu, Z., Norrbom, M., Prakash, T.P., O'Reilly, D., Sharma, V.K., Damha, M.J., Watts, J.K., Rigo, F. *et al.* (2018) Activation of Frataxin Protein Expression by Antisense Oligonucleotides Targeting the Mutant Expanded Repeat. *Nucleic acid therapeutics*, **28**, 23-33.

224. Yoon, T. and Cowan, J.A. (2003) Iron-sulfur cluster biosynthesis. Characterization of frataxin as an iron donor for assembly of [2Fe-2S] clusters in ISU-type proteins. *Journal of the American Chemical Society*, **125**, 6078-6084.

225. Yoon, T. and Cowan, J.A. (2004) Frataxin-mediated iron delivery to ferrochelatase in the final step of heme biosynthesis. *The Journal of biological chemistry*, **279**, 25943-25946.

226. Bulteau, A.L., O'Neill, H.A., Kennedy, M.C., Ikeda-Saito, M., Isaya, G. and Szweda, L.I. (2004) Frataxin acts as an iron chaperone protein to modulate mitochondrial aconitase activity. *Science (New York, N.Y.)*, **305**, 242-245.

227. Stehling, O., Elsasser, H.P., Bruckel, B., Muhlenhoff, U. and Lill, R. (2004) Iron-sulfur protein maturation in human cells: evidence for a function of frataxin. *Human molecular genetics*, **13**, 3007-3015.

228. Condo, I., Malisan, F., Guccini, I., Serio, D., Rufini, A. and Testi, R. (2010) Molecular control of the cytosolic aconitase/IRP1 switch by extramitochondrial frataxin. *Human molecular genetics*, **19**, 1221-1229.

229. Cherubini, F., Serio, D., Guccini, I., Fortuni, S., Arcuri, G., Condo, I., Rufini, A., Moiz, S., Camerini, S., Crescenzi, M. *et al.* (2015) Src inhibitors modulate frataxin protein levels. *Human molecular genetics*, **24**, 4296-4305.